

AD-A283 509

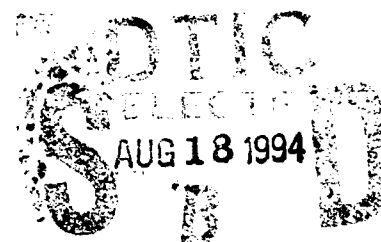


ARMY RESEARCH LABORATORY



METHODS OF MODELING RADIANT ENERGY EXCHANGE IN RADIATION FOG AND CLOUDS

John M. Davis
2413 Cedarwood Drive
Fort Collins, CO 80526



Under Contract DAAL03-91-C-0034
Contract Monitor Robert A. Sutherland

ARL-CR-103

June 1994

94-25947



Approved for public release; distribution is unlimited.

94 25947

NOTICES

Disclaimers

The findings in this report are not to be construed as an official Department of the Army position, unless so designated by other authorized documents.

The citation of trade names and names of manufacturers in this report is not to be construed as official Government indorsement or approval of commercial products or services referenced herein.

Destruction Notice

When this document is no longer needed, destroy it by any method that will prevent disclosure of its contents or reconstruction of the document.

Accession For	
NTIS GRA&I	<input checked="checked" type="checkbox"/>
DTIC TAB	<input type="checkbox"/>
Unannounced	<input type="checkbox"/>
Justification	
By _____	
Distribution/Availability	
Availability Codes	
Dist	Small and/or Special
A-1	

REPORT DOCUMENTATION PAGEForm Approved
OMB No. 0704-0188

Public reporting burden for this collection of information is estimated to average 1 hour per response, including the time for reviewing instructions, searching existing data sources, gathering and maintaining the data needed, and completing and reviewing the collection of information. Send comments regarding this burden estimate or any other aspect of this collection of information, including suggestions for reducing this burden, to Washington Headquarters Services, Directorate for Information Operations and Reports, 1215 Jefferson Davis Highway, Suite 1204, Arlington, VA 22202-4302, and to the Office of Management and Budget, Paperwork Reduction Project (0704-0188), Washington, DC 20503.

1. AGENCY USE ONLY (Leave blank)

2. REPORT DATE
June 19943. REPORT TYPE AND DATES COVERED
Final, June 92 - March 93

4. TITLE AND SUBTITLE

Methods of Modeling Radiant Energy Exchange in Radiation
Fog and Clouds

5. FUNDING NUMBERS

DAADL03-91-C-0034

6. AUTHOR(S)

John M. Davis
Robert A. Sutherland contract monitor*

7. PERFORMING ORGANIZATION NAME(S) AND ADDRESS(ES)

John M. Davis
2413 Cedarwood Dr.
Fort Collins, CO 805268. PERFORMING ORGANIZATION
REPORT NUMBER

ARL-CR-103

*US Army Research Laboratory, WSMR, NM 88002-5501

9. SPONSORING/MONITORING AGENCY NAME(S) AND ADDRESS(ES)

U.S. Army Research Office
PO Box 12211
Research Triangle Park, NC 2770910. SPONSORING/MONITORING
AGENCY REPORT NUMBER

TCN 92341

11. SUPPLEMENTARY NOTES

Task was performed under a Scientific Service Agreement issued by Battelle,
Research Triangle Park Office, Research Triangle Park, NC 27709

12a. DISTRIBUTION/AVAILABILITY STATEMENT

Approved for public release; distribution is unlimited.

12b. DISTRIBUTION CODE

13. ABSTRACT (Maximum 200 words) This report describes several types of parameterizations commonly used in cloud and fog models to calculate the effects of radiant energy exchange in both the infrared and solar portions of the spectrum. The types of parameterizations used in several models of radiation fog have been summarized in the main text and detailed in the appendix, along with a few summaries of supporting studies. In general, the treatment of radiant exchange includes spectral resolution at the level of band models, whether band models are used explicitly or whether the radiation stream has been divided using "a sum of exponentials" approach. All of the studies use a plane parallel approximation in one form or another and all assume spherical particles for droplets and aerosols. The more sophisticated studies use a delta-two stream approach to account for the effects of multiple scattering. A few of the models include a prognostic equation that links the change in the microphysical distribution with the radiation field. The more advanced models also include a carefully designed surface flux exchange model. The strengths and deficiencies of the approaches are discussed and recommendations of a proper radiative parameterization are listed.

14. SUBJECT TERMS

radiation fog models, radiation parameterizations, radiation
models

15. NUMBER OF PAGES

97

16. PRICE CODE

17. SECURITY CLASSIFICATION
OF REPORT

Unclassified

18. SECURITY CLASSIFICATION
OF THIS PAGE

unclassified

19. SECURITY CLASSIFICATION
OF ABSTRACT

unclassified

20. LIMITATION OF ABSTRACT

SAR

Table of Contents

1.0 Introduction	1
2.0 Overview of the requirements	2
2.1 A qualitative description	2
2.2 The structure of the fog model	3
2.3 The nature of the radiative fluxes	4
3.0 Approximations and parameterizations	7
3.1 In the infrared	8
3.2 In the solar region	14
3.3 Some remarks about the parameterizations	21
4.0 The evaluation of parameterizations used in radiation fog models	22
4.1 Listing of models reviewed	22
4.2 Completeness of the parameterizations	23
4.3 Aspects and limitations of radiative treatment common to all models	25
4.4 Inclusion of the effects of solar radiation	26
4.5 Treatment of radiation in the infrared	28
4.6 Treatment of processes related to radiation exchange	30
4.7 Summary of major modeling efforts	31
5.0 Recommendations for naturally occurring and for multi-component fog modeling .	41
5.1 The role of horizontal non-homogeneity	41
5.2 The need for modeling of the role of surface vegetation	42

5.3 The multi-component fog scenario	42
6.0 Summary	44
Acknowledgement	44
References	45
APPENDIX	52
A.1.0 Introduction	52
A.2.0 Cloud Topped Mixed Layer Models	52
A.2.1 Lilly (1968) and Schubert (1977)	52
A.2.2 Oliver, Lewellen and Williamson (1977)	53
A.3.0 Fog models	56
A.3.1 Zdunkowski, Welch and Cox's Radiation Fog Model	56
A.3.2 Practical Improved Flux Method (PIFM) by Zdunkowski <i>et al.</i> (1980)	58
A.3.3 Radiation scheme for circulation and climate models by Zdunkowski <i>et al.</i> (1982)	61
A.3.4 The radiation fog model of Brown and Roach (1976)	72
A.3.5 A numerical study of radiation fog by Brown (1980)	74
A.3.6 Formation and evolution of radiation fog and stratus fogs in the atmospheric boundary layer, by Buykov and Khvorost'yanov (1977).	77
A.3.7 A numerical study of the formation and the dissipation of radiation fogs by Ohta and Tanaka (1986)	78
A.3.8 Prediction of quasi-periodic oscillations in radiation fogs. Part I: Comparison of simple similarity approaches by Welch, Ravichandran and Cox (1986)	81
A.3.9 Assessing the role of latent heat in the development of nighttime cooling fogs, by L.P. Bykova (1986).	81

A.3.10 A comparison of a numerical model of radiation fog with detailed observations by Turton and Brown (1987)	82
A.3.11 The effects of radiative exchange on the growth by condensation of a population of droplets by Guzzi (1986)	82
A.3.12 Numerical simulation of a fog event with a one-dimensional boundary layer model by Luc Musson-Genon (1987)	84
A.3.13 A one-dimensional numerical study to simulate the influence of soil moisture, pollution and vertical exchange on the evolution of a radiation fog by Forkel, Panhans, Welch and Zdunkowski (1984)	88
A.3.14 Fog Modeling with a new treatment of the chemical equilibrium condition by Forkel <i>et al.</i> (1987)	88
A.3.15 The diurnal cycle of the marine stratocumulus layer. A higher-order model study by Bougeault (1981).	88
A.3.16 A radiative fog model with a detailed treatment of the interaction between radiative transfer and fog microphysics, by Bott, Sievers and Zdunkowski (1990).	89
A.3.17 Properties of aerosols on the life cycle of radiation fogs, by Bott (1991)	93
A.3.18 Radiation fog: A comparison of model simulations with detailed observations by Duynkerke (1991)	94
A.3.19 Computing solar heating in a fog layer: a new parameterization, by Vehil and Bonnel (1988)	96
A.3.20 Study of the radiative effects (long-wave and short-wave) within a fog layer, Vehil <i>et al.</i> (1989)	96
A.3.21 A numerical study of radiation fog over the Changjiang River by Qian and Lei (1990)	97
A.3.22 Numerical simulations with a three-dimensional cloud model: Lateral boundary condition experiments and multicellular severe storm simulations, by Clark (1979)	97
A.3.23 Mathematical modeling of acid deposition due to radiation fog, by Pandis and Seinfeld (1989)	97

1.0 Introduction

There is arguably no other short-term natural atmospheric phenomenon that is more strongly affected by the exchange of radiant energy than the development, maintenance and dissipation of radiation fog. Over the past fifteen years many models treating the evolution of the fog process have appeared in the literature that utilize various methods of accounting for the effects of the radiant energy exchange. This report presents a review of what is believed to be every significant entry in this collection, focussing on the aspects of each model that determine the role played by radiation transfer. In attempting this summary, it is acknowledged at the start, that the subject of the review is not the effects of the radiant exchange but rather the manner in which the treatment of the radiant exchange is incorporated into the model. Also, it is not the intent here to present a detailed recipe of any of the approaches although some are presented in more detail than others. The possibilities span a wide range of completeness, from simply specifying the radiational cooling of a fog layer as a constant, to including the radiant effects into the droplet growth equation, the surface energy balance and approximating all relevant scattering and absorption processes. The degree of sophistication with which the radiation exchange is incorporated into the models has been found to be a function of the history of a particular modeling effort and the primary focus of the individual studies. This being the case, no attempt is being made in this report to assess the value of any effort, since each model may have as its primary focus any of a number of important physical processes.

There are of course many sophisticated treatments of radiation transfer that have as their goal the accurate simulation of radiative processes. However, as is the case in many atmospheric simulations, the radiative processes are only one aspect of the fog modelling problem and only a limited fraction of the total resources may be allocated to any process. Thus, the radiative treatments that are described in this report fall into the category of parameterizations, not only due to the limitations of computational resources, but also because many of the physical quantities required for complete radiation treatments are not available within the fog model. Nevertheless, the reader will find by following a chronological path through the various efforts, that at the present time the parameterizations are becoming quite sophisticated and are approaching some of the stand alone radiative transfer models.

This report is organized into three sections. In this the main part of the report, various aspects of the parameterizations are discussed including at least one approach that has not as yet found its way into the fog models. A discussion of the merits and limitations of the approaches will also be found in the main text. Next, a summary of the models with the most complete treatment of radiational exchange will be presented which includes a one-page summary that attempts to give a brief, if cursory overview of the methods employed. The final part of the report is an appendix that gives an account of several of the efforts found in the literature review. It is hoped that sufficient information can be gleaned from the appendix that further research in assessing the best modeling approaches will prove unnecessary.

2.0 Overview of the requirements

This section attempts to overview the manner in which radiation interacts with the fog in its life cycle and also the physical process which affect the transfer of radiative energy in the various stages of fog development.

2.1 A qualitative description

In constructing a model that accurately simulates the life cycle of radiation fog it is necessary to calculate the effect of the radiative energy exchange on the process. A simple qualitative description of the fog life cycle demonstrates the need to accurately account for the radiative exchange. One such scenario might be described as follows. On the evening before fog formation the lower troposphere consists of a moist boundary layer beneath a relatively clear sky. The temperature of the surface and the boundary layer have been determined by conditions on the synoptic scale and the radiation conditions of the day. The layer will include an atmospheric aerosol dictated by the location. After the sun sets the surface cools to space by emission of infrared radiation primarily in the infrared window region, which will be defined as the spectral region with wavelengths between 8.0 and 12.0 μm . At the same time the entire surface layer in the lowest meters of the atmosphere cools to space via the same mechanism. It may result that due to the relatively higher surface emissivity, the surface temperature drops below that of the air immediately above. This allows the air to cool, not only to space but also to the surface, and a strong inversion is set up in the lowest part of the atmosphere.

As the cooling continues the air reaches near saturation conditions with respect to water vapor. A water haze forms as the air becomes nearly saturated and haze droplets, whose size distribution is primarily determined by the pre-existing aerosol size distribution, compete for the existing water vapor. Small scale turbulence, induced by the temperature gradient of the inversion mix the layer's water vapor and droplets. Once larger droplets are formed infrared cooling is dramatically enhanced in the upper regions of the fog allowing haze droplets to activate and grow as a function of the aerosol nuclei type and the net radiation budget at the droplet surface which selectively enhances the growth of larger droplets. The depth of the fog layer grows as the moisture is mixed to higher levels and heat is mixed downward, the existence of the layer is sustained by radiation loss at the top of the fog layer, now primarily to space as the fog filled intermediate layers become more opaque to the radiation from the fog layer above. As haze droplets are converted to fog droplets gravitational settling becomes important. Larger drops settle out of the layer forming dew at the surface and altering the liquid water budget within the layer. Short term (15 to 20 minute) oscillations may be observed as the fog layer alternately thickens by growing drops in a high radiative loss environment and then thins as large drops settle to the ground. This process continues in the absence of changing synoptic conditions until after sunrise.

With sunrise the solar radiative stream's ability to heat the layer sufficiently to dissipate the fog depends on the optical properties of the layer. Geometrically thick layers or layers with a high

concentration of small droplets may be particularly resistant to solar burn off. The dissipation of the fog becomes more likely with the decrease in the solar zenith and is likely to be a combined process of absorption by the droplets (depending on the absorption coefficient again related to the type of condensation nucleus as well as the size of the droplet) and heating of the surface by the transmitted solar irradiance. After the fog dissipates the likelihood of recurrence of the event is again governed by conditions dictated by the synoptic situation as sunset approaches.

This description of what may transpire in the fog's life cycle is fairly typical of the scenario most modelers adhere to. There are of course a great number of possible variations on what was described, but it is not the intent to describe variations of the fog life cycle here. Rather, the brief description was offered as an indication of the ways radiation influences the genesis, maintenance and dissipation of the fog layer. Infrared radiation plays the crucial role in the initiation of the layer by cooling the layer to near saturation conditions. The ability of the ground surface to radiate to space is also active in this first stage. Upon activation of the haze droplets the total radiative environment in which the droplet is immersed influences the growth rate of the droplets selectively enhancing the growth of the larger drops and enhances the cooling of the upper few meters of the fog. In daytime conditions the ability of the solar radiation to penetrate further into the fog, relative to the infrared radiation, is important in the break up or burn off of the fog. As will be seen below, in spite of the complex interactions between radiative and dynamic processes, it is possible to grow a fog layer with a fairly simple radiation model, and if the modeler's expertise is focussed on other aspects of the fog's development, this course is often taken. Nevertheless, in order to simulate a more detailed history of the fog's life cycle, the radiative process must be carefully modeled.

2.2 The structure of the fog model

While it is not the purpose of this report to document the numerical methods used in simulating the dynamics of the fog, it is useful at the outset to examine the structure of the governing set of equations in order to see how the radiative term is included in the model. Most all of the efforts reviewed in this study had a similar basic set of equations, with one exception which is noted later. The equations must describe the budgets of horizontal and vertical momentum, heat and water. They must also treat in some degree of approximation the processes of turbulent transport, radiative exchange and microphysical droplet growth and settling. As an example, the theoretical equations of Bott (1990) are presented below in which u and v are the horizontal components of velocity for which the subscript g denotes the geostrophic values, f is the Coriolis parameter, θ is the potential temperature, p and p_0 are the pressure at height z and at the surface, c_p is the specific heat at constant pressure, ρ the density of air, L is the heat of condensation for water, q the specific humidity, and $f(a,r)$ is the microphysical droplet distribution for droplets of radius r with condensation nuclei of radius a .

$$\begin{aligned}
\frac{\partial u}{\partial t} &= \frac{\partial}{\partial z} \left(k_m \frac{\partial u}{\partial z} \right) + f(v - v_g) \\
\frac{\partial v}{\partial t} &= \frac{\partial}{\partial z} \left(k_m \frac{\partial v}{\partial z} \right) - f(u - u_g) \\
\frac{\partial \theta}{\partial t} &= \frac{\partial}{\partial z} \left(k_m \frac{\partial \theta}{\partial z} \right) - \left(\frac{p_0}{p} \right)^{0.286} \frac{1}{c_p \rho} \left(\frac{\partial E_n}{\partial z} + LC \right) \\
\frac{\partial q}{\partial t} &= \frac{\partial}{\partial z} \left(k_h \frac{\partial q}{\partial z} \right) + \frac{C}{\rho} \\
\frac{\partial f(a, r)}{\partial t} &= \frac{\partial}{\partial z} \left(k_h \frac{\partial f(a, r)}{\partial z} \right) - \frac{\partial}{\partial z} (w_t f(a, r)) - \frac{\partial}{\partial r} \left(\frac{dr}{dt} f(a, r) \right),
\end{aligned}$$

where k_m and k_h are the turbulent mixing coefficients for momentum and heat, E_n is the net radiative flux density, C is the condensation rate and w_t is the droplet terminal fall velocity.

The single exception to this general set of equations that is of interest in this report is the second order closure model of Oliver *et al.* (1978), which differs in the way in which the turbulent transports are modeled. Another higher order model was identified (Bougeault 1981) but it did not include any treatment of the radiative processes.

The net radiative flux in the thermodynamic equation results from the difference between the absorption of shortwave and longwave fluxes and the emission of the longwave flux by the layer. The remainder of this report is concerned with the manner in which the net flux is calculated by various models. It will be seen that although there are several variations on the methodology, most of the approaches are basically similar.

2.3 The nature of the radiative fluxes

Because of the large difference between the radiating temperatures of the sun and the earth's atmosphere there is a natural spectral division between the solar and terrestrial radiative streams. This division occurs around $3 \mu\text{m}$; radiation from roughly 0.28 to $2.8 \mu\text{m}$ being considered in the solar regions and radiation beyond being considered in the longwave regime. Of course, this is not totally accurate since absorption of solar radiation by water vapor is usually taken into account out to beyond $6.0 \mu\text{m}$. In the solar region the radiative stream is subject to the processes of scattering by aerosols (which includes water droplets) and air molecules and absorption by water vapor, carbon dioxide, ozone and aerosols. Solar radiation interacts with other atmospheric constituents to a lesser extent. Scattering is not as important in the infrared for which the most important processes are absorption and emission primarily by water vapor, carbon dioxide, ozone and by water droplets; however, scattering is considered important in the infrared in some applications in the region of the atmospheric window from 8.0 to $12.5 \mu\text{m}$. In the application of modeling of fog evolution scattering in the infrared is important because it enhances the absorption and/or emission of the radiative energy by extending the optical path through which the radiation passes. Of the two types, infrared radiation is generally considered most important in the fog life cycle since it is possible to model the onset and intensification of the fog without any consideration of the solar radiation. This is in accord with the tendency for fogs to form during the nocturnal hours; however, solar radiation is considered important in the

dispersion stage of the fog, although some studies indicate that fogs can be dispersed under the influence of an increase in downwelling infrared radiation as might happen if a low or middle level cloud were advected over the fog layer.

The relatively brief listing of the important processes affecting the transfer of radiation in the atmosphere is misrepresentative of the difficulty of quantifying its effects. There are two complications in the infrared; one is the extremely fine spectral scale and large number of absorption lines offered by the possible molecular transitions of the gases. The total number of absorption lines which may be considered by detailed "line by line" models is of the order of 10^4 . The difficulty of treating the sheer number of such lines is complicated by the second factor; the effects of non-homogeneous paths in the atmosphere. As the molecules are exposed to differing temperature and pressure environments the shapes of the absorption lines change in their line strengths and in their widths, overlapping other lines of the same and foreign gases. It is currently not possible to treat the absorption and emission of infrared radiation at this level of detail in a numerical model in which radiation is but one of the important physical quantities. Such models simulate fogs in time steps of from a few tenths of seconds to a few minutes depending on which physical processes are important. Calculation of the infrared spectrum on a modern work station using a "line by line" model may take up to a few hours depending on the nature of the problem being solved. Even with the advances being made in processing speed it is difficult to imagine when treatment of infrared radiation in numerical models will advance to the level of detail at which the spectra are currently understood. Thus, some type of parameterization must be constructed which approximates the more detailed treatment. The parameterization must account for the absorption and emission by water vapor from 3.5 to 8.75 μm and from 12.5 to 100 μm , by the 15 μm CO_2 band, and by the 9.6 μm ozone band. In the atmospheric window, besides ozone there is the continuum absorption by the water vapor dimer. Aerosols and liquid water absorb and emit infrared radiation across the entirety of the longwave spectrum. Figure 1 shows the measured downwelling infrared radiation for a clear sky case and for stratocumulus overcast, which is similar to what would be observed at the bottom of a fog layer. Notable is the masking of the individual bands by the nearly grey body emission by the droplets forming the cloud layer.

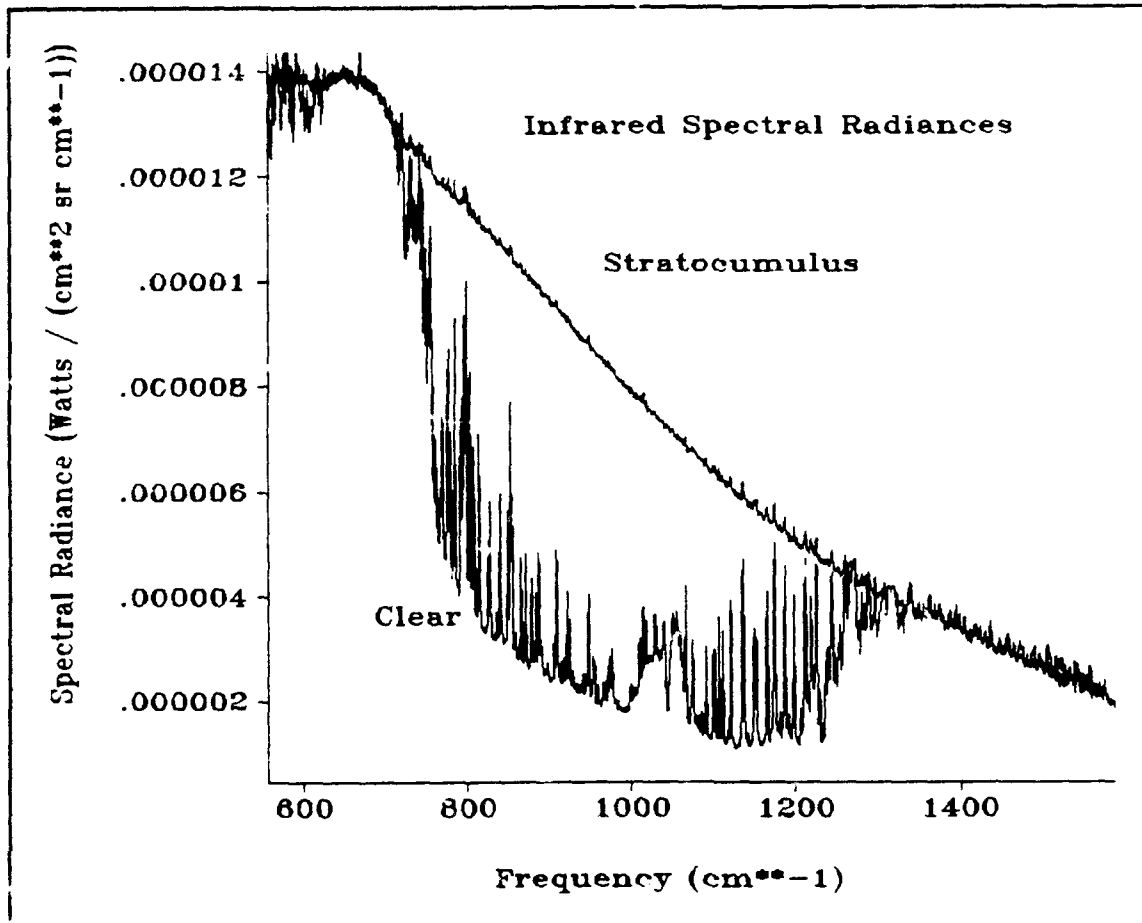


Figure 1 Measured downwelling IR spectral radiance for a clear sky and for stratocumulus overcast.

In the solar portion of the spectrum the primary processes are absorption and scattering. Solar radiation is absorbed primarily by water vapor in bands centered at 0.94, 1.1, 1.38, 1.87, 2.7, 3.2 and 6.3 μm , by ozone in the mid visible and to a lesser extent by CO_2 in bands centered at 1.4, 1.6, 2.0, 2.7, 4.3, 4.8, and 5.2 μm . In some sense the treatment of solar radiation is simpler due to the absence of emission since the spectral distribution of the energy is known at the top of the atmosphere and is changed only by selective absorption, whereas in the infrared the spectral properties change due to emission by the gases at various pressures and temperatures within the atmosphere. However the role of scattering is greatly enhanced in the shortwave and becomes the major complication in the presence of aerosols or water droplets and to a much smaller extent by Rayleigh scattering from air molecules. The most important parameters of scattering are the extinction coefficient which determines the total attenuation through a path containing a given concentration of particles, the single scattering albedo which determines the amount of absorption relative to attenuation through the same path and the phase function (or in the case of simplified scattering models the asymmetry parameter) which determines the angular distribution of the scattered radiation. Figure 2 shows a plot of the extraterrestrial solar radiation and the radiation transmitted through a clear mid-latitude winter atmosphere.

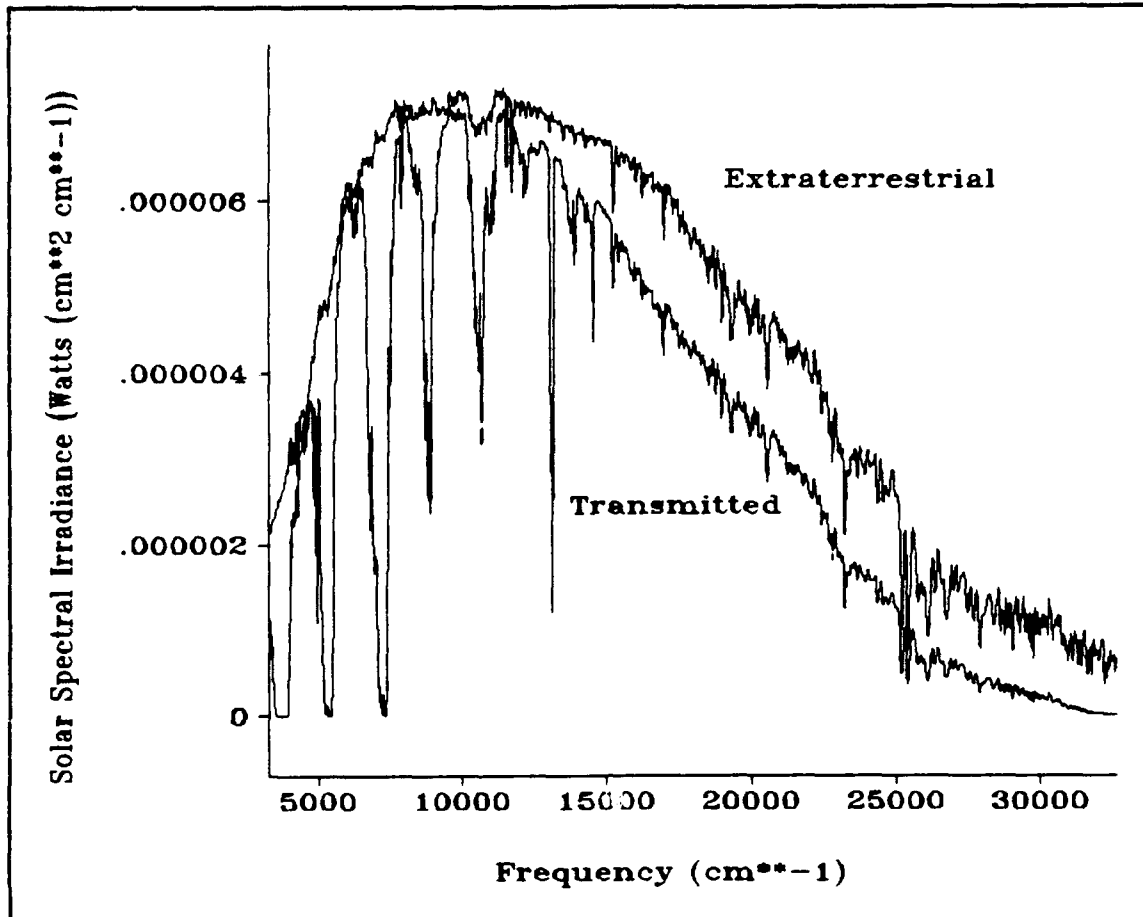


Figure 2. Spectral solar irradiance at the top of the atmosphere and transmitted through a mid-latitude winter atmosphere.

3.0 Approximations and parameterizations

The numeric model must approximate the transfer of radiant exchange in a time frame acceptable for model execution. If all of the quantities required for this calculation are not predicted or diagnosed by the dynamic and hydrodynamic equations of the model, then parameterizations must be invoked. Stephens (1984) presents a review of parameterizations which are useful in General Circulation Models (GCMs) or in climate models. Many of these same approaches are used in fog models. In fact, two efforts use a direct adaptation of the GCM version of radiative transfer effects for the application to fog models. This section deals with the nature of the approximations which are used in the numerical models. Much of this information has been condensed from the Stephens (1984) review article. In section 4 the specific types of parameterizations used in the fog models which have been reviewed will be presented.

3.1 In the infrared

The governing equations for the transfer of the upwelling $F\uparrow(z)$ and downwelling $F\downarrow(z)$ infrared fluxes at a level z are given by Liou (1980) as

$$F\uparrow(z) = \int_0^\infty \pi B_\nu(0) \tau_\nu(z, 0) d\nu + \int_0^z \int_0^\infty \pi B_\nu(z') \frac{d\tau_\nu^f}{dz'}(z, z') dz' d\nu$$

$$F\downarrow(z) = \int_0^\infty \int_z^\infty \pi B_\nu(z') \frac{d\tau_\nu^f}{dz'} dz' d\nu$$

where $B(z)$ represents the Planck emission function, ν is the frequency in wavenumbers (cm^{-1}), and τ_ν^f is the diffuse transmission. The diffuse or flux transmissivity is defined as

$$\tau_\nu^f(z, z') = 2 \int_0^1 \tau_\nu(z, z', \mu) \mu d\mu,$$

where μ is the cosine of the zenith angle for the direction in which the infrared radiance is travelling. The diffuse transmission is often approximated as

$$\tau_\nu^f(z, z') \approx \tau_\nu(z, z', 1/\beta),$$

where β is the diffusivity factor often taken to be 1.66, and where the spectral transmissivity is defined as

$$\tau_\nu(z, z', \mu) = \exp\left[-\frac{1}{\mu} \int_{u(z)}^{u(z')} k_\nu(p, T) du\right],$$

where $k_\nu(p, T)$ is the spectral extinction coefficient and u is the path normally given in units of (molecules cm^{-2}), although units of (g cm^{-2}) or (atmospheric centimeters at normal temperature and pressure) are also used. Use of the diffusivity factor allows the computation of a flux transmissivity from an intensity transmissivity rather than an integration of the intensity transmissivity over the hemisphere. This is usually considered to be a good approximation and is invoked in the infrared by almost all of the models reviewed.

If one follows the order of considerations presented in Stephens (1984), another concern is the value of $k_\nu(p, T)$, since radiation passes through highly variable pressure and temperature paths while the value of the absorption coefficient is normally determined in a laboratory under homogeneous conditions. One approach to the problem attributed to Goody (1964a) assumes optical depth ($k_\nu u$) may be separated into two factors

$$k_\nu u = k_\nu(p_0, T_0) \int \frac{\phi(p, T)}{\phi(p_0, T_0)} du = k_\nu(p_0, T_0) u^*,$$

where p_0 , and T_0 are the reference temperature and pressure. Then the variation in the atmosphere is usually absorbed into the expression for the path amount and u^* is given by

$$u^* = \int \left(\frac{p}{p_0} \right)^n \left(\frac{T}{T_0} \right)^m du.$$

The other approximation for the effects of inhomogeneous path is the so called Curtis Godson approximation for which the absorption along a nonhomogeneous path is calculated by adjusting the path and the pressure according to

$$\begin{aligned} p^* u^* &= \int p du, \\ u^* &= \int du. \end{aligned}$$

This approximation is considered to be more accurate than the previous for the effects of variable path.

The variability of the IR radiative spectrum and the dramatic effect of the cloud layer as shown in Fig. 1 is, to say the least, a challenge to the modeler trying to include these effects. Calculation of the heating or cooling from the infrared requires a convolution of the spectral transmittance with the Planck function in the integrals for the equation of transfer. Since consideration of individual lines is enormously expensive in the context of a numerical GCM or fog model, band models have been developed. One such model attributed to Goody (1952) assumes a form similar to that of an individual Lorentz line and is given by

$$\tau_{\nu}^f = \exp \left[- \frac{\overline{S} u \beta}{d} \left(1 + \frac{\overline{S} u \beta}{\pi \overline{\alpha}} \right)^{-1/2} \right],$$

where the overbar indicates an average over a subspectral interval $\Delta \nu$, where in the single line formula for absorption, S is the line strength, α is the halfwidth at half maximum. In the band model these parameters as well as d should be considered parameters of the fit. Through an inhomogeneous path the band model is used by replacing the path parameter with that from the Curtis Godson approximation and multiplying the halfwidth by (p^*/p_0) where p_0 is the reference pressure at which the halfwidth is originally determined. Even with this level of approximation it typically requires approximately 20 spectral intervals to approximate the radiative contribution in the infrared spectrum.

A large fraction of the IR cooling from lower tropospheric layers occurs in the atmospheric window region. Within this region there is a smoother absorption caused by water vapor and termed continuum absorption. This effect is not totally understood but is believed to be due to a combination of absorption in the wings of the surrounding water vapor bands and to *e-type* absorption by water vapor. At any rate it depends on the water vapor partial pressure. One

expression for the absorption coefficient for *e*-type is given by

$$k_v(p, T) = \frac{\phi(T)}{\phi(T_0)} \psi(v, T_0) e,$$

where

$$\phi(T) = \exp(1800/T),$$

and

$$\psi(v, T_0) = 4.18 + 5578 \exp(-0.00787 v) g^{-1} \text{ cm}^2 \text{ atm}^{-1},$$

with $T_0 = 296 \text{ K}$, and v in cm^{-1} .

Another important consideration is the overlap of the H_2O vapor and CO_2 emission lines especially in the $15 \mu\text{m}$ region. According to Stephens (1984), the combined transmittance, which may be expressed as the product of the individual transmittances (strictly valid only in a monochromatic sense) is only valid for transmission models based on the random distribution of absorption lines and not for the flux emissivity approximations which are prevalent in fog numerical models. Examples of transmission models for the combined emission may be found in Ramanathan (1976), Ellingson and Gille (1978) and Fels and Schwartzkopf (1981).

The most accurate form of "quadrature" for integration over frequency is the k distribution method. A thorough treatment of this method may be found in Chou and Arking (1980, 1981), for the infrared and solar portion of the spectrum respectively. The essence of this method is in effect a reordering of spectral absorption coefficients into groups of common strengths. This is valid since the absorption over a fairly wide spectral interval depends on the fraction of the interval that is associated with a particular value of k . This method is also attractive since it may be used when scattering is also an important process. Implementation of the method is ultimately performed by interpolating for a value of a parameter $G(w^*, T)$ defined as

$$G(w^*, T) = \sum_{i=1}^n B_i(T) \tau_i^*(w^*) \Delta v_i,$$

where

$$w^*(p_1, p_2) = \int_{p_1}^{p_2} \frac{1}{g} \frac{p}{p_r} \left[\frac{T_r}{T(p)} \right]^{0.5} q(p) dp,$$

$$\tau^*(u_v) = 2E(u_v) = 2 \int_1^\infty e^{-u_v t} t^{-n} dt,$$

and

$$u_v(p_1, p_2) = \int_{p_1}^{p_2} g^{-1} k_v(p, T(p)) q(p) dp,$$

in which $q(p)$ is the specific humidity and g the gravitational acceleration. G is a rather smoothly varying function tabulated as a function of w and T separately for the band wings and the band center regions. The IR cooling rate may be expressed directly in terms of G and its partial derivative with respect to temperature.

One of the most common approaches used for calculating IR cooling is to use what has been termed a flux emissivity approach to solve the equation of transfer in a broadbanded fashion. The flux equations are written in the form

$$F^\uparrow(z) = \int_0^\infty B_v [1 - A_v(z, 0)] dv + \int_0^z \int_0^\infty \pi B_v(z') \frac{dA_v}{dz'}(z, z') dz' dv$$

$$F^\downarrow(z) = \int_0^\infty \int_z^\infty \frac{dA_v}{dz'}(z, z') \pi B_v(z') dz' dv,$$

where $A_v = (1 - \tau_v)$ is the absorptivity of the gas. The flux emissivity may then be defined as

$$e(z, z') = \frac{1}{\sigma T^4} \int_0^\infty A_v(z, z') \pi B_v(T) dv.$$

After which the equations for the upward and downward flux may be written as

$$F^\uparrow(z) = \sigma T^4 (1 - e(z, 0)) + \int_0^z \sigma T^4(z') \frac{de}{dz'}(z, z') dz'$$

$$F^\downarrow(z) = \int_z^\infty \frac{de}{dz'}(z, z') \sigma T^4(z') dz$$

Stephens (1984) points out that it is not always possible to accurately evaluate $d\epsilon(z, z')/du$, so an alternate emissivity form may be introduced which is suggested by integration of the equations of IR radiative transfer by parts to obtain

$$F\downarrow(z) = \int_0^{\infty} B_v(z=0) dv + \int_0^z \int_0^{\infty} A_v(z, z') \frac{dB_v(z')}{dz'} dz' dv,$$

and

$$F\downarrow(z) = \int_z^{\infty} \int_z^{\infty} A_v(z, z') \frac{dB_v(z')}{dz'} dz' dv.$$

If the following quantity is defined,

$$e'(z, z') = \int_0^{\infty} A_v(z, z') \frac{dB_v}{d\sigma T^4(z')} dv,$$

then the equations may be transformed into

$$F\downarrow(z) = \int_z^{\infty} e'(z, z') \frac{d\sigma T^4(z')}{dz'} dz'$$

$$F\downarrow(z) = \sigma T_s^4 + \int_0^z e'(z, z') \frac{d\sigma T^4(z')}{dz'} dz'$$

which is apparently more accurately evaluated in numerical modeling applications.

There is also some advantage in evaluating the IR cooling rates by separating the problem into two parts: one part is the exchange of the radiative streams with layers above and below the layer whose cooling/heating is being calculated; the other part is the consideration of the fraction of the radiation which is lost to space directly. Some studies apparently have indicated that it is more appropriate to treat each of these portions in different ways in order to achieve the maximum accuracy for a given expenditure of computational resources. There is some similarity to this philosophy in a few of the fog models which in essence treat the upper part of the atmosphere as a given quantity and concentrate only on the mutual exchange between the layers within the fog when calculating the radiative effects.

When fog droplets begin to activate from aerosol haze a dramatic change begins to take place regarding the IR radiative budget within the fog layer. As explained qualitatively above the emission by the upper levels of the fog provides the temperature gradient setting up turbulent transports within the layer. This is one area where fog numerical models have a distinct advantage over the GCMs designed to simulate larger scale (both in time and space) circulations. This results from the smaller space and time scales which allow, in a few of the more recent efforts, a prognostic equation for the microphysical droplet distribution. This allows a direct

computation of the droplet absorption coefficient. If it is assumed that scattering in the IR is not important compared to absorption (almost all fog numerical models make this assumption; see Section 4 for a complete discussion of the single exception), then the absorption $A(z, z')$ and optical thickness have a simple relationship

$$A_v(z, z') = 1 - \exp[-\delta_v(z, z')],$$

where $\delta(z, z')$ is the optical depth between levels (z, z') and is given by

$$\delta_v(z, z') = \frac{1}{\mu} \int_z^{z'} \kappa_v(z'') dz''.$$

The droplet absorption coefficient is given by

$$\kappa_v(z'') = \pi \int_0^\infty n(r, z'') r^2 Q_{abs}(v, r) dr,$$

where Q_{abs} is derived from Mie theory as the absorption efficiency of a spherical droplet of radius r , and $n(r, z)$ is the number density of the droplets. All of the models reviewed assumed spherical droplets through the use of various assumptions or parameterizations. If the absorption coefficient is known as a function of frequency then it may be combined in the equation of transfer with that for gaseous absorption and the droplets contribution to the IR cooling may be computed. Many of the models reviewed for this study did not include a prognostic equation for the droplet distribution so a direct calculation of the absorption coefficient was not possible. Instead a very common type of parameterization was used which expresses the absorption coefficient as a function of liquid water path. The liquid water path is usually deduced from a total (liquid plus gaseous) water budget together with prognostication of saturation conditions. If the absorption coefficient κ , is divided by the density of liquid content in the fog there results a mass absorption coefficient for liquid water,

$$k_v^c(z'') = \frac{\kappa_v(z'')}{w(z'')} = \frac{3}{4} \frac{\int_0^\infty n(r, z'') r^2 Q_{abs}(v, r) dr}{\int_0^\infty n(r, z'') r^3 dr},$$

where $w(z'')$ is the liquid water content of the fog at z'' . For particles small compared to the wavelength it is approximately true that $Q_{abs}(v, r) = c(v)r$. Then the mass absorption coefficient may be written as $k_{vc} = 3/4 c(v)$, after which the absorptivity may be expressed as

$$A_v(z, z') = 1 - \exp(-k_v^c W(z, z') \mu^{-1}),$$

where

$$W(z, z') = \int_z^{z'} w(z'') dz''.$$

This type of parameterization would normally apply in fogs where the droplets have a modal radius of about $5 \mu\text{m}$ according and the IR wavelengths are mainly above this limit. A flux emissivity is then obtained by integrating ϵ_v over zenith angle or introducing a diffusivity approximation

$$\epsilon_v^f = 1 - \exp(-\beta k_v^c W).$$

A broadband flux emissivity is obtained after integration over wavenumber weighted by the Planck function;

$$\epsilon_v^f = \frac{\int_{\Delta v} B_v(T) \epsilon_v^f dv}{\int_{\Delta v} B_v(T) dv}.$$

Since the absorption coefficient for liquid water is relatively smooth the broadband flux emissivity is usually written as

$$\epsilon_v^f = 1 - \exp(-\beta k_v^c W),$$

where the absorption coefficient has been averaged over the wavelength interval.

3.2 In the solar region

In the solar region the determination of clear sky fluxes is fairly straightforward and usually based on a simple parameterization. The solar radiation arriving at a level z from the direction of the solar zenith angle with a cosine represented by μ_0 is given as

$$S\downarrow(z, \mu_0) = \int_0^\infty S_v(\infty) \tau_v(z, \infty, \mu_0) dv,$$

where $S(\infty)$ is the extraterrestrial solar flux density and τ , the spectral transmissivity. The spectral transmissivity is expressed in terms of an absorption coefficient k_v as

$$\tau_v(z, \infty, \mu_0) = \exp\left(-\frac{1}{\mu_0} \int_z^\infty k_v du\right),$$

where u is the optical mass. At large zenith angles there is often an adjustment for passage of the solar radiation through a curved atmosphere but this has little relevance in the current situation. The expression for the downward and upward fluxes may be written as summations according to

$$S\downarrow(z) = \mu_0 \sum_{i=1}^N S_i(\infty) \tau_{\bar{v}_i}(u),$$

and

$$S\uparrow(z) = \mu_0 \sum_i^N \alpha_{gi} S_i(\infty) \tau_{\bar{v}_i}(u^*),$$

where the transmittances are expressed as average values of a spectral subinterval and u^* is the path adjusted for the more or less diffuse radiance field reflected from the surface with albedo α_s . The value of u^* may be taken as $u_0 / \mu_0 + (u_0 - u) m^*$, where u_0 is the optical path for a vertical path through the atmosphere and m^* is a factor for the diffuse nature of the radiation and has a value of 1.9 for water vapor and 5/3 for ozone.

In the clear sky for solar wavelengths absorption by water vapor plays the major role in heating the lower atmosphere. There are several clear sky parameterizations for absorption by water vapor such as Korb *et al.* (1956), McDonald (1960), Yamamoto (1962), Sasamori *et al.*, (1972), Lacis and Hansen (1974), and Liou and Sasamori (1975). Most of these are based on the original measurements of Howard *et al.* (1956), whose original expressions are usable as well. According to Stephens (1984), one of the most useful formulations is due to Lacis and Hansen (1974), whose absorption by water vapor fits the Yamamoto (1962) absorption curve to within 1% for $0.001 < u^* < 10$ cm. It is expressed as

$$\bar{A} = \frac{2.9 u^*}{(1 + 141.5 u^*)^{0.635} + 5.925 u^*},$$

where u^* is the water vapor path in precipitable centimeters scaled by the Curtis Godson approximation with $T_0 = 273$ K and $p_0 = 1013$ mbar.

Despite the seemingly simpler problem of computing heating rates in the solar region for a cloud free atmosphere, Stephens (1984) indicates that among various parameterizations differences of 50% are possible depending on the altitude used in the comparison. At the surface the spread is about 20% for a mid-latitude summer atmosphere and closer to 40% for a sub-arctic winter atmosphere. These discrepancies exist despite the fact that almost all of the parameterizations use the original water vapor absorption data as indicated above.

Ozone absorbs in the solar region roughly from 0.28 to 0.65 μm . Clear sky parameterization for ozone assume most of the absorption occurs high in the atmosphere where little scattering takes place. This assumption is not valid for fog models. Even for fog free computations

enhanced boundary layer concentrations of O₃ due to the effects of air pollution can not be disregarded. Most of the fog models do not include the effects of ozone absorption. Those that do (Bott *et al.*, 1990 and Ohta and Tanaka 1984) for example, include the effects of molecular scattering which would accommodate the enhancement of absorption. Nevertheless, for clear sky calculations the parameterizations of Lacis and Hansen (1974) are often employed. They have the simple form

$$A_{ozone}^{vis} = \frac{0.02118 \nu}{1 + 0.042 \nu + 0.000323 \nu^2},$$

which is applicable for $0.0001 < \nu < 10$ cm (NTP) to four figure accuracy. In the UV for $0.0001 < \nu < 1$ cm (NTP) the absorption is given by

$$A_{ozone}^{uv} = \frac{1.082 \nu}{(1 + 138.6 \nu)^{0.805}} + \frac{0.0658}{(1 + 103.6 \nu)^3},$$

and the total absorption by ozone is obtained as the sum of the those given by the reactions above.

Except in the case noted above of a polluted boundary layer, the treatment of scattering by air molecules or Rayleigh scattering is probably more critical in GCMs than in fog models. This is because GCMs are concerned with heating in the entire atmospheric layer and radiation diffusely reflected by air molecules will be absorbed to a greater extent than will collimated radiation by the same layer, particularly for the upper atmospheric layers where ozone absorption is most important. Two approaches are listed by Stephens (1984). The first and simplest simply replaces the integrated solar constant by one which is reduced by 7%, an average global value for reflectance by Rayleigh scattering. This approach is least accurate for heating in the upper atmosphere but is probably more acceptable in fog models, again with the possible exception of the ozone polluted boundary layer. The other formulation composites the reflection by the surface and the lowest layer and specifies that

$$\bar{\alpha}(\mu_0) = \alpha_R(\mu_0) + [1 - \alpha_R(\mu_0)] [1 - \alpha_R^*] \frac{\alpha_g}{1 - \alpha_R^* \alpha_g},$$

where

$$\alpha_R(\mu_0) = 0.219 / (1 + 0.816 \mu_0) ; \quad \alpha_R^* = 0.144.$$

The function $\alpha_R(\mu_0)$ is computed by standard methods for a non-absorbing layer. Afterwards, the composite albedo is used as a replacement for the surface albedo in the GCM. In the fog model of Ohta and Tanaka (1984) it is simply stated that Rayleigh scattering is included. In the Bott *et al.*, (1990) model it is stated that the scattering coefficients for air molecules are solar energy weighted average values of the same over the appropriate spectral intervals. Only in Fouquart and Bonnel (1980) is the formulation actually given as

$$R_R = 0.5 \tau_R / (\mu_i + \tau_R),$$

where τ_R is the Rayleigh optical thickness given by $\tau_R = 0.06(p - p^+) / p_0$, where p^+ and p^- are the upper and lower pressure boundaries of the layer and p_0 is the surface pressure.

Of course, the greatest complication in the shortwave portion of the spectrum is devising an efficient method to treat scattering by aerosols, which will be taken as including scattering by water droplets. When droplets are present much attention is placed on how to handle the effects of multiple scattering. The simplest approach, and one that is often taken in GCMs is to assign precalculated values for the reflectance and transmittance by high middle and low clouds. While this practice may be disputed as it applies to GCMs it would certainly not qualify as a "state of the art method" in a radiation fog model. The rationale for seeking a more interactive approach is twofold. First, in the more advanced models the necessary ingredients are available for evaluating the appropriate values of fog reflection, transmission and absorption by the droplets. More specifically, some models now have the ability to predict the microphysical droplet distribution which may be used to evaluate the single scattering parameters which may then be used in a multiple scattering recipe. Second, the dissipation stage in the fog life cycle is thought to be very sensitive to the penetration of solar radiation into the fog deck and this implies a changing value of transmission (also reflection and absorption) at each time step in the model. Obviously, fixed values are not appropriate in this application. The equation of transfer for solar radiation may be written

$$\begin{aligned} \mu \frac{dI(\delta, \mu)}{d\delta} = & -I(\delta, \mu) + \frac{\omega_0}{2} \int_{-1}^{+1} \bar{P}(\delta, \mu, \mu') I(\delta, \mu') d\mu' \\ & + \frac{S_0}{4\pi} \bar{P}(\delta, \mu, \mu_0) e^{-\delta/\mu_0} \end{aligned}$$

where $I(\delta, \mu)$ is the monochromatic radiance at an angle whose cosine is μ at a level in the atmosphere whose optical thickness is δ that is comprised of the optical thicknesses for scattering δ_s (aerosol plus air molecules), that due to absorption by aerosols δ_a (including water droplets), and that due to absorption by gases δ_g . The single scattering albedo ω_0 is the ratio of scattering to total extinction by droplets or δ_s / δ . The directional nature of the scattering is characterized by the phase function $p(\delta, \mu, \mu')$, which for wavelengths in the visible and droplet sizes typical in fogs, has relatively much larger values in the directions of scatter near the forward direction compared to the sides or backscatter direction. For the assessment of solar heating rates the exact shape of the phase function is not terribly important because of the effects of multiple scattering which tends to smooth out the effects of the strong forward peak. A more useful parameter is the asymmetry parameter g , defined as

$$g = \frac{1}{2} \int_{-1}^{+1} p(\delta, \mu, \mu') \mu d\mu.$$

For clouds g is typically between 0.7 and 0.9. The asymmetry parameter may be used to approximate the phase function when the exact shape of the phase function is not important as in the calculation of heating rates which result from flux divergences, basically a hemispheric integral of the radiance field. The Henyey Greenstein phase function is approximated in this way and is given by

$$P(\delta, \mu, \mu') = \frac{1 - g^2}{1 + g^2 - 2g\mu\mu'}.$$

There remains the problem of solving the equation of transfer in a scattering medium. Several methods have been discussed in the literature which solve the equation with varying degrees of approximation. Most of these methods are not acceptable for use in a GCM or a fog model because of the amount of computer resources required to compute the solutions. A commonly used method which offers rapid solution to the scattering problem is the "two stream" method, so called because it solves for single streams in the upward and downward directions. This level of approximation is quite common in fog models and has been studied extensively in the literature; see for example, Stephens (1984), Zdunkowski *et al.* (1980) and Harshvardhan and King (1993). The numerical recipe for the Practical Improved Flux Method, which is a delta-two stream method may be found in the appendix section A.3.2. In general if the spectral flux density $S(\delta)$ is obtained from the radiant intensity $I(\delta, \pm\mu)$ according to

$$S^{\pm}(\delta) = \int_0^1 \mu I(\delta, \pm\mu) d\mu,$$

then the equation of transfer may be written as

$$\left. \begin{aligned} \frac{dS^+}{d\delta} &= \gamma_1 S^+ - \gamma_2 S^- + \frac{S_0}{4} \omega_0 \gamma_3 e^{-\delta/\mu_0} \\ \frac{dS^-}{d\delta} &= \gamma_2 S^+ - \gamma_1 S^- + \frac{S_0}{4} \omega_0 \gamma_4 e^{-\delta/\mu_0} \end{aligned} \right\},$$

where some functional approximation of I on μ has been assumed that allows the flux density to be obtained from the radiance analytically. When the intensity is approximated in this way the coefficients γ_1 , γ_2 and γ_3 are expressed as a function of κ_0 , δ and g . The "gamma" coefficients may be defined in various ways in terms of the scattering albedo, the optical depth and the asymmetry parameter; see the Appendix sections A.3.2 and A.3.3. Apparently none of the two stream methods are accurate over all ranges of the optical thickness and single particle scattering albedo. Zdunkowski *et al.* (1980) indicate the PIFM has the best overall performance while Harshvardhan and King (1993) recommend a delta Eddington approach. The delta phase function approach more accurately approximates the effects of the highly forward scattering phase functions typical of fogs and water clouds. In it the phase function is approximated using a delta function so that

$$p(\delta, \mu, \mu') = 2f\delta_{\mu, \mu'} + (1-f)(1+3g'\mu\mu'),$$

where $f = g^2$ is the fraction of radiation scattered into the forward peak and $\delta_{\mu, \mu'}$ is the Dirac delta function. When this approximation is made the solution follows the same method of solution as the original Eddington approximation with scaled values of δ , κ_0 and g ; see Shettle and Weinman (1970). The scaling relations are

$$\left. \begin{aligned} \delta' &= (1 - \omega_0 f) \delta \\ \omega'_0 &= (1 - f) \omega_0 / (1 - \omega_0 f) \\ g' &= (g - f) / (1 - f) \end{aligned} \right\}.$$

Stephens (1984) lists eight choices for the gamma coefficients for various solutions and Zdunkowski *et al.* (1980) consider additional possibilities.

One of the major considerations in solving a two stream or any other method for multiple scattering is the degree of spectral resolution that can be maintained in the model. In general the two stream solution must be exercised for each spectral band used in the approximation. Some of the methods for modeling fogs use four or five spectral divisions in the solar region; and further subdivide each of these into six or seven intervals using various methods; see the discussion of Zdunkowski *et al.* (1980) in the Appendix section A.3.3. Others attempt to use a mono-spectral approach as Fouquart and Bonnel (1980), which is used in the fog model of Musson-Genon, (1987); see Appendix section A.3.12. This topic will be discussed further in the next section. Also, there is the added complication that the spectral regions where water vapor and water droplets overlap. Thus it is not correct to treat the scattering fog or cloud layer separately from the atmosphere in which it is immersed, since the absorption by the droplets will be altered by the amount of water vapor absorption which has occurred above the layer. It is common to employ a formulation based on the k distribution mentioned above in which the transmission is expressed as

$$\tau_{\Delta\lambda}(u^*) = \int_{\Delta\lambda} f(k) e^{-ku^*} dk = \sum_{n=1}^N f(k_n) e^{-k_n u^*}$$

where $f(k)$ is the distribution of k absorption coefficient values and u^* the optical mass. Then in the two stream solution for scattering by droplets the optical depth δ is replaced by an augmented optical depth $\delta_n = \delta + k_n u^*$, and the single particle scattering albedo ω_0 by $\omega_n = \omega_0 \delta / \delta_n$, and the two stream method is solved for each value of n for a solar flux S_n and the value of solar flux for the spectral interval $\Delta\lambda$ is given by

$$S_{\Delta\lambda} = \sum_{n=1}^N f(k_n) S_n(k_n).$$

Examples of this approach can be found in the Zdunkowski models discussed later. Another approach is to use photon path length distributions $N(l)$ calculated *a priori* using a Monte Carlo algorithm for a desired cloud type. The transmission $\tau_{\Delta\lambda}$ over a spectral band of width $\Delta\lambda$ is then given by

$$\tau_{\Delta\lambda} = \int N(l) \tau(lu^*, p^*) dl \approx \sum_l N(l) \tau(lu^*, p^*),$$

where $\tau(lu^*, p^*)$ is the band model transmission along a path with scaled quantities u^* and p^* . This approach is used in the Luc Musson model that uses the parameterizations of Fouquart and Bonnel (1980) and is discussed later on.

In either case it is important to approximate the single scattering properties of the droplets as accurately as possible. This is a much easier task in fog models which have a prognostic equation for the droplet distribution such as the model whose equations are listed above in section 2.2. In this case the single particle scattering albedo could be computed from Mie theory for a range of microphysical distributions and a table look up accessed from within the dynamic model. This allows an approximation to a time dependent value of the absorption coefficient, extinction coefficient (thus determining the single particle scattering albedo) and the asymmetry parameter. If the microphysical distribution is not diagnosed in the model other parameterizations must be employed. An approximation for the optical depth that is commonly used in fog and cloud models is more or less derived from the basic principles. It begins with the expression for optical depth due to water droplets:

$$\delta = \int_0^{\Delta\lambda} \int_0^\infty n(r) \pi r^2 Q_{\text{ext}}\left(\frac{2\pi r}{\lambda}, m_\lambda\right) dr d\lambda,$$

where $n(r)$ is the droplet size distribution, Q_{ext} is the efficiency for extinction from Mie theory for spherical drops of radius r and radiation of wavelength λ and index of refraction m_λ . By using the fact that Q_{ext} asymptotically approaches a value of 2.0 for droplets large compared to the wavelength of the light, and the definition of the equivalent radius,

$$r_e = \frac{\int_0^\infty n(r) r^3 dr}{\int_0^\infty n(r) r^2 dr},$$

Stephens (1978b) showed that the optical depth could be approximated in terms of the liquid water path W by $\delta = \frac{3}{2} W r_e^{-1}$. The liquid water path is often available in fog models from via a water budget equation.

The value of the single particle scattering albedo is important in determining the droplet absorption in the fog; see Vehil and Bonnel (1988). One parameterization by Liou (1980) is in terms of the complex part of the index of refraction k' and is given by,

$\omega_0 = 1 - 1.7 k' r_e$, where r_e is defined above. Vehil and Bonnel (1988) present newer parameterizations for both the asymmetry parameter and the single scattering parameter specifically for fog. Another approximation applies if the real part of the index of refraction n_r approaches unity. The anomalous diffraction theory gives an approximation of

$$1 - \omega_0 = \frac{1}{2} \left(\frac{4}{3} \rho \tan \Gamma - \rho^2 \tan^2 \Gamma \right),$$

where

$$\rho = \frac{4 \pi r}{\lambda} (n_r - 1),$$

and

$$\Gamma = \arctan \left(\frac{k'}{n_r - 1} \right).$$

This type of parameterization is of interest for application to situations in which the chemical composition of nucleation aerosols is considered important since their effect might be taken into account through variation of the index of refraction $m = n_r - ik'$. A more exact treatment of the effects of aerosol chemical solution may be found in the discussion of the Bott *et al* (1990) model in the Appendix; see section A.3.16.

3.3 Some remarks about the parameterizations

The sections above have summarized many of the parameterizations commonly used in numerical simulations of atmospheric processes in which radiation plays a role but is not the main focus of the modeling effort. It is safe to conclude that all of the models for studying the behavior of radiation fog utilize algorithms which are closely related to those described above, if not identical in form. The sections above provide a number of approaches to the problem of approximating radiative effects without specifying which is most accurate or most rapid. It is not possible in a study of this type to evaluate all approaches, but it is somewhat reassuring that those described have been accepted by various groups as reasonable approaches. It is quite likely that no single

parameterization is optimum for all types of cloud or fog modelling and one of the purposes of this study is to characterize the strengths and weaknesses of approaches actually used in published accounts of radiation fog models. The next section summarizes the types of approximations that have been used in fog models, the strengths and weaknesses of each, and, in particular, which approximations are best suited for application to multi-component fog models. However, the specific question of what approach is optimum must be addressed by dedicated numerical studies and verified by measurements of the scenarios of interest. No attempt is being made here to specify the single best approach.

4.0 The evaluation of parameterizations used in radiation fog models

The previous sections have established the nature of the problem and the types of parameterizations usually applied for the purposes of calculating cooling and heating rates in dynamic models such as GCMs, cloud or fog models. The Appendix provides a rather detailed summary of the treatment of radiation for each fog model which was reviewed. As mentioned above the techniques in the fog models are closely related to those already described. Nevertheless, there are some variations and extensions of these methods to be noted. Also, there are specific questions which need to be addressed regarding the use of the approximations. The following sections address these issues in the form of an evaluation of the methods and serve as a link to the specific formulations found in models described in the Appendix. Understanding of the scope of the methods in each model will be enhanced by reading the entry for the model in the paragraphs below and the corresponding entry in the Appendix. Finally, this section concludes with single page summaries of the treatment of radiation in several of the more complete efforts.

4.1 Listing of models reviewed

The models included in this study are those found in the open literature from 1975-1992. The list of all entries relating to radiation fog numbers several dozen or so, but only a subset of these describe modeling efforts (as opposed to observational studies for example) and of those only a subset provide detail on the treatment of radiation. Some papers, which do not describe dynamic models, but rather add clarification and detail to the discussion of the fog models are also included. The final set actually reviewed is comprised of the entries in the Appendix and are merely listed here. The set includes the following:

Lilly (1968);
Schubert (1977), Schubert (1976), Steiner and Schubert (1977), Schubert *et al.* I and II (1979);
Oliver, Lewellen and Williamson (1977);
Welch *et al.* (1986);
Zdunkowski *et al.* (1980);
Zdunkowski *et al.* (1982);
Brown and Roach (1976);
Brown (1980);
Buykov and Khvorost'yanov (1977);

Ohta and Tanaka (1986);
Bykova (1986);
Turton and Brown (1987);
Guzzi (1980);
Musson-Genon(1987);
Forkel *et al.* (1984), (1987);
Bougeault (1981);
Bott *et al.* (1990);
Bott (1991);
Duynderke (1991);
Vehil and Bonnel (1988);
Vehil *et al.* (1989);
Qian and Lie (1990);
Clark (1979);
Pandis and Seinfeld (1989).

4.2 Completeness of the parameterizations

Radiation enters into the equations of the dynamic fog model according to the model equations in section 2.2. One way to evaluate the treatment of radiant energy is merely by the number of interactions which are included. In this section the completeness of the various models concerning the treatment of radiation is discussed. The models span a wide range of detail as depicted in the following chart. The models' treatment of radiation increases in complexity from top to bottom in the table. The table does not include all of the features of the models that have been reviewed. Rather, the aspects of the models are necessarily limited to a fairly brief description. Additional details from each may be found in the Appendix. Nevertheless, the table does show the progression of completeness found in the various efforts.

<p>Net radiation is treated as a constant with no interaction with model dynamics. Example: Schubert (1976) section A.2.1</p>
<p>Infrared radiation only is included based on absorption models. Examples: Brown and Roach (1976), Brown (1980) and Buykov and Khvorost'yanov (1977), sections A.3.4, A.3.5 and A.3.6</p>
<p>Solar and infrared radiation is included but only using transmission functions, i.e. no scattering. Examples: Oliver <i>et al.</i> (1976), Bykova (1986) sections A.2.2 and A.3.9</p>
<p>Scattering is included in the solar region using a delta two stream method but not in the infrared which is treated using a flux emissivity method. Example: Musson Genon (1987), section A.3.12</p>
<p>Scattering is included in the solar and in the atmospheric window region using a delta two stream method. In other portions of the infrared a flux emissivity method is used with a grey body term included. Droplet settling is included as well as boundary layer aerosols complete with effects of humidity on aerosol size. A surface moisture model is included. Spectral features of the radiation exchange are more fully resolved. Example: Zdunkowski <i>et al.</i> section A.3.3</p>
<p>Scattering is included in the solar and in the atmospheric window region using a delta two stream method. In other portions of the infrared a flux emissivity method is used with a grey body term included. Droplet settling is included as well as boundary layer aerosols complete with effects of humidity on aerosol size. A joint aerosol-droplet growth equation is included with the effects of the solute on the value of the index of refraction. A surface moisture model is included. Spectral features of the radiation exchange are more fully resolved. Example: Bott <i>et al.</i> (1990), Bott (1991), sections A.3.16 and A.3.17</p>

Table 1. Table indicating the degree of completeness offered by selected models

In addition to the models listed in the table, there were some entries which are discussed in the Appendix that are in fact more detailed in their treatment of a particular process but have not been included above because they are not truly fog models. An example of this is the entry by Guzzi *et al.* (1980), section A.3.11, which details the effect of the radiative environment on the droplet growth but does not consider many of the other processes required to fully simulate the fog life cycle.

In evaluating the model's treatment of radiation the following aspects will be examined: a) Does the model account for the effects of solar radiation? Although a fog model can simulate the onset of a radiation fog without including solar radiation there will be a loss of generality since doing so eliminates the effects of solar absorption in the boundary layer for the afternoon period preceding the onset of the fog. Also, the dissipation of the fog cannot be modeled since absorption of solar radiation is the primary mechanism responsible for dissipation. b) Does the model include multiple scattering? The calculation of heating rates will only be approximate if multiple scattering is neglected. c) To what degree is the fog considered as a homogeneous layer in the vertical and horizontal? The assumption of horizontal homogeneity will also affect the flux divergence. d) Are the effects of aerosols included. Aerosols affect especially solar absorption but also alter the fog's microphysics especially in a polluted boundary layer or if the model is to be applied to multi-component fogs such as those which might be encountered in a battlefield environment. e) What detail is included concerning the aspects of single scattering *i.e.*, do the fog particles consist of water only or is allowance made for solution effects when calculating the absorption coefficients. Also, the ability to treat non-spherical particles would be a plus for modeling of multi-component fogs as in a battlefield environment. f) The degree of spectral resolution, or equivalently the effort to find accurate limited resolution schemes is relevant. g) Although the dynamic aspects of the model are not under scrutiny here, any unique aspects of the coupling of the radiative heating with the dynamic equations will be noted.

4.3 Aspects and limitations of radiative treatment common to all models

In order to avoid repetition it is worthwhile to list properties which are common to all the models. First, it can be said that all models treat the fog or cloud particles as spheres thus implying that the results of Mie theory are assumed. This limitation may not be explicit because some models do not calculate Mie parameters; however, the parameterizations used invoke artifacts of Mie theory which assumes spherical droplets. The extent of the shortcomings of this treatment is not clear since no studies were found which detailed the effects of non-spherical particles in cloud or fog models except for application more appropriate to ice particles in cirrus clouds. Also, at the level of sophistication of currently accepted parameterizations (see sections 3.1 and 3.2), it is certainly not clear how the single scattering properties of irregularly shaped particles might be introduced into a dynamically evolving fog layer.

Second, regarding homogeneity, all of the models treat the scattering or emitting process using plane parallel techniques. Some clarification on this point is in order. There are non-homogeneous effects which are caused by variation of liquid water content in the vertical (since many of the radiative properties are parameterized in terms of the liquid water content). However, even though such non-homogeneities will affect the value of absorption or emission for a layer or even for a given grid volume for a 2-dimensional model, the effects of finite geometry on the scattering or emission process itself are not included. Instead a plane parallel radiative approximation is applied in each layer or each grid box as if the values affecting the scattering or emission in the layer or grid volume extended infinitely far in the horizontal direction. According to Welch *et al.* (1980), the width to height ratio of a cloud, 0.46 km thick, must approach a value of 240 before the energy escaping the sides is insignificant compared to

the absorption.

Third, almost all of the models include thermal emission since it is the radiative process responsible for the formation of the fog. Clark (1979) and Bougeault (1981) are the exceptions. Clark (1979) describes a dynamic cloud model for vigorously developing systems as in thunderstorms in which the role of radiation is considered to be secondary. Bougeault (1981) describes a higher order closure model and ignores the effects of radiation.

Fourth, all the models introduce the effects of radiative heating/cooling in the thermodynamic energy budget equation in more or less the same way; see section 2.2. The only discussion of a possible exception to this convention is in the second order closure model of Oliver *et al.* (1976) in which second order correlations between the radiative flux and optical mass, virtual temperature or mixing ratio are mentioned but disregarded because the coefficients needed to include such correlations are completely unknown.

The following sections will discuss the remaining aspects of radiation modeling pertinent to the fog model as they are handled in the various efforts.

4.4 Inclusion of the effects of solar radiation

Solar radiative effects are included in a few of the models reviewed but with varying degrees of sophistication. The Schubert papers (1976 and section A.2.1) all use a diurnally varying monospectral solar absorption value. While this allows some influence of solar radiation to be examined it does not permit the investigation of an accurate assessment of solar absorption due to droplets and aerosols. Modeling of the effects of aerosols in solution and the effect of solar radiation on droplet growth are thus excluded. Thus, this approach is not desirable for treating the effects of multi-component fogs. The only advantage of entering the solar absorption in this way is the economy of the computing resources which would otherwise need to be allocated to the calculation. The model concentrates on the boundary layer and the net solar radiation is input as an energy source for the layer. No consideration is given to cloud free conditions within the boundary layer.

In Oliver *et al.* (1976 and A.2.2) and Bykova (1986 and A.3.9), solar radiation is considered without the effects of scattering by using a transmission function. The transmission function uses a constant for the absorption coefficient, which has been averaged over the solar spectrum. As a result, the absorption of the direct beam has no interaction with changing cloud microphysics except for coupling to the liquid water content in the usual exponential expression for transmission. The transmission function takes into account the absorption by water vapor, CO₂ and the water droplets which constitute the cloud or fog. No detail of the averaging procedure regarding spectral resolution or overlap is given. The method is not adaptable to treatment of multi-component fogs unless new transmission functions are derived for that situation. The reader is referred to the Appendix for listing of the boundary conditions.

A unique approach to the role of multiple scattering is presented by Ohta and Tanaka (1986 and

A.3.7), who describe a P_3 method that actually solves for the radiance or intensity rather than the irradiance. In some sense this order of calculation is more sophisticated than the two stream methods used in almost every other instance for calculating the effects of multiple scattering. There is no advantage to adding this level of definition of the radiative stream since it is only the heating rate which ultimately enters the dynamic system and this is determined solely by the vertical flux divergence. However, if the effects of non-spherical particles were desired, it may be advantageous to use a treatment of multiple scattering with greater angular resolution than the more common two-stream approaches since it is likely that the angular variation of the intensity would become important. The effects of Rayleigh scattering and scattering by cloud droplets are included. Absorption by ozone and water vapor is modeled, but no detail of the exact transmission functions is given. Spectral resolution is at the band model level; *i.e.* for water vapor band absorption models centered at 0.94, 1.10, 1.38, 1.87, 2.70 and 3.40 μm were used. A separate band model was used for ozone. This method improves upon those above for the treatment of solar radiation and is probably adequate as long as multi component fogs are not modelled (here again unless an entire new approach is used for the transmission functions). Horizontal homogeneity is assumed. Boundary conditions are given in the Appendix.

The numerical model of Musson-Genon (1987 and A.3.12) uses a parameterization for solar radiation designed for use in a GCM. The parameterization has been named the "SUNRAY" algorithm and is the subject of a separate paper by Fouquart and Bonnel (1980). The parameterization has been tailored so that especially the total column heating or cooling rates would compare favorably with other parameterizations. The effects of Rayleigh scattering are included by modifying the reflection coefficients of the layers above and below the layer of interest. Horizontal non-homogeneity is approximated by maintaining the fraction of unscattered radiation entering a given layer from above and treating the other fraction as an isotropic field below the cloud through which it scattered, although this feature is not carried over into the fog model application. Spectral resolution is achieved using methods based on the k distribution approach discussed in section 3.2 and similar to the EAM (Exponential Absorption Method) and the EFM (Exponential Fit Method) as discussed in Zdunkowski *et al.* (1982 and Section A.3.3), and apparently a monospectral approach was developed. Scattering by droplets is considered by specifying values of reflectance and transmittance for high, middle and low clouds, although the effect of the cloud's multiple scattering on column absorption is accounted for by using predetermined photon path distribution statistics. This parameterization appears to be well conceived and fairly comprehensive for use in a GCM. It does not necessarily follow that it is an appropriate treatment of solar radiation in fog models. For example, it is not until a paper by Vehil and Bonnel (1988 and section A.3.19) that the scattering properties are adjusted for fog microphysics. The approximation for horizontal inhomogeneity is on a spatial scale that is likely inappropriate for use in fog models even if it had been used. Transmission and reflection of clouds are fixed (at least in the model description cited) and thus no allowance is made for changing microphysics and therefore limiting application to water clouds only until new transmission and reflectance values are introduced. Finally, there is no interaction between the droplet growth and the radiative environment.

The most sophisticated treatment of solar radiation in the fog models reviewed here is that which

has evolved in a series of papers by Zdunkowski's group including; Bott *et al.* (1990 and section A.3.16), Bott (1991 and section A.3.17), Forkel *et al.* (1984 and section A.3.13, 1987 and section A.3.14), Welch *et al.* (1976, 1986 and section A.3.8), Zdunkowski and Nielson (1969), Zdunkowski *et al.* (1966, 1979, 1980 and section A.3.2, 1982 and section A.3.3). The history of the model's development is not important so only the most recent version will be discussed. The model uses a delta-two stream method called the PIFM (Practical Improved Flux Method) to account for the effects of multiple scattering. According to Zdunkowski *et al.* (1980 and section A.3.2) the PIFM is the most physically relevant of many of the two stream methods; however, Harshvardhan and King (1993) indicate the delta-Eddington to be most generally acceptable. Particles are assumed spherical through the expression of critical scattering parameters in terms of the Legendre expansion coefficients from Mie theory, although if the same parameters are available from other calculations or measurements one could argue that this limitation could be removed. The same condition would apply to all similar two stream models. Spectral resolution has been thoroughly treated. The solar spectrum is divided into four regions and each of these broken down into several sub regions (from 5 to 7) using the EFM and EAM discussed in sections 3.2 and A.3.3. The spectrum was resolved separately for each attenuating material including scattering by dry air, aerosols and water drops, and absorption by water vapor, ozone, NO₂, and CO₂. Spectral overlap was accounted for. In the later versions of the model, Bott (1991), specific aerosol distributions were specified as part of the initial conditions for model simulation. The radiative effects on droplet growth as they affect the joint aerosol-droplet distribution were included. The solute effects on the index of refraction were also accounted for, although treatment of the joint distribution as a function of wavelength required a table look up from the results of 1.2×10^6 Mie calculations. This type of treatment could in theory be applied to multi-component fogs; however, as is evident from the number of Mie calculations required, if more than two components are included the approach could require a tremendous investment in computer resources even though these calculations may be carried out *a priori*. As in all other models reviewed horizontal homogeneity was assumed even though the model was originally compiled for a GCM in which cloudy and clear columns were separately maintained.

4.5 Treatment of radiation in the infrared

The simplest treatment of the infrared radiation exchange is included in the Schubert (1976 and section A.2.1) stratocumulus model for which the net flux divergence is specified as a constant of 90.0 watts m⁻² and is applied at an infinitesimally thin layer at the top of the cloud layer. Arguments similar to those made concerning the treatment of solar radiation apply in the IR as well. The value was based on measurements typical of top of the marine stratocumulus boundary layer. The constant value allowed dedication of the limited computer resources of the mid 1970s to be concentrated on the dynamics of the simulation.

A flux transmission method is applied in Oliver *et al.* (1977 and A.2.1). The value of the absorption coefficient is taken from Feigelson (1970) and is an average over wavelength and applied for a mean drop size of 6.0 μm. Scattering is ignored. Consistent with the treatment of solar radiation there is no interaction between the droplet growth rate and the radiative

environment. The spectral resolution is limited to the single averaged value for the absorption coefficient, which takes into account the effects of water droplets, water vapor and carbon dioxide. Cloudy/foggy conditions are simulated by merely adding the droplet absorption coefficient to the value for the clear sky conditions. This method is simple to apply but is not applicable to multi-component fogs unless new absorption coefficients are derived. Values of the fluxes imposed at the boundaries may be found in the Appendix.

The flux transmission method is also applied in Brown and Roach (1976 and section A.3.4), and in Brown (1980 and section A.3.5) except that the parameterization of the absorption efficiency factor in terms of the particle radius is cited (as in section 3.1) in order to obtain the absorption coefficients. A separate value of the coefficient for the regions inside and outside the atmospheric window define the spectral resolution and include the effects of water vapor, carbon dioxide and droplets. There is no treatment of scattering in the infrared. The parameterization of the absorption coefficient becomes more important in the later paper by Brown with the introduction of a droplet growth equation which is a function of the radiative environment of the droplets. This coupling is a significant formal advance in the numerical model; however, the model only follows the growth of the number of droplets in each of several droplet size bins. The method introduces some complications because it does not conserve the liquid water content adequately. This inclusion of a droplet growth equation in conjunction with the parameterization of the absorption coefficient is a first step toward the ability to handle multi-component fogs but it is unclear if a proper parameterization for the absorption coefficient could be formulated for such a medium.

In Buykov and Khvorost'yanov (1977 and section A.3.6) the infrared radiation transfer is handled in much the same manner as in Brown (1980) except that it uses alternate expressions for the droplet growth equation and a different form of the parameterization of the absorption coefficient. Spectral resolution is moderate with radiative heating calculated at 32 wavelengths between 5 and 32 μm . At this level of review it is not possible to determine the differences in the effects caused by the two approaches. For similar reasons as stated above the approach does not lend itself to application in a multi-component fog scenario.

The same level of approximation is found in the Musson-Genon (1987 and section A.3.12) model. A flux emissivity approach is used where the emissivity for water vapor rotation and vibration regions, for carbon dioxide and for the water dimer are taken from separate band models and the transmissivity due to droplets is computed from a flux transmission function using a constant absorption coefficient which implies a monospectral treatment for transmission due to droplets.

A P_j method which is similar to the one used in the solar is also used for the IR transfer in Ohta and Tanaka (1986 and section A.3.7), with the Planck function in the source term. As mentioned above, the method solves for an approximate intensity rather than a flux value. Except for the possible benefit when used with non-spherical particles, this level of angular resolution is also questioned in the application in the infrared where again flux divergences only are required. The method requires that the Planck function be expressed as a function of optical

thickness only and this is accomplished using a third order polynomial; however, it is not clear how temperature variations are retained in this formulation. Either the entire fog layer is assumed to be isothermal in this approach or several isothermal layers must be modeled using a separate solution in each layer. The IR spectrum was resolved into three regions, from 4.2-8.0 μm for the water vapor vibration band, from 8.0-12.0 μm for which a dimer model is used and from 12.0-65.0 μm which includes the 15.0 μm carbon dioxide and water vapor rotation bands.

The only modeling approach which considers scattering in the IR is the group of models put forth by Zdunkowski's group. The latest of these efforts retains most of the features of the 1982 radiation model that is rather thoroughly described in section A.3.3. This model uses the same PIFM delta-two stream approach as was used in the solar region to include the effects of scattering in the IR window region. The absorption from ozone, water vapor, the water vapor dimer and droplets is also included using methods listed in the tables of section A.3.3. Spectral overlap is accounted for. In the spectral regions surrounding the window, where absorption plays a more significant role, a flux emissivity method is used. However, this method is somewhat advanced relative to that described in section 3.1 since it includes a separate grey body emission term for aerosols and clouds. In the early versions of the model, droplet distributions were selected as a function of the fog life cycle. Later, a droplet growth equation was incorporated and in the last upgrade in this area, a joint droplet-aerosol distribution was used in which the droplet's growth is affected both by the solution and radiative effects. The solute effects on the index of refraction of the droplet are also used to determine the absorption coefficient. This model is close to the point at which it could be adapted for use with a multi-component fog. In its latter form with joint aerosol-droplet distributions, an interpolation in a table computed from 1.2 million Mie computations spanning wavelength, and aerosol and droplet size ranges is used. From this figure it is clear that the approach would require a large ancillary effort if more than two components are used and if the size distribution of each is allowed to change.

4.6 Treatment of processes related to radiation exchange

The majority of this report has concentrated directly on the treatment of the radiative exchange itself. At this point it is worthwhile to note that various other processes affect the rates of radiative heating or cooling indirectly, but which are nevertheless rather strongly coupled to the radiative effects. One of these which has been mentioned several times above is the coupling of the rate of droplet growth with the radiative environment. One of the earlier accounts of this effect may be found in Roach (1976), and it is incorporated in the radiation fog model by Brown (1980 and section A.3.5). A different approach found in Buykov and Khvorost'yanov (1977 and section A.3.6) includes a term to account for the temperature difference between the droplet and its surroundings. This is an approximation to include the IR effects on the growth of the droplets. Guzzi (1980 and section A.3.11) studies this effect in detail with the conclusion that the larger droplets grow at the expense of the smaller drops when the radiative term is included. The most complete treatment of this effect is in Bott *et al.* (1990 and section A.3.16) wherein it is postulated that one of the contributing factors to short term oscillations in the droplet density is the enhanced growth of larger droplets and subsequent gravitational settling. The treatment indicates the need to integrate the radiance field over the surface of the droplet in order to obtain

the correct contribution to the radiative budget of the drop. This feature is important for the modeling of multi-component fogs from at least two standpoints. First, if a fog includes particles with a low scattering albedo, especially if droplets grow with some of these particles as nuclei, then the absorption of solar radiation by the modified droplets may dramatically alter its rate of growth. Second, if the foreign particles are non-spherical, then the angular variability of the incident radiance field must be taken into account to adequately evaluate the effects of the non-sphericity during initial stages of growth, again assuming the particle serves as host nuclei.

The next process which affects the radiative exchange, and which is related to the size of the drop, is the modeling of the droplet fall speed. The fall speed depends on the size of the droplet and is coupled into the equations through the prognostic equation for the size distribution as a loss term for a droplet of a given radius. The correct modeling of the fall speed is important then since it affects the size distribution of the droplets. Additionally, this process is important in order to evaluate the surface emissivity. As the droplets fall to the surface the emissivity changes and, depending on when this occurs in the fog life cycle, may significantly affect the IR budget of the lower layers of the fog.

Finally, it is important to consider the exchange of surface fluxes between the atmosphere and the ground. Although almost all models include a term for the exchange of radiant energy with the surface, only a few consider sensible heat, vapor and liquid water fluxes. In the initial stages of the fog life cycle the radiative exchange of the surface layer with the surface may play a crucial role in the initial fog formation. This exchange will depend on the surface emissivity, as the fog develops fluxes of sensible and latent heat and water fluxes. Little has been included in this report concerning this aspect of the fog model. More information may be found in Forkel *et al.* (1984).

4.7 Summary of major modeling efforts

The next several pages are one page summaries of the radiation models which typify those of the fog/cloud modeling efforts.

Cloud Topped Mixed Layer by Schubert (1976) and Lilly (1968)

SOLAR

Scattering	Scattering is not explicitly calculated; a precalculated fixed value for flux divergence at cloud top is used.
Absorption	Absorption is calculated a priori.

INFRARED

Scattering	Single a priori calculation of flux divergence, no separate modeling of these processes within model.
Absorption	Same as above.
Emission	Same as above.

GENERAL

Geometry	Plane parallel approximation - horizontal homogeneity
Homogeneity	Net flux divergence introduced in an infinitesimal layer at the top of the mixed layer
Spectral Resolution	No explicit spectral resolution ... net radiation entered as a single constant
Numerical Methods	Single value of flux divergence is introduced with into thermodynamic energy equation.
Coupling with dynamics	No coupling to dynamics.

The Interaction Between Turbulence and Radiative Transport in the Development of Fog and Low Level Stratus by Oliver, Lewellen and Williamson 1976

SOLAR

Scattering	Not included
Absorption	Water vapor, carbon dioxide and droplets

INFRARED

Scattering	Not included
Absorption	Water vapor, carbon dioxide and droplets
Emission	Water vapor, carbon dioxide and droplets

GENERAL

Geometry	Plane parallel approximation in both the solar and infrared
Homogeneity	Non homogeneity is introduced by variations in the water vapor mixing ratio and liquid water content which determine the value of the absorption coefficients.
Phase Function Constraints	Phase functions are not calculated in this two stream model.
Spectral Resolution	Radiation stream divided into a single broadbanded solar and single broadbanded infrared spectral interval.
Numerical Methods	Transmission functions are derived from the work of Feigel'son (1970). Droplet distributions are not calculated.
Coupling with dynamics	Coupling is indirect via changes in water vapor and liquid water, although the possibility of including the perturbation in radiative energy in the second order decay terms is discussed.

Radiation Fog by Welch, Zdunkowski and Cox

SOLAR

Scattering	Droplets and aerosols
Absorption	Water vapor, carbon dioxide, ozone, droplets and aerosols

INFRARED

Scattering	Droplets and aerosols (window region only)
Emission	Water vapor, ozone, carbon dioxide, droplets and aerosols (aerosols in window region only)
Absorption	Water vapor, ozone, carbon dioxide, droplets and aerosols (aerosols in window region only)

GENERAL

Geometry	Plane parallel approximation is used in both the solar and infrared.
Homogeneity	Non homogeneity is apparently introduced by the variability of liquid water content and water vapor mixing ratio and their effects on transmission and on and volume extinction coefficients.
Phase Function	Phase functions are not explicitly calculated. Instead, a delta method is used which determines the significant scattering parameters in terms of the fractional backscattering coefficients for diffuse and primary scattered parallel light, the fraction of primary light scattered into the forward peak and diffusivity factors.
Spectral Resolution	The solar spectrum is divided into four main intervals. In each of these the water vapor transmission function is expanded in a series of five or six exponential terms which are each assigned individual volume extinction and absorption coefficients for droplets and aerosols. The window region is treated in much the same manner as the solar in which a four term EFM method is used for ozone and a water dimer calculation is included. Droplets and aerosols are assumed to be grey in the window region.
Numerical Methods	Droplet size distributions are not calculated in model. Volume extinction and absorption coefficients are calculated a priori by assuming a modified gamma distribution for droplets which are characteristic of various stages of the fog life cycle and are fit as a function of liquid water content and wavelength.
Coupling with dynamics	Net radiation enters the thermodynamic energy equation. Coupling is indirect via changes in water vapor and liquid water, although the fog layer is coupled to the surface via the surface radiation budget.

The Physics of Radiation Fog by Brown and Roach (1976)

SOLAR

The effects of solar radiation are not included in the model.

INFRARED

Scattering	Scattering is not included in the model.
Emission	Water vapor, carbon dioxide and droplets (no aerosols)
Absorption	Water vapor, carbon dioxide and droplets (no aerosols)

GENERAL

Geometry	Plane parallel approximation is used.
Homogeneity	Non homogeneity is apparently introduced in the vertical by the variability of liquid water content and water vapor mixing ratios and their effects on transmission and absorption efficiencies.
Phase Function	Phase functions are not calculated since scattering is not included.
Spectral Resolution	The infrared spectrum is divided into two broad intervals, one for the atmospheric window and the other for the remainder of the spectrum.
Numerical Methods	Droplet size distributions are not calculated in model. Volume absorption coefficients are approximated using a linear relationship between absorption efficiency and droplet radius, resulting in functional relationship between droplet transmission and liquid water content.
Coupling with dynamics	Net radiation enters the thermodynamic energy equation. Coupling is indirect via changes in water vapor and liquid water in the vertical only. Surface emission is included.

A numerical study of radiation fog with explicit formulation of the microphysics by Brown (1980)

SOLAR

The effects of solar radiation are not included in the model.

INFRARED

Scattering	Scattering is not included in the model.
Emission	Water vapor, carbon dioxide and droplets (no aerosols)
Absorption	Water vapor, carbon dioxide and droplets (no aerosols)

GENERAL

Geometry	Plane parallel approximation is used.
Homogeneity	Non homogeneity is apparently introduced in the vertical by the variability of liquid water content and water vapor mixing ratios and their effects on transmission and absorption efficiencies.
Phase Function	Phase functions are not calculated since scattering is not included.
Spectral Resolution	The infrared spectrum is divided into two broad intervals, one for the atmospheric window and the other for the remainder of the spectrum.
Numerical Methods	Droplet size distributions are approximated in model as a function of height. Volume absorption coefficients are calculated by integrating the absorption efficiency over the size distribution and applying a diffusivity factor to estimate the correction for nonparallel radiation streams.
Coupling with Dynamics	Net radiation enters the thermodynamic energy equation. Coupling is direct via changes in droplet distributions. Coupling of radiation with droplet growth included in droplet growth equation. Surface emission is included. Visual range may be calculated since droplet distribution is known.

Formation and evolution of radiation fog and stratus clouds in the atmospheric boundary layer by
M.V. Buykov and V. L. Khvorost'yanov (1977)

SOLAR

The effects of solar radiation are not included in the model.

INFRARED

Scattering Scattering is not included in the model.

Emission Water vapor and droplets (no aerosols)

Absorption Water vapor and droplets (no aerosols)

GENERAL

Geometry Plane parallel approximation is used.

Homogeneity Non homogeneity is apparently introduced in the vertical by the variability of liquid water content and water vapor mixing ratios and their effects on transmission and absorption efficiencies.

Phase
Function Phase functions are not calculated since scattering is not included.

Spectral
Resolution The infrared spectrum (5-35 μm) is divided 32 wavelength regions.

Numerical
Methods Droplet size distributions are approximated in model as a function of height. Volume absorption coefficients are calculated by integrating the absorption efficiency over the size distribution and applying a diffusivity factor to estimate the correction for nonparallel radiation streams. Droplet absorption coefficients are calculated using exact Mie calculations and Shifrin's interpolation formula. Wavelengths are chosen in such a way as to approximate the spectral trend in the vapor absorption coefficients.

Coupling
with
Dynamics Net radiation enters the thermodynamic energy equation. Coupling is direct via changes in droplet distributions. Coupling of radiation with droplet growth not explicitly included in droplet growth equation, but a factor which accounts for the difference in droplet and air temperatures is included. Surface emission is included. Visual range may be calculated since droplet distribution is known.

SOLAR

Scattering	Air molecules in the visible, water droplets and surface reflection. Matrix adding method is used. No scattering in the near infrared by gases
Absorption	Water vapor and ozone.

INFRARED

Scattering	Scattering is not included in the IR
Emission	Water vapor, carbon dioxide and droplets (no aerosols)
Absorption	Water vapor, carbon dioxide and droplets (no aerosols)

GENERAL

Geometry	Plane parallel approximation is used.
Homogeneity	Non homogeneity is apparently introduced in the vertical by the variability of liquid water content and water vapor mixing ratios and their effects on transmission and absorption efficiencies and also possibly by vertical variation in the concentration of O ₃
Phase Function	Phase functions are calculated from Mie theory for droplets only using a modified gamma distribution.
Spectral Resolution	For absorption, a band in the visible is included for ozone which includes scattering. In the near infrared, band models at 0.73, 0.81, 0.94, 1.1, 1.38, 1.87, 2.7, and 3.4 μm are included without scattering. The infrared is divided into three spectral regions; 4.2-8.0, 8.0-12.0 and 12.0-62.5 μm regions. The first region includes only the effects of the 6.3 μm water vapor band. In the window a dimer continuum model is used. The 12.0-62.5 μm region includes the 15.0 μm CO ₂ band and the pure rotation band due to water vapor.
Numerical Methods	Droplet size distributions are calculated a priori and are not adjusted in the model. Droplet extinction coefficients are calculated from Mie theory from this distribution. In the visible a matrix adding method is used to consider the effects of scattering due to air molecules. Otherwise a P ₃ method is used to include scattering by droplets and emission as a source function.
Coupling with dynamics	Net radiation enters the thermodynamic energy equation. No coupling through size distribution. A rather thorough treatment of the surface heat transfer is included.

Numerical simulation of a fog event with a one-dimensional boundary layer model by Luc
Musson-Genon (1987)

SOLAR

Scattering	Rayleigh scattering, cloud reflection and transmission calculated at a single conservative wavelength. Reflectivity is fixed (apparently) computed by modified exponential kernel method.
Absorption	Water vapor, ozone and carbon dioxide by approximating the absorber amount based on path derived from conservative scattering $c_{39} \cdot \tau^{\text{U}^{\text{R}}}$ $\tau^{\text{U}^{\text{R}}} \rightarrow \tau^{\text{R}}$
Scattering	No scattering in the infrared
Emission	Water vapor and dimer, carbon dioxide and droplets (no aerosols).
Absorption	Water vapor and dimer, carbon dioxide and droplets (no aerosols).

GENERAL

Geometry	Plane parallel approximation is used.
Homogeneity	Non homogeneity is apparently introduced in the vertical by the variability of liquid water content and water vapor mixing ratios and their effects on transmission and absorption efficiencies and also possible by vertical variation in the concentration of O_3 . Sub grid scale saturation relaxed in radiative treatment.
Phase Function	Phase functions are calculated from Mie theory for droplets only in solar using "delta" approximation.
Spectral Resolution	In IR band models are used. A single band is for the each of the following: the $6.3 \mu\text{m}$ water vapor band, the $15 \mu\text{m}$ CO_2 band, the water vapor dimer in the atmospheric window and an additional band for water vapor at $15 \mu\text{m}$. The transmission in the IR through water droplets is handled with a simple exponential using a fixed extinction coefficient. In the solar scattering is considered at a conservative wavelength after which absorption by gases are calculated using two term (strong plus weak) formulation.
Numerical Methods	A solar radiation heating scheme that was tailored for use in a GCM is used. Cloud reflectivities are calculated for conservative scattering after which photon path lengths are estimated and absorption due to strong and weak intervals for gases are calculated. A mean drop radius of $5.0 \mu\text{m}$ is used. Droplet distributions are not adjusted. Sub grid scale saturation algorithm is used in dynamics but not in radiative scheme. Visibility field is calculated.
Coupling with dynamics	Net radiation enters the thermodynamic energy equation. No coupling through size distribution. A large scale 3D model is used to calculate temperature and moisture fields before the 1D fog model is applied.

A Radiation Fog Model with a Detailed Treatment of the interaction between radiative transfer and fog microphysics, by Bott, Sievers and Zdunkowski (1990)

SOLAR

Scattering	Droplets and aerosols
Absorption	Water vapor, ozone, carbon dioxide, droplets and aerosols

INFRARED

Scattering	Droplets and aerosols (aerosols in window region only)
Emission	Water vapor, ozone, carbon dioxide, water dimer, droplets and aerosols (aerosols in window region only)
Absorption	Water vapor, ozone, carbon dioxide, water dimer, droplets and aerosols (aerosols in window region only)

GENERAL

Geometry	Plane parallel approximation is used in both the solar and infrared.
Homogeneity	Non homogeneity is apparently introduced by the variability of liquid water content and water vapor mixing ratio and their effects on transmission and on volume extinction coefficients.
Phase Function	Phase functions are not explicitly calculated. Instead, a delta method is used which determines the significant scattering parameters in terms of the fractional backscattering coefficient for diffuse and primary scattered parallel light, the fraction of primary light scattered into the forward peak and diffusivity factors.
Spectral Resolution	The solar spectrum is divided into four main intervals. In each of these the water vapor transmission function is expanded in a series of five or six exponential terms which are each assigned individual volume extinction and absorption coefficients for droplets and aerosols. The window region is treated much like the solar with a 4-term EFM method for ozone, a continuum model for water vapor and grey body emission for aerosols and droplets.
Numerical Methods	A joint aerosol-droplet growth equation is used which includes the effects of the radiative environment on the growth rates. Volume extinction and absorption coefficients are calculated a priori by assuming a modified gamma distribution for droplets and aerosols from 1.2 million Mie calculations. Table look up is performed in model to obtain extinction and scattering coefficients. Solute effects are included in calculation of index of refraction.
Coupling with dynamics	Net radiation enters the thermodynamic energy equation. Coupling is direct via effects of radiation on droplet growth.

5.0 Recommendations for naturally occurring and for multi-component fog modeling

The previous sections have summarized the types of radiative parameterizations used in GCMs and climate models and those used specifically in fog models. The Appendix presents a rather detailed summary of the radiative treatments found in fog models. Some of the fog models incorporate a fairly comprehensive treatment of the radiative exchange. In fact, if one is concerned with investigating naturally occurring fog events, the model described by Bott *et al.* (1990 and section A.3.16) is arguably a state of the art effort and would be a valuable tool for investigating the behavior of the fog life cycle. The model includes a carefully thought out resolution of the spectrum in both the solar and infrared, includes all the known absorption mechanisms including aerosols, accounts for the radiative effects on droplet growth, accounts for droplet settling, includes a sophisticated treatment for the exchange of surface fluxes, and accounts for the effects of multiple scattering in both the solar and infrared in the atmospheric window region. In fact, the parameterization seems relatively complete; however, there are at least two areas where improvements may be considered.

Recommendation: *For naturally occurring fogs, the Bott et al. (1990) model represents a valuable tool for investigation of the fog life cycle. Specifically, the two stream approach may be used for including the effects of multiple scattering. In fact, several variations of the delta two stream approach are easily programmed and the best method might be determined from comparison with measurements. Horizontal non-homogeneities may be important in studies of convective dissipation of fog layers.*

5.1 The role of horizontal non-homogeneity

The first is in the area of fog homogeneity. Research which dates back to the early 1970s indicates that radiative transfer in media with finite horizontal dimensions requires special treatment due to the ability of the radiative energy to exit or enter the sides of the media Busygin *et al.* (1973), McKee and Cox (1974), Davis *et al.* (1979). This aspect of radiative transfer has received a good deal of attention in the past twenty years without a truly suitable solution. The original investigations used Monte Carlo methods to explore the effects of the finite geometry and methods more analytic in nature have been used more recently to generate results; however, both the original Monte Carlo approaches and the newer analytical approaches are extremely CPU intensive. Thus, it is unlikely that either approach is suitable for use in a dynamic fog model which may only allocate a fraction of the total computational resources to the radiative computation. In a radiation fog scenario the finite geometrical effects apply more in the sense of non-homogeneities or "patchiness" rather than the isolated cloud structures which attracted so much attention early on. It is interesting to note that for this type of structure results from Monte Carlo modeling indicate only slight differences between plane parallel results and finite geometry calculations. For example, Welch *et al.* (1980) show results of Monte Carlo calculations which indicate virtually no difference occurs in values of solar radiation absorbed by clouds whose extinction coefficient fluctuates randomly throughout a horizontally infinite layer compared to the same calculation for a homogeneous layer using the average of the variable extinction coefficient. Due to the relatively more isotropic nature in the IR radiance field the

results for calculations in the infrared are likely to show even smaller differences. Thus, these results would seem to indicate that finite geometrical effects are not crucially important in considering the effects of multiple scattering if average values of variable optical parameters can be determined and used in a plane parallel radiative transfer model.

Recommendation: *Modeling the effects of horizontal non-homogeneity may not be crucial to understanding the fog life cycle. Efforts should be placed in understanding the magnitude of horizontal non-homogeneities in quantities affecting the radiation exchange (such as liquid water) so that average optical parameters could be derived for the fog layer and used in a plane parallel multiple scattering model.*

5.2 The need for modeling of the role of surface vegetation

The second area which has largely been neglected is the treatment of the effects of surface vegetation. The only study to mention the possible effects on the emissivity of surface vegetation was in Brown and Roach (1976 and section A.3.4), although Forkel *et al.* (1984 and section A.3.13) study the effects of a dry or moist surface layer. In the initial period of fog formation the amount of IR radiative exchange between the atmosphere and the ground is of critical importance. The value of the emissivity of the surface may impact this exchange process to a large extent depending on the temperature differences between the lower atmosphere and the surface. Thus, the extent to which the surface is covered by vegetation is important. The vegetation will also have a role in the exchange of the other fluxes as well (especially in the moisture flux) at the surface.

Recommendation: *The early development of the model's treatment of radiation should allow for the effects of a time variation in the surface emissivity and attention should be placed on the vertical resolution of the lower atmospheric layers so that proper radiative exchange with the surface can be modeled.*

5.3 The multi-component fog scenario

One of the goals of this review is to comment on the applicability of current models to multi-component fog scenarios. Although the Bott *et al.* (1990) effort comes the closest to providing the framework to include these effects, deficiencies still exist. Thus, some specific recommendations are in order regarding the multi-component fog scenario. First, it is necessary to specify the optical properties of the fog layer. In the more advanced treatments of radiation great care was taken to assess the requirements of spectral resolution. If foreign substances are introduced there is a need to reevaluate the way absorption is modeled. If new gases are involved it would be worthwhile to consider a modified k-distribution approach to specifying the absorption for the combined foreign and natural gases, even to the extent of modifying the temperature used in the calculation of line intensities. Temperatures more typical of the lower atmosphere might be considered and spectral overlap could be taken into consideration at this level.

Recommendation: *If multi-component fogs would include the introduction of foreign gases into the atmosphere spectral resolution should be modeled using an approach such as the k-distribution method to model the absorption including regions of spectral overlap with the naturally occurring gases.*

It is more likely that a multi-component fog scenario implies the presence of aerosols which have been artificially introduced to achieve a desired effect. Such aerosols will be referred to as foreign aerosols hereafter. In this case it is important to know if the aerosols are hygroscopic. If not, their introduction causes no unusual complication barring the effects of non-spherical particles; see below. In the case of particles which can be considered spherical, the treatment would take an analogous course as with the water droplets. If it is assumed that the size distribution of the foreign aerosol is constant then Mie calculations would be made *a priori* for the size distributions and at a spectral resolution compatible with the spectral resolution imposed by consideration of the gaseous components. The resulting extinction, absorption and scattering coefficients would be combined with those of the gases and naturally occurring aerosols to form composite optical depths. Composite single scattering albedos and other scattering parameters as may be required by the multiple scattering algorithm would be a weighted combination of the various constituents using the respective extinction, absorption and scattering coefficients as weighting coefficients.

If the microphysical distribution of the foreign aerosols changes as a function of time the individual Mie calculations of the extinction, absorption and scattering efficiency factors would be maintained as a function of size and wavelength. As the respective sizes of droplets and foreign aerosols change (independently assuming the foreign aerosol is non-hygroscopic), appropriate extinction, absorption and scattering efficiencies may be integrated over the size range of the respective distributions of foreign aerosols and droplets and independent extinction, absorption and scattering coefficients derived and used as weighting coefficients as described above in the implementation of the multiple scattering algorithm.

The case of hygroscopic foreign aerosols presents perhaps the most difficult challenge. If the foreign aerosols act as nucleation aerosols or merely form water coatings then the microphysical distributions may not be considered as independent. This case is similar to that described in Bott *et al.* (1990 and section A.3.16) in which the microphysics of nucleation aerosol and fog droplets are described by a joint distribution. In that study a droplet growth equation was used to generate a time dependency of the joint distribution. A similar approach could be taken if more than one aerosol type is involved although the size of the required tabulations might become prohibitively large. For example, in order to retain the necessary information to calculate volume extinction, absorption and scattering coefficients for a single type of nucleation aerosol, 1.2 million Mie calculations were performed and the results tabulated *a priori* in the Bott *et al.* study. Within the fog model the results of the tabulations were interpolated as a function of size and wavelength to obtain the extinction, absorption and scattering efficiencies of the joint distribution. Introducing a third component would expand this tabulation requirement by a factor equal to the number of size increments for the foreign aerosol. The number enters as a factor because of the requirement to combine separate values of indices of refraction, weighted by the

volume fraction of the drop which is comprised by each component, to form the effective index of refraction in the Mie calculations of extinction, absorption and scattering efficiencies. If the foreign aerosol is hygroscopic, an alternate approach might be to examine the anomalous diffraction approach for the parameterization of the single particle scattering albedo as mentioned at the end of section 3.2 above.

Recommendation: *Determine early in the development of the model the properties of the foreign aerosols and select an acceptable approach to the multi-component problem.*

Finally, it is possible that multi-component fogs will introduce the complication of non-spherical particles. It would seem that non-spherical particles introduce no additional complications other than that their single particle scattering features must be obtained by means other than computations based on Mie theory. If the non-spherical particles are not hygroscopic then separate determination of their scattering features may be pursued using an algorithm such as the discrete dipole method. Alternately, it may be possible to obtain field or laboratory measurements which supplant the need for calculations. If the particles are hygroscopic then Mie scattering calculations may again be used for the nucleated or coated droplet.

Recommendation: *Determine if non-spherical particles are part of the multi-component fog scenario. Determine the single scattering features of the aerosols using an approach such as the discrete dipole algorithm.*

6.0 Summary

This report has presented several types of parameterizations commonly used in cloud and fog models in order to calculate the effects of radiant energy exchange in both the infrared and solar portions of the spectrum. The types of parameterizations used in several models of radiation fog have been summarized in the main text and detailed in the Appendix along with a few summaries of supporting studies. In general, the treatment of radiant exchange includes spectral resolution at the level of band models, whether band models are used explicitly or whether the radiation stream has been divided using "a sum of exponentials" approach. All of the studies use a plane parallel approximation in one form or another and all assume spherical particles for droplets and aerosols. The more sophisticated studies use a delta-two stream approach to account for the effects of multiple scattering. A few of the models include a prognostic equation which links the change in the microphysical distribution with the radiation field. The more advanced models also include a carefully designed surface flux exchange model. The strengths and deficiencies of the approaches have been discussed and recommendations for design of a proper radiative parameterization have been listed.

Acknowledgement

This work was supported by the Atmospheric Sciences Laboratory (Dr. Robert A. Sutherland) under the auspices of the U.S. Army Research Office Scientific Services Program administered by Battelle (Delivery Order 410, Contract No. DAAL03-91-C-0034).

References

- Bignell, K. J., 1970: The water vapour infrared continuum. *Quart. J. Roy. Meteor. Soc.*, **96**, 390-403.
- Bougeault, Ph., 1981: The diurnal cycle of the marine stratocumulus layer. A higher-order model study. *J. Atmos. Sci.*, **38**, 2429-2439.
- Bott, A., U. Sievers, and W. Zdunkowski, 1990: A radiation fog model with a detailed treatment of the interaction between radiative transfer and fog microphysics. *J. Atmos. Sci.*, **47**, 2153-2166.
- Bott, A., 1991: Properties of aerosols on the life cycle of radiation fogs. *Bound. Lay. Meteor.*, **56**, 1-31.
- Brogniez, C., 1975: Calcul approche des flux radiatifs en milieu diffusant. Application aux mesures de Venera 8. These de 3e cycle, Universite des Sciences et Techniques de Lille.
- Brown, R. and W. T. Roach, 1976: The physics of radiation fog: II- A numerical study. *Quart. J. Roy. Meteor. Soc.*, **102**, 335-354.
- _____, 1980: A numerical study of radiation fog with an explicit formulation of the microphysics. *Quart. J. Roy. Meteor. Soc.*, **106**, 781-802.
- Busygin, V. P., N. A. Yevstratov and Ye. M. Feygel'son. 1973: Optical properties of cumulus and radiant fluxes for cumulus cloud cover. *Atmos. Ocean. Phys.*, **9**, 1142-1151.
- Buykov, M. V. and V. I. Khvorost'yanov, 1977: Formation and evolution of radiation fog and stratus clouds in the atmospheric boundary layer. *Izvestiya, Atmos. and Oceanic Physics*, **13**, 251-260.
- Bykova, L. P., 1986: Assessing the role of latent heat in the development of nighttime cooling fogs. *Izvestiya, Atmospheric and Oceanic Physics*, **22**, 446-451.
- Chou, M. D. and A. Arking, 1980: Computation of infrared cooling rates in the water vapor bands. *J. Atmos. Sci.*, **37**, 855-867.
- _____, and _____, 1981: An efficient method for computing the absorption of solar radiation by water vapor. *J. Atmos. Sci.* **38**, 798-807.
- Clark, T. L., 1979: Numerical simulations with a three-dimensional cloud model: Lateral boundary condition experiments and multicellular severe storm simulations. *J. Atmos. Sci.*, **36**, 2191-2215.

- Cowling, T. G., 1950: Atmospheric absorption of heat radiation by water vapour. *Phil. Mag.*, London, **41**, 109-123.
- Cox, S. K., 1973: Radiation components of the energy budget for BOMEX. *Atmos. Sci. Paper No. 208*, Department of Atmospheric Science, Colorado State University, Fort Collins, CO 80523, 43 pp.
- Davies, R., 1985: Response of cloud supersaturation to radiative forcing. *J. Atmos. Sci.*, **42**, 2820-2825.
- Davis, J. M., S. K. Cox, and T. B. McKee, 1979: Total shortwave radiative characteristics of absorbing finite clouds. *J. Atmos. Sci.*, **36**, 508-518.
- Duynkerke, P. G., 1991: Radiation fog: A comparison of model simulation with detailed observations. *Mon Wea. Rev.*, **119**, 324-341.
- Ellingsen, R. G., and J. C. Gille, 1978: An infrared radiative transfer model. Part I: model description and comparison of observations with calculations. *J. Atmos. Sci.*, **35**, 523-545.
- Elsasser, W. M., and M. F. Culbertson, 1960: *Atmospheric Radiation Tables*. Meteor. Monogr. No. 23, 44 pp.
- Feigl'son, E. M., 1964: *Light and Heat Transfer in a Cloudy Atmosphere*. Moscow, Nauka, 245 pp. (English translation by Israel Program for Scientific Translation, 1966.)
- _____, 1970: *Radiant Heat Transfer in a Cloudy Atmosphere*. Leningrad, Gidrometeor., 191 pp. (English translation by Israel Program for Scientific Translations, 1973.)
- Fels, S., and M. D. Schwartzkopf, 1975: The simplified exchange approximation. A new method for radiative transfer calculations. *J. Atmos. Sci.*, **32**, 1475-1488.
- Forkel, R., W. G. Panhans, R. M. Welch, and, W. Zdunkowski, 1984: A one-dimensional numerical study to simulate the influence of soil moisture, pollution and vertical exchange on the evolution of radiation fog. *Contrib. Atmos. Phys.*, **57**, 72-91
- _____, U Sievers, and W. Zdunkowski, 1987: Fog modelling with a new treatment of the chemical equilibrium condition. *Contrib. Atmos. Phys.*, **60**, 340-360.
- Fouquart, Y., K. Laval, and R. Dadourny, 1978: The LMD general circulation model. Note LMD no. 86, Laboratoire de Meteorologie Dynamique, Ecole Normale Supérieure, 24, rue Lhomond, Paris, 24 pp.
- _____, and B. Bonnel, 1980: Computation of solar heating in the earth's atmosphere: a new parameterization. *Contrib. Atmos. Phys.*, **53**, 35-62.

- Fowle, F. E., 1915: The transparency of aqueous vapor. *Astrophys. J.*, 42, 394-411.
- Golubitski, B. M., and N. I. Moskalenko, 1968: Spectral transmission functions in the H₂O and CO₂ bands. *Atmos. Ocean. Phys.*, 4, 194-203.
- Goody, R. M. 1952: A statistical model for water vapour absorption. *Quart. J. Roy. Meteor. Soc.*, 78, 165-169.
- _____, 1964: *Atmospheric Radiation*, Oxford University Press, London England, 436 pp.
- Guzzi, R., and R. Rolando, 1980: The effects of radiative exchange on the growth by condensation of a population of droplets. *Contrib to Atmos. Phys.*, 53, 351-365.
- Harshvardhan, and M. D. King, 1993: Comparative accuracy of diffuse radiative properties computed using selected multiple scattering approximations. *J. Atmos. Sci.* 15, 247-259.
- Herman, B. M., 1962: Infrared absorption, scattering and total attenuation cross sections for water spheres. *Quart. J. Roy. Meteor. Soc.*, 88, 143-150.
- Howard, J. N., D. R. Burch, and D. Williams, 1955: Near-infrared transmission through synthetic atmospheres. Geophysics Research Directorate, AFCRC, Air Force and Development Command.
- _____, _____, and _____, 1956: Infra-red transmission of synthetic atmospheres. *J. Opt. Soc. Amer.*, 46, 237-245.
- Joseph, J. H., Wiscombe, W. J. and Weinmann, J. A., 1976: The delta-Eddington Approximation for radiative flux transfer. *J. Atmos. Sci.*, 33, 2452-2459.
- Korb, G., J. Michalowsky and F. Moller, 1956: Investigation on the heat balance of the troposphere. Tech. Rep. No. 1, Contract AF61(514)-863, August, 94pp. [OTS No. PB127016--obtainable from Library of congress].
- Kerschgens, M., U. Pilz, and E. Raschke, 1978: A modified two-stream approximation for the computations of the solar radiation budget in a cloudy atmosphere. *Tellus XXX*, 429-435.
- Kovetz, A., and B. Olund, 1969: The effect of coalescence and condensation on rain formation in a cloud of finite vertical extent. *J. Atmos. Sci.*, 26, 1060-1065.
- Lacis, A. A., and J. E. Hansen, 1974: A parameterization for the absorption of solar radiation in the earth's atmosphere. *J. Atmos. Sci.*, 31, 131-133.
- Lilly, D. K., 1968: Model of cloud-topped mixed layers under a strong inversion. *Quart. J. Roy. Meteor. Soc.*, 94, 292-309.

Liou, K. N., and T. Sasamori, 1975: On the transfer of solar radiation in aerosol atmospheres. *J. Atmos. Sci.*, **32**, 2166-2177.

_____, 1980: *An Introduction to Atmospheric Radiation*, *Int. Geophys. Ser.*, Vol 25, Academic Press, 392 pp.

McKee, T. B. and S. K. Cox, 1974: Scattering of visible radiation by finite clouds. *J. Atmos. Sci.* **31**, 1885-1892.

Moskalenko, N. I., 1969: The spectral transmission functions in the bands of water vapor. O₃, N₂O, and N₂ atmospheric components. *Atmos. Ocean. Phys.*, **5**, 678-684.

McCumber, M. C., and R. A. Pielke, 1981: Simulation of the effects of surface fluxes of heat and moisture in a mesoscale numerical model. *J. Geophys. Res.*, **86**, 9929-9938.

McDonald, J. D., 1960: Direct absorption of solar radiation by atmospheric water vapor. *J. Atmos. Sci.*, **17**, 319-328.

_____, 1963: The saturation adjustment in numerical modelling of fog. *J. Atmos. Sci.*, **20**, 476-478.

Mellor, G. L., and T. Yamada, 1974: A hierarchy of turbulence closure models for planetary boundary-layer. *J. Atmos. Sci.*, **31**, 1791-1806.

Musson-Genon, L., 1987: Numerical simulation of a fog event with a one-dimensional boundary layer model. *Mon. Wea. Rev.*, **115**, 592-607.

Ohta, S. and M. Tanaka, 1984: A P₃-approximation method as applied to foggy and cloudy atmospheres. *J. Meteor. Soc. Japan*, **62**, 146-157.

_____, and _____, 1986: A numerical study of the formation and the dissipation of radiation fogs. *J. Meteorol. Soc. Japan*, **64**, 65-77.

Oliver, D. A., W. S. Lewellan, and G.G. Williamson, 1978: The interaction between turbulent and radiative transport in the development of fog and low level stratus. *J. Atmos. Sci.*, **35**, 301-316.

Pandis, S. N., and J.H. Seinfeld, 1989: Mathematical modeling of acid deposition due to radiation fog. *J. Geophys. Res.*, **94**, (D10), 12,911-12923.

Pielke, R. A., 1984: *Mesoscale Meteorological Modeling*, Academic Press, Orlando, 612 pp.

Pruitt, W. O., D. L. Morgan, and F. J. Lourence, 1973: Momentum and mass transfer in the surface boundary layer. *Quart. J. Roy. Meteor. Soc.*, **92**, 370-386.

Pruppacher, H. R., and J. D. Klett, 1980: *Microphysics of clouds and Precipitation*. D Reidel, 714 pp.

Ramanathan, V., 1976: Radiative transfer within the earth's troposphere and stratosphere: A simplified radiative-convective model. *J. Atmos. Sci.*, **33**, 1330-1346.

Roach, W. T., R. Brown, S. J. Caughey, J. A. Garland, and C. J. Readings, 1976: The physics of radiation fog: I - A field study. *Quart. J. Roy. Meteor. Soc.*, **102**, 313-333.

Rogers, C. D., and C. D. Walshaw, 1966: The computation of infrared cooling rate in planetary atmospheres. *Quart. J. Roy. Meteor. Soc.*, **92**, 67-92.

Sasamori, T., 1968: The radiative cooling calculations for application to general circulation experiments. *J. Appl. Meteor.*, **7**, 721-729.

_____, J. London, and D. Hoyt, 1972: *Radiative budget of the Southern Hemisphere*. *Meteor. Monogr.* No. 35, 9-23.

Schubert, W. H., 1976: Experiments with Lilly's cloud-topped mixed layer model. *J. Atmos. Sci.*, **33**, 436-446.

_____, J. S. Wakefield, E. J. Steiner, and S. K. Cox, 1979: Marine stratocumulus convection. Part I: Governing equations and horizontally homogeneous solutions. *J. Atmos. Sci.*, **36**, 1286-1307.

_____, _____, _____, and _____, 1979: Marine stratocumulus convection. Part II: Horizontally inhomogeneous solutions. *J. Atmos. Sci.*, **36**, 1308-1324.

Selby, J. E. A., E. P. Shettle and R. A. McClatchey, 1976: Atmospheric transmittance from 0.25 to 28.5 μm : Supplement Lowtran 3 B. *AFGL-TR-76-0258*.

Shaffer, W. A., and P. E. Long, 1975: A predictive boundary layer model. *NOAA Tech. Memo*, NNS-TDL-57, 43pp. [Techniques Development Laboratory, Silver Spring, Md.]

Shettle, E. P. and J. A. Weinman, 1970: The transfer of solar irradiance through inhomogeneous turbid atmospheres evaluated by Eddington's Approximation. *J. Atmos. Sci.* **27**, 1048-1055.

Shifrin, K. S., 1955: Calculation of the radiation properties of clouds. Tr. CGO, No. 46.

Sievers, U., 1984: The turbulent atmosphere and the inclusive system of model equations. *Contrib. Atmos. Phys.*, **57**, 324-345.

Steiner, E. J., 1977: Stratocumulus convection off the west coast of South America. *Atmos. Sci. Paper No. 270*, Department of Atmospheric Science, Colorado State University, Fort Collins, CO 80523, 97 pp.

Stephens, G. L., 1978: Radiation profiles in extended water clouds I: Theory. *J. Atmos. Sci.*, **35**, 2111-2122.

_____, 1984: The parameterization of radiation for numerical weather prediction and climate models. *Mon. Weath. Rev.*, **112**, 826-867.

Tampieri, F. and C. Tomasi, 1976: Size distribution models of fog and cloud droplets in terms of the modified gamma function. *Tellus*, **28**, 333-347.

Tanaka, M., 1971: Radiative transfer in turbid atmospheres. I. Matrix analysis for the problem of diffuse reflection and transmission. *J. Meteor. Soc. Japan*, **49**, 296-312.

Turton, J. K., and R. Brown, 1987: A comparison of a numerical model of radiation fog with detailed observations. *Quart. J. Roy. Meteor. Soc.*, **113**, 37-54.

Vehil, R., and B. Bonnel, 1988: Computing solar heating in a fog layer: A new parameterization. *Atmos. Res.*, **22**, 73-84.

_____, J. Monerris, D. Guedalia, and P. Sarthou, 1989: Study of the radiative effects(Long-wave and shortwave) within a fog layer. *Atmos. Res.*, **23**, 179-194.

Veyre, P., B. Sommeria, and Y. Fouquart, 1980: Modelisation de l'effet des heterogeneites du champ radiatif infrarouge sur la dynamique des nuages. *J. Rech. Atmos.*, **14**, 89-108.

Wang, L., 1972: Anisotropic non-conservative scattering in a medium. *Astrophys. J.*, **174**, 671-678.

Welch, R. M., and W. G. Zdunkowski, 1976: A radiation model of the polluted atmospheric boundary layer. *J. Atmos. Sci.*, **33**, 2170-2184.

_____, S. K. Cox, and J. M. Davis, 1980: *Solar Radiation and Clouds. Meteor. Monogr. No. 39*, 96 pp.

_____, M. G. Ravichandran, and S. K. Cox, 1986: Prediction of quasi periodic oscillations in radiation fogs. Part I: Comparison of simple similarity approaches. *J. Atmos. Sci.*, **43**, 633-651.

Yamamoto, G., 1962: Direct absorption of solar radiation by atmospheric water vapour, carbon dioxide and molecular oxygen. *J. Atmos. Sci.*, **19**, 182-188.

Zdunkowski, W. G., and R. J. Junk, 1974: Solar radiative transfer in clouds using Eddington's Approximation, *Tellus XXVI*, 361-368.

_____, and B. C. Nielson, 1969: A preliminary prediction analysis of radiation fog. *Pure Appl. Geophys.*, 75, 278-299.

_____, R. E. Barth, and F. A. Lombardo, 1966: Discussion on the Atmospheric Radiation Tables by Elsasser and Culbertson. *Pure Appl. Geophys.*, 63, 211-219.

_____, R. M. Welch, and P. Breslin, 1979: A numerical test of two approximate solutions to the radiative transfer equation using the Elsasser Scheme. *Pure Appl. Geophys.* 117, 927-934.

_____, R. M. Welch, and G. Korb, 1980: An investigation of the structure of typical two-stream methods for the calculation of solar fluxes and heating rates in clouds. *Beitr. Phys. Atmos.*, 53, 147-166.

_____, W. G. Panhans, R. M. Welch and G. N. Korb, 1982: A radiation scheme for circulation and climate models. *Contrib. Atmos. Phys.*, 55, 215-237.

APPENDIX

A.1.0 Introduction

This appendix is a summary of various models used to predict the onset, maintenance and in some cases the dissipation of radiation fogs. The order of the summaries is more or less in a chronological order with some exceptions made for the sake of coherency. In each summary the main focus is the treatment of the radiation exchange. Some detail is also given concerning the physical processes related to radiation exchange; for example, the modeling of droplet growth and droplet fall rate may receive some attention. The earlier models have received more attention to the supporting dynamic structure and the later entries have mentioned these processes only if they are significantly different from their predecessor. The original notation has been retained so that the reader may easily refer to the complete document if desired. Some papers are merely mentioned if they did not introduce new aspects of the radiative treatment even if they utilize sophisticated methods that had been previously introduced. This was normally the case if the main focus of the paper was some other aspect of the fog development process.

A.2.0 Cloud Topped Mixed Layer Models

The first group of models studied is more aptly included in the grouping of models of clouds which at times propagate to the ground and are thus basically interpreted as ground fog. Several papers are found in the literature with two distinct levels of detail in the treatment of radiative exchange.

A.2.1 Lilly (1968) and Schubert (1977)

The first group was spawned from a study by Lilly (1968), and include Schubert (1976), Steiner and Schubert (1977), and Schubert *et al.* Parts I and II (1979). For the present purposes only the first two in this list need be given consideration. These models were constructed in order to explain the large areas of marine stratocumulus clouds that typically form in the descending branch of the Hadley circulation near the west coasts of major land masses. Although they are cloud models *per se.*, the role of infrared radiation is a major one, thus their inclusion in this study.

The contribution of radiation to this model's behavior is concentrated at the top of the mixed layer based on independent calculations of the jump in net radiation ΔF_R . The calculation of ΔF_R is not coupled to the state variables in the model, but is merely an estimate of typical radiation conditions at the top of a marine stratus cloud. Schubert (1976) extends the model to a time dependent calculation in which the net radiation jump is given by

$$\Delta F_R = 90.00 - 69.77 \max \left\{ \begin{array}{c} 0.202 + 0.779 \cos \left(\frac{2\pi t_d}{24} \right) \\ 0 \end{array} \right\} \text{ Wm}^{-2}$$

where t_d is the time of day measured in hours from local noon. The first term is the net upward longwave flux, while the second term is the solar radiation absorbed by the cloud. The two terms are based on analysis of the BOMEX radiation budget measurements Cox (1973), for typical moisture and temperature profiles, but conditions decoupled from the thermodynamics of the cloud model. The flux values were derived from a budget analysis of measurements that were tuned with calculations in which multiple scattering is included only via a diffusivity factor. Even though the calculation of radiation is not directly coupled to the model, radiative effects are striking. In fact, it is the vigorous emission of radiation from cloud top which provides the instability needed to drive the turbulence in the mixed layer and maintain the cloud against the dry subsiding air aloft.

The radiative flux enters the model through an application of the budget equations for the moist static energy (h) and the total water mixing ratio ($q+l$) to an infinitesimally thin layer at the cloud top. The moist static energy $h = c_p T + gz + Lq$, where T is temperature, z is height, q is the water vapor mixing ratio and c_p , g and L are the constants for specific heat, gravity and the latent heat of water respectively, and l is the mixing ratio for liquid water. The result is that the jump in the radiative flux ΔF_R relates to the jump in moist static energy by

$$-\frac{1}{g} \left(\frac{\partial p_B}{\partial t} - \omega_B \right) \Delta h + (F_h)_B = \Delta F_R$$

where p_B and ω_B are the pressure and pressure velocity at the top of the mixed layer and F_h is the flux of moist static energy.

The radiative jump ΔF_R is directly related to the value of the moist static energy in the mixed layer and to the thickness of the layer.

A.2.2 Oliver, Lewellen and Williamson (1977)

The next model studied brings more physical detail to bear on the subject of fog/cloud dynamics. The model as described in Oliver, Lewellen, and Williamson (1977) studies the interaction between turbulent and radiative transport in the development of fog and low-level stratus. Although this model occurs early in the collection which has been examined, the modeling of the transports by turbulence is significantly different in that it is a second order closure model. This entails a budget equation for second order correlations in contrast to the "K theory" parameterizations used almost without exception in the other studies. A prognostic equation is included in the model for each of the second order correlations.

$$\begin{aligned}
\overline{u'_i u'_j} & \text{ (Reynolds stresses)} \\
\overline{u'_i \theta'_v} & \text{ (heat flux)} \\
\overline{u'_i H'} & \text{ (moisture flux)} \\
\overline{\theta'^2_v} & \text{ (temperature-humidity} \\
\overline{H'^2} & \text{ correlations/variances)}
\end{aligned}$$

where u'_i , θ'_v , and H' represent perturbations in component velocity, virtual potential temperature and mixing ratio respectively.

The radiative energy enters the model through a mean thermodynamic balance equation,

$$\frac{D\bar{\theta}_v}{Dt} = -\frac{\partial}{\partial x_j} (\overline{u'_j \theta'_v}) + \kappa_s \bar{S} + \kappa_g \Gamma w$$

where S is the source term for radiative energy, Γ is the adiabatic lapse rate, w is the vertical velocity and κ_s and κ_g coefficients generated from the vapor saturation function whose definition is not important in the present discussion. Radiative influence would also enter the scheme through the budget equations for the second order correlations listed above via terms involving correlations of the form

$$\overline{S' u'_i}, \overline{S' \theta'_v} \text{ and } \overline{S' H'}.$$

These fluctuations arise from variation in the radiation absorption coefficient due to changes in ξ , the liquid mixing ratio. The authors argue that to include such terms would necessitate a modification of the coefficients of turbulent decay terms in the equations for the second order correlations listed above, and that the required separate coefficients for molecular diffusion and radiative diffusion have not been empirically established. Thus, introducing radiation into the budgets for the second order correlations would require a theory or measurements not yet established. Presumably second order effects are not totally suppressed however since the radiative absorption coefficients are influenced by the value of total mixing ratio H and perturbation components for the total water mixing ratio are solved for in the second order correlation equations.

The physics of radiative transfer are approximated using a spectrally averaged two stream model; i.e. the radiation intensities are represented by frequency and angular averaged values F^+ and F^- for the respective upwelling and downwelling streams. The streams are separated into broadband solar and infrared values. The governing equations for these intensities were taken from Goody (1964) and are given as

$$F^+(z) = [F^+(z_0) - \sigma(z_0)] \tau(z_0, z) + \sigma(z) - \int_{z_0}^z \tau(z', z) \frac{\partial \sigma}{\partial z'} dz'$$

and

$$F^-(z) = [F^-(h) - \sigma(h)] \tau(h, z) + \sigma(z) - \int_h^z \tau(z', z) \frac{\partial \sigma}{\partial z'} dz' ,$$

where $\sigma(z)$ and $\tau(z_0, z)$ represent the source function at z and the transmittance between levels z_0 and z , and the top and bottom of the layer are at h and z_0 respectively. The radiative heat flux for either the solar or infrared field is given as $q_z^{rad} = F^+ - F^-$, and the total heat flux is the sum of the direct heat flux and the infrared heat flux. The source term for solar radiation is set to zero as scattering and emission are omitted in the solar and scattering is omitted in the infrared.

For solar radiation the transmission function includes the effects of absorption by water vapor and CO_2 . Transmission by liquid water is modeled as $\tau_{liq}^s(z_1, z_2) = \exp(-\alpha^s m)$,

where m is the liquid water path expressed in units of grams per square centimeter and α^s is the absorption coefficient for direct solar radiation by water droplets. Values of α^s tabulated by Feigel'son (1964) are integrated over the solar spectrum to produce an average value of the coefficient of $16 \text{ cm}^2 / \text{gm}$.

For the infrared portion of the spectrum the source function σ is set to the integrated Planck function. At the boundaries $F^+(z_0)$ is set to the surface Planck function and at the top of the layer $F^-(h)$ is given by the downward flux emitted by the upper atmosphere. The transmission function for water vapor and carbon dioxide are again taken from Feigel'son (1970), with the liquid water contribution included as a factor in the transmission given by

$\tau_{liq}^T = \exp(-\alpha^T m)$. In this equation α^T is the averaged liquid water absorption coefficient which does depend strongly on the droplet size, ranging from $200\text{--}1700 \text{ cm}^2 / \text{gm}$ for drop sizes ranging from 4.5 to $7.0 \mu\text{m}$. In the model the variation of α^T with drop size is maintained. It is implied that droplets are considered to be monodispersed in the media; however, it is not clear if drop size is a function of the liquid water content or if the drop size is constant, which obviously would fix the value of α^T as well. Alternately the droplet density could be fixed and the mean size allowed to change with ξ . The authors state that a mean size distribution for fog and stratus is $6.0 \mu\text{m}$ which corresponds to a value of $600 \text{ cm}^2 / \text{gm}$.

The authors state that one of the most significant aspects of their study relating to radiative energy is the ability of the model to incorporate the effects of the dramatic differences between the absorption coefficients for solar and terrestrial radiation. For example, if we consider a fog with an average liquid water content of 0.2 g / kg , the mean free path for solar radiation is $2,700 \text{ m}$ while that for infrared radiation is only 83 m when each is averaged over its respective portion of the spectrum. Thus, while infrared exchange is confined to a region near cloud top (if the fog interior is nearly isothermal compared to the free atmosphere above), solar radiation is absorbed much deeper in the fog interior and its heating turbulently mixed to much greater

depths. As a result the fog can be evaporated from within rather than burned off at the top while the infrared radiation maintains the cooling necessary for continued turbulence production.

A.3.0 Fog models

The preceding section considered models of a cloud capped boundary layer. The models are important when considering the evolution of a fog scenario since they do include the condition of a stratus extending to the ground. There are of course other mechanisms leading to ground fogs; for example, fogs are categorized as advective or stemming from radiation conditions. This section deals with the radiative treatment given to models which may be included in these classes. The first model described has a relatively complete treatment of radiative exchange and may set the standard for this aspect of the model procedure.

A.3.1 Zdunkowski, Welch and Cox's Radiation Fog Model

This model is perhaps one of the most complete from the standpoint of including most of the relevant physical processes. For example, treatments of dew formation, droplet settling, effects of aerosols and response to variation of the large scale geostrophic wind are included in addition to energy and moisture exchange with the surface and the relatively thorough treatment of radiative exchange. Although the treatment of turbulence is not as physically realistic as the second order closure model discussed above, it utilizes eddy exchange coefficients which are scaled using the Monin-Obukhov profile function as adjusted for stability. The framework is presented for a more realistic handling of diffusion fluxes and phase fluxes; however, ultimately the time rates of change of concentrations of water vapor and liquid water are determined diagnostically, in much the same manner as simpler formulations. Also, diffusion fluxes for water vapor, liquid water and aerosol are modeled in terms of exchange coefficients and it is not clear if eddy exchange of aerosol is included in the model.

The description of the treatment of radiative energy is taken from the brief description given in the paper on the fog model and from separate papers which detail the Practical Improved Flux Method (section A.3.2) and a description of the general circulation version of the radiation model (section A.3.3). The net radiative flux vector S enters the prognostic scheme in the equation for temperature;

$$c_{p_0} \frac{\overline{Dp\theta}}{Dt} + \nabla \cdot \left(\frac{Y^{\theta}}{\bar{\pi}} \right) + \frac{1}{\bar{\pi}} \nabla \cdot S = \frac{1}{\bar{\pi}} (\epsilon - \sum_i f^i \hat{h}_i),$$

where, c_{p_0} is the specific heat at constant pressure, $\bar{\pi} = \left(\frac{\bar{p}}{p_0} \right)$ $\theta = \frac{T}{\bar{\pi}}$, where T is the

temperature, p the pressure, ρ the density, ϵ the rate of energy dissipation, h_i the partial specific enthalpy, Y^{θ} the sensible heat flux vector, f^i is the phase flux of species i (dry air, water vapor, liquid water and dry aerosol for $i = 0, 1, 2, 3$) and the overbar indicates a simple average. Also,

in the above, the derivative is in flux form

$$\frac{D\bar{\cdot}}{Dt} = \frac{\partial \bar{\cdot}}{\partial t} + \nabla \cdot (\bar{V} \bar{\cdot}),$$

in which the symbol $\bar{\cdot}$ implies a density weighted average and V is the velocity vector.

The net radiative flux is described as a vector S which includes the effects of absorption by water vapor and carbon dioxide, droplets and aerosols, and multiple scattering by particles in the entire solar spectrum using a scheme dubbed the Practical Improved Flux Method, which is outlined separately in the next sub-section. Less the term vector be interpreted as having application in three dimensional radiative transfer, it should be stated that there is no indication that this is anything more than a two stream calculation, and the terminology undoubtedly stems from division of the radiative stream into six components comprised of the direct solar radiation and upward and downward diffuse streams, each of which are further separated into fluxes in the clear and cloudy atmosphere. In the description of this model's application in a general circulation model, the radiative flux is described as the diagonal of a matrix which of course may also be interpreted as a vector. A separate section on the Practical Improved Flux Method and the general circulation version of the radiative transfer model seem in order and will follow. At any rate the method uses a delta function approach Joseph *et al* (1976) to approximate highly anisotropic phase functions of aerosols and water droplets. Here again, the report is somewhat unclear since flux methods do not use phase functions explicitly. Instead, the phase function is used to calculate the fraction of scattered radiation contained in the forward peak and the diffusivity factors which then scale the asymmetry parameter and the single scattering albedo. In the atmospheric window absorption and emission by water vapor, droplets and aerosols is accounted for in addition to multiple scattering by all particles. In the regions of the strong absorption by water and carbon dioxide multiple scattering by droplets is ignored as is the contribution by aerosols. In the window an emissivity approach is used which accounts for the mutual overlap of gases and particles.

Spectral resolution consists of dividing the solar spectrum into four intervals which are each characterized by constant particle attenuation coefficients. The tables in the next sections detail the spectral resolution in the model. Transmissions by water vapor and carbon dioxide are calculated by expanding each of the solar intervals into a series of five or six exponential terms in which extinction and scattering coefficients of droplets and aerosols are utilized for calculating the optical path length and single scattering albedo of each subinterval. Weighted asymmetry parameters are calculated for the mixture of droplets and aerosols and the effects of Rayleigh scattering. Notably, aerosol extinction parameters are adjusted for moisture effects in the entire humidity range. Flux calculations are subsequently made for each subinterval, and the results summed to obtain the net solar flux. The atmospheric window is treated as a single interval where water vapor absorption is assumed to be independent of wavelength.

One of the strengths of the model is the use of a modified gamma drop size distribution whose parameters are adjusted on the basis of the fog life cycle. Mie calculations (implying spherical

particles) are performed *a priori* on droplet distributions measured during various phases of the fog life cycle by Tampieri and Tomasi (1976), as a function of wavelength, to obtain the volume absorption coefficients. Then, because droplet attenuation can be approximated as a function of liquid water content, the entire set of attenuation coefficients is parameterized in the form $\beta = aW_l^b$, where β is the attenuation coefficient, W_l the liquid water content and a and b are coefficients of the fit. In the window region a value of a and b is tabulated for wavelengths of 8, 9, 10, 11 and 12 microns for both the extinction and absorption coefficients. In the solar spectrum the fit for the entire region is given as $\beta_s = (106.51 + 2.55\lambda) W_l^{(0.70-0.01\lambda)}$, where λ is in microns and W_l is in g/m³. In the solar region the value of β_s is highly variable and is obtained by defining another coefficient k_s , such that $k_s = \beta_s / \beta_o$. Presumably k_s is less variable than β_s and is also tabulated as a set of curve fits with liquid water the parameter.

A.3.2 Practical Improved Flux Method (PIFM) by Zdunkowski *et al.* (1980)

The model described in section 3.1 uses a delta-flux method termed the Practical Improved Flux Method or PIFM. The method is described in Zdunkowski *et al.* (1980), wherein several flux methods are compared. The PIFM fixes the manner in which the monochromatic radiative flux is transported in a plane parallel medium once the optical properties of the atmosphere have been dictated. The method does not specify the manner in which aerosols are introduced, the formulation of water vapor or carbon dioxide transmissions, nor the nature of the spectral quadratures or expansions. Of the flux methods presented, the PIFM is shown to yield the most physically consistent results for the range of optical parameters considered. It is shown that the flux models considered are all described by the following system:

$$\begin{aligned}\frac{dF_1}{d\tau} &= \alpha_1 F_1 - \alpha_2 F_2 - \alpha_3 \frac{S}{\mu_0} \\ \frac{dF_2}{d\tau} &= \alpha_2 F_1 - \alpha_1 F_2 + \alpha_4 \frac{S}{\mu_0} \\ \frac{dS}{d\tau} &= -(1 - \tilde{\omega} f) \frac{S}{\mu_0}\end{aligned}$$

where S is the solar direct beam flux, μ_0 is the cosine of the solar zenith angle, and f is the fraction of radiation contained in the diffraction peak. In this system the quantities α_1 , α_2 , α_3 , and α_4 are defined as follows:

$$\begin{aligned}\alpha_1 &= U_1 (1 - \tilde{\omega} (1 - \beta_o)) \\ \alpha_2 &= U_2 \beta_o \tilde{\omega} \\ \alpha_3 &= (1 - f) \tilde{\omega} \beta(\mu_0) \\ \alpha_4 &= (1 - f) \tilde{\omega} (1 - \beta(\mu_0))\end{aligned}$$

where $\bar{\omega}$ is the single scattering albedo, β_0 is the fractional mean backscattering coefficient for diffuse radiation, $\beta(\mu_0)$ is the mean backscattering coefficient for primary scattered parallel solar radiation and U_1 and U_2 are the reciprocals of the mean effective cosines of the zenith angles for upward and downward radiation, respectively. The authors show that several flux methods have a common solution, and that only the method of assigning values to f , β_0 , $\beta(\mu_0)$, U_1 , and U_2 differentiate the methods. If the atmosphere is divided into $i = 1 \dots N$ layers increasing in an upward direction and if a layer is bounded by the levels $(i, i+1)$, then the general solution for layer i is given by

$$\begin{pmatrix} S_i \\ F_{2,i} \\ F_{1,i+1} \end{pmatrix} = \begin{pmatrix} a_{1,i} & 0 & 0 \\ a_{2,i} & a_{4,i} & a_{5,i} \\ a_{3,i} & a_{5,i} & a_{4,i} \end{pmatrix} \begin{pmatrix} S_{i+1} \\ F_{2,i+1} \\ F_{1,i} \end{pmatrix}.$$

Boundary conditions are

$$\begin{aligned} S_{N+1} &= \mu_0 S_0 \\ F_{2,N+1} &= 0 \\ F_{1,1} &= A_s(\mu_0) S_1 + A_g F_{2,1} \end{aligned}$$

where S_0 is the spectral solar constant. The coefficients in the above have the values

$$\begin{aligned} a_{1,i} &= e^{-(1-\bar{\omega}f)\Delta\tau_i/\mu_0} \\ a_{2,i} &= -a_{4,i}\gamma_{2,i} - a_{5,i}\gamma_{1,i}a_{1,i} + \gamma_{2,i}a_{1,i} \\ a_{3,i} &= -a_{5,i}\gamma_{2,i} - a_{4,i}\gamma_{1,i}a_{1,i} + \gamma_{1,i} \\ a_{4,i} &= E_i(1 - M_i^2) / (1 - E_i^2 M_i^2) \\ a_{5,i} &= M_i(1 - E_i^2) / (1 - E_i^2 M_i^2) \end{aligned}$$

where

$$\begin{aligned} E_i &= e^{-e_i \Delta\tau_i}, \quad M_i = \frac{\alpha_{2,i}}{\alpha_{1,i} + e_i}, \quad e_i = \sqrt{\alpha_{1,i}^2 - \alpha_{2,i}^2} \\ \gamma_{1,i} &= \frac{(1 - \bar{\omega}f)\alpha_{3,i} - \mu_0(\alpha_{1,i}\alpha_{3,i} + \alpha_{2,i}\alpha_{4,i})}{(1 - \bar{\omega}f)^2 - e_i^2 \mu_0^2} \\ \gamma_{2,i} &= \frac{-(1 - \bar{\omega}f)\alpha_{4,i} - \mu_0(\alpha_{1,i}\alpha_{4,i} + \alpha_{2,i}\alpha_{3,i})}{(1 - \bar{\omega}f)^2 - e_i^2 \mu_0^2}. \end{aligned}$$

The methods compared are the flux method of Zdunkowski and Junk (1974), the flux method of Kerschgens *et al.* (1978), the Eddington type methods, delta Eddington type methods, the discrete ordinate method, a delta discrete ordinate method, the improved flux method and the PIFM. As mentioned above the PIFM gives the physically most consistent results for the various atmospheres considered, which include variations in optical thickness, solar zenith angle and single particle scattering albedo. The PIFM is a simplification of the improved flux method for which

$$\beta(\mu_0) = \frac{1}{2} \int_0^1 d\mu \sum_{l=0}^N P_l^T(-1)^l P_l(\mu) P_l(\mu_0),$$

where the expansion coefficients p_l^T of the Legendre polynomials are obtained from the requirement that the primary scattered light is reduced by the fraction f . The original phase

function is truncated at a cut-off angle $\theta_1 = \cos^{-1}(\frac{P_1}{3})$. The truncated phase function is

normalized and expanded into a series of Legendre polynomials yielding the coefficients p_l^T , and the cut off fraction is determined from

$$f = \frac{1}{4\pi} \int_{\omega} [P(\cos\theta) - P^T(\cos\theta)] d\omega,$$

where $P(\cos\theta)$ and $P^T(\cos\theta)$ are the normal and truncated phase functions respectively. Note that determination of $\beta(\mu_0)$ and f in this manner requires an expansion of the phase function which is of course computationally demanding depending on the size distribution. The authors state that these values may be adequately approximated as

$$\begin{aligned} \beta_0 &= \frac{3 - P_1}{8} \\ f &= (P_1/3)^2 \\ \beta(\mu_0) &= \frac{1}{2} - \frac{\mu_0}{4} \frac{P_1 - 3f}{1 - f} \\ U_1 &= U_2 = 2. \end{aligned}$$

This determination is, of course, less demanding.

There is nothing in the PIFM which limits its application in any fog model if scattering is included as a relevant process and if scattering parameters are calculated from Mie theory. As noted previously however, the method does not specify the optical properties of the atmosphere or the method of spectral averaging or integration which is required to consider all relevant wavelength regimes.

A.3.3 Radiation scheme for circulation and climate models by Zdunkowski *et al.* (1982)

This paper details a radiative transfer scheme which is referenced in the Zdunkowski and Welch fog model. The paper is very detailed in its presentation of the relevant equations. It is questionable if reproducing the level of detail is justified, but because of the lack of detail used in most other descriptions of the radiative treatments, the radiation sub-model will be fully described. Also there are a few aspects of the model as described in this subsection which are obviously not relevant to the radiation fog scenario or have not been mentioned in the original fog model description. These aspects will be noted.

Some of the description in this section is similar to that of the section above, which concentrates on the aspects of the PIFM model that make it better suited than other 2-stream methods as a solution to the monochromatic radiative transfer equation. This section explains how the method is actually applied as in a general circulation or climate model. For example it details the way in which the major spectral intervals are divided, the manner of calculating optical paths, which atmospheric constituents are included in the calculation and how the transfer of infrared energy is included.

Again the description begins with a statement of the basic differential flux equations from monochromatic radiation; however the equations have been formally extended to include infrared radiation. Letting F_1 and F_2 stand for the upward and downward diffuse flux densities and S to represent the direct beam solar flux on a horizontal surface, with τ the optical depth, μ_0 the cosine of the solar zenith angle ω the single particle scattering albedo, B is used to represent the Planck function, β_0 the backscattering coefficient for diffuse light, and $\beta(\mu_0)$ the backscattering coefficient for primary scattered solar radiation, the following equations apply.

$$\begin{aligned}\frac{dF_1}{d\tau} &= \alpha_1 F_1 - \alpha_2 F_2 - \alpha_3 J \\ \frac{dF_2}{d\tau} &= \alpha_2 F_1 - \alpha_1 F_2 + \alpha_4 J \\ \frac{dS}{d\tau} &= -(1 - \omega f) \frac{S}{\mu_0}\end{aligned}$$

where the symbols have the following definitions using (s) to denote the definition when applied to solar radiation and (i) to denote their use for the infrared portion of the spectrum,

$$\begin{aligned}\alpha_1 &= U(1 - \omega)(1 - \beta_0) & (s, i) \\ \alpha_2 &= U\beta_0\omega & (s, i)\end{aligned}$$

$$\alpha_3 = \begin{cases} (1 - f) \omega B(\mu_0) & (s) \\ \alpha_1 - \alpha_2 = U(1 - \omega) & (i) \end{cases}$$

$$\alpha_4 = \begin{cases} (1 - f) \omega (1 - B(\mu_0)) & (s) \\ \alpha_3 & (i) \end{cases}$$

$$J = \begin{cases} S / \mu_0 & (s) \\ \pi B & (i) \end{cases}$$

$$U = \begin{cases} 2 & (s) \\ 1.66 & (i) \end{cases}$$

In theory when the model is applied in a general circulation or climate model the fluxes for both cloudy and cloud free portions of the atmosphere above or below the layer in question are maintained separately as they enter the layer. These fluxes are modified using the properties of the layer including the fractional cloudiness and new fluxes emanating from cloudy and cloud free portions of the layer are calculated. Even in these applications, it is noted by the authors that since clouds are not truly black body radiators, using this partial cloudiness approach is numerically time consuming since the grey body clouds overlap with the emission spectra of the gases and a spectrally detailed emission must be retained although its detail is somewhat masked by the clouds. It is numerically more efficient to treat clouds as black body radiators. Thus, in the application to a general circulation model, atmospheric columns are treated as totally clear or totally cloudy. Then, because using a vertical resolution of n independent layers allows 2^n possible column configurations, additional limits are placed on the layers in which clouds are allowed. The practice is to limit the cloudiness to the typical high, middle and low cloud types and thus the number of column calculations is limited to eight.

In the fog model there is no mention of merging fog and clear radiances. The model has not been extended beyond the plane parallel approximation. Nevertheless, in what follows the cloudy and clear notation will be carried through because the fog model does treat clear and foggy atmospheres separately, and the formulation is different for each.

In order to express the solution in a compact form the authors define quantities they call black body flux deficiencies. The superscripts c and f stand for cloudy and cloud free values and C denotes the fractional cloud cover in a layer. The first subscript denotes upward (1) or downward (2) values and the second subscript stands for the levels (i) which increase from the surface up.

The black body flux deficiencies are defined as

$$\begin{aligned} F_{1,1,1}^{*c} &= C_1 \pi B_{1,1} - F_{1,1,1}^c \\ F_{2,1}^{*c} &= C_1 \pi B_1 - F_{2,1}^c \\ F_{1,1,1}^{*f} &= (1 - C_1) \pi B_{1,1} - F_{1,1,1}^f \\ F_{2,1}^{*f} &= (1 - C_1) \pi B_1 - F_{2,1}^f \end{aligned}$$

Then the authors write the solution in the compact form

$$\begin{pmatrix} S_1^c \\ F_{2,1}^{*c} \\ F_{1,1,1}^{*c} \end{pmatrix} = \begin{pmatrix} a_{1,1}^{*c} & 0 & 0 \\ a_{2,1}^{*c} & a_{4,1}^{*c} & a_{5,1}^{*c} \\ a_{3,1}^{*c} & a_{6,1}^{*c} & a_{4,1}^{*c} \end{pmatrix} \begin{pmatrix} Q_{1,1}^c \\ b_{3,1} F_{2,1,1}^{*c} + (1 - b_{1,1}) F_{2,1,1}^{*f} \\ b_{4,1} F_{1,1}^{*c} + (1 - b_{2,1}) F_{1,1}^{*f} \end{pmatrix}$$

$$\begin{pmatrix} S_1^f \\ F_{2,1}^{*f} \\ F_{1,1,1}^{*f} \end{pmatrix} = \begin{pmatrix} a_{1,1}^{*f} & 0 & 0 \\ a_{2,1}^{*f} & a_{4,1}^{*f} & a_{5,1}^{*f} \\ a_{3,1}^{*f} & a_{6,1}^{*f} & a_{4,1}^{*f} \end{pmatrix} \begin{pmatrix} Q_{1,1}^f \\ (1 - b_{3,1}) F_{2,1,1}^{*c} + b_{1,1} F_{2,1,1}^{*f} \\ (1 - b_{4,1}) F_{1,1}^{*c} + b_{2,1} F_{1,1}^{*f} \end{pmatrix}$$

with

$$Q_{1,1}^c = \begin{cases} b_{3,1} S_{1,1}^c + (1 - b_{1,1}) S_{1,1}^f & (s) \\ C_1 \pi (B_1 - B_{1,1}) & (i) \end{cases}$$

$$Q_{1,1}^f = \begin{cases} (1 - b_{3,1}) S_{1,1}^c + b_{1,1} S_{1,1}^f & (s) \\ (1 - C_1) \pi (B_1 - B_{1,1}) & (i) \end{cases}$$

$$a_{1,1}^* = \begin{cases} a_{1,1} & (s) \\ 0 & (i) \end{cases}, a_{2,1}^* = \begin{cases} -a_{2,1} & (s) \\ a_{6,1} & (i) \end{cases}, a_{3,1}^* = \begin{cases} -a_{3,1} & (s) \\ -a_{6,1} & (i) \end{cases}$$

$$a_{4,1}^* = a_{4,1}, \quad a_{5,1}^* = a_{5,1} \quad (s, i)$$

with

$$a_{6,1} = (1 - a_{4,1} + a_{5,1}) / (\alpha_{1,1} + \alpha_{2,1}) \Delta \tau_1,$$

and if $a_{e,i} = 0/0$, then set $a_{e,i} = 1$. The definitions of the remaining $a_{i,j}$ are given in the discussion of the PIFM method above.

The $b_{i,j}$ coefficients relate to the cloud fraction of the layer and have the following definitions

$$\left. \begin{aligned} b_{1,i} &= (1 - \text{Max}(C_i, C_{i-1})) / (1 - C_{i-1}) \\ b_{2,i} &= (1 - \text{Max}(C_i, C_{i-1})) / (1 - C_{i-1}) \\ b_{3,i} &= (\text{Min}(C_i, C_{i-1})) / C_{i-1} \\ b_{4,i} &= (\text{Min}(C_i, C_{i-1})) / C_{i-1} \end{aligned} \right\} = 1 \text{ if } 0 / 0$$

The authors note that in applying the equations to the solar region of the spectrum the B terms must be set to zero so that thermal emission from $3-6\mu\text{m}$ is not accounted for twice.

The authors give a physical interpretation for each of the $a_{i,j}^{c,e}$; however, these will not be repeated here.

Next, it is important to note special cases which may occur in the system above. First, for the case of conservative scattering, the following relations apply:

$$\left. \begin{aligned} \omega &= 1 \\ \alpha_{1,i} &= \alpha_{2,i} \\ a_{4,i} &= \frac{1}{1 + \alpha_{1,i} \Delta \tau_i} \\ a_{5,i} &= \frac{\alpha_{1,i} \Delta \tau_i}{1 + \alpha_{1,i} \Delta \tau_i} \end{aligned} \right\}.$$

Second, if the process is completely absorptive,

$$\left. \begin{aligned} \omega &= 0 \\ \alpha_{1,i} &= U \\ \alpha_{2,i} &= \alpha_{3,i} = \alpha_{4,i} = 0 \\ a_{2,i} &= a_{3,i} = a_{5,i} = 0 \\ a_{4,i} &= e^{-(U \Delta \tau_i)} \\ \alpha_{6,i} &= \frac{1 - e^{-(U \Delta \tau_i)}}{U \Delta \tau_i} \end{aligned} \right\}.$$

Finally, if there is no attenuation,

$$\left. \begin{aligned} \Delta \tau_i &= 0 \\ a_{1,i} &= a_{4,i} = a_{6,i} = 1 \\ a_{2,i} &= a_{3,i} = a_{5,i} = 0 \end{aligned} \right\}.$$

The authors note that the physically relevant fluxes in the infrared must be obtained by going back to the definition of the flux deficiencies. Then the relevant flux at any level i is obtained from

$$\left. \begin{aligned} S_i &= S_i^c + S_i^f \\ F_{2,i} &= F_{2,i}^c + F_{2,i}^f \\ F_{1,i} &= F_{1,i}^c + F_{1,i}^f \\ F_{NET,i} &= F_{1,i} - (F_{2,i} + S_i) \end{aligned} \right\}.$$

Next, the boundary conditions are stipulated. At the upper boundary $i = N + 1$,

$$\left. \begin{aligned} S_{N+1}^c &= 0 \\ S_{N+1}^f &= \mu_0 S_0 \\ F_{2,N+1}^c &= F_{2,N+1}^f = 0 \\ F_{2,N+1}^f &= F_{2,N+1}^c = 0 \end{aligned} \right\} (s)$$

and

$$\left. \begin{aligned} F_{2,N+1}^c &= F_{2,N+1}^f = 0 \\ F_{2,N+1}^f &= \pi B_{N+1} \\ F_{2,N+1}^c &= 0 \end{aligned} \right\} (i).$$

The lower boundary conditions for level $i = 1$ are

$$\left. \begin{aligned} F_{1,1}^c &= -F_{1,1}^f = -A_s (\mu_0) S_1^c - A_s F_{2,1}^c \\ F_{1,1}^f &= -F_{1,1}^c = -A_s (\mu_0) S_1^f - A_s F_{2,1}^f \end{aligned} \right\} (s)$$

where A , and ϵ , are the surface albedo and emissivity respectively, and

$$\left. \begin{aligned} F_{1,1}^c &= (1 - \epsilon_g) [F_{2,1}^c + C_1 \pi (B_g - B_1)] \\ F_{1,1}^f &= (1 - \epsilon_g) [F_{2,1}^f + (1 - C_1) \pi (B_g - B_1)] \\ F_{1,1}^c &= (1 - \epsilon_g) F_{2,1}^c + C_1 \epsilon_g \pi B_g \\ F_{1,1}^f &= (1 - \epsilon_g) F_{2,1}^f + (1 - C_1) \epsilon_g \pi B_g \end{aligned} \right\} (i).$$

with

$$\begin{aligned} F_{1,1}^{*c} &= C_1 \pi B_g - F_{1,1}^c \\ F_{1,1}^{*f} &= (1 - C_1) \pi B_g - F_{1,1}^f \end{aligned}$$

The equations above apply in a monochromatic sense to the entire solar and infrared regions; however, the number of monochromatic calculations required to produce meaningful heating rates would be enormously computationally expensive. The authors have thus decided on the following methods of spectral integration. In the solar region and atmospheric window (8.75 - 12.25 μm) a combination of the exponential fit method (EFM) and effective absorber amount method (EAM) has been adopted by which scattering may be included. In the regions of high emissivity by water vapor and carbon dioxide (3.5 - 8.75 μm) and (12.25-100 μm) a flux emissivity method is used in which scattering is discounted as an important physical process.

The exponential fit method expresses the band transmission for a gas over a limited spectral region as a sum of exponentials. If u_m is the reduced absorber amount for gas m , then the transmission for a limited band T_{band} is written as

$$T_{band}(u_m) = \sum_{l=1}^{L_m} a_{m,l} e^{-k_{m,l} u_m}$$

This requires the solution using the extended PIFM method to be performed L_m times for each band. Then the flux over the band is obtained by summing the weighted individual results using the $a_{m,l}$ as weighting factors as in

$$\bar{F}_{m,i} = \begin{pmatrix} S_m^c \\ S_m^f \\ F_{2,m}^c \\ F_{2,m}^f \\ F_{1,m}^c \\ F_{1,m}^f \end{pmatrix} = \bar{F}_{m,k}^{(EFM)} = \sum_{l=1}^{L_m} a_{m,l} \begin{pmatrix} S^c(k_{m,l}) \\ S^f(k_{m,l}) \\ F_2^c(k_{m,l}) \\ F_2^f(k_{m,l}) \\ F_1^c(k_{m,l}) \\ F_1^f(k_{m,l}) \end{pmatrix}_i$$

in which the summation applies to all elements of the flux vector.

To further develop the spectral integration methodology the authors also introduce a solution flux vector which would be calculated from the equations governing monochromatic radiation transfer but which contain the influence of grey body absorption. This vector excludes the effects of band absorbers.

$$\bar{E}_{0,i} = \begin{pmatrix} S_0^c \\ S_0^f \\ F_{2,0}^c \\ F_{2,0}^f \\ F_{1,0}^c \\ F_{1,0}^f \end{pmatrix}_i$$

The authors introduce the notion of a transmission matrix,

$$\Pi_{m,i}^{(EFM)} = \text{Diag} \left\{ \sum_{l=1}^{L_m} a_{m,l} \left[\frac{S^c(k_{m,l})}{S_0^c}; \frac{S^f(k_{m,l})}{S_0^f}; \frac{F_{2,0}^c(k_{m,l})}{F_{2,0}^c}; \frac{F_{2,0}^f(k_{m,l})}{F_{2,0}^f}; \frac{F_{1,0}^c(k_{m,l})}{F_{1,0}^c}; \frac{F_{1,0}^f(k_{m,l})}{F_{1,0}^f} \right] \right\}_i$$

Then the approximation of the exponential fit method may be written as

$$\bar{F}_{m,i} \approx \bar{F}_{m,i}^{EFM} = \Pi_{m,i}^{EFM} \cdot \bar{F}_{0,i}$$

In some regions of the solar spectrum an even greater efficiency is achieved using what the authors term the effective absorber amount method. This method is similar to an approximation used by Musson-Genon (1987), discussed in section A.3.12 below. In this application the authors express the effective absorber amount as a function of the absorption coefficient k_m , and express an effective path for each element of the flux vector as

$$\bar{u}_i(k_m) = \text{Diag} \{ (u_s^c; u_s^f; u_2^c; u_2^f; u_1^c; u_1^f)(k_m) \}_i$$

And the values of the effective absorber vector may be approximated by taking the limiting value of the above as $k_m \rightarrow 0$, or

$$\begin{aligned} \bar{u}_i(k_m) &\approx \bar{u}_i(k_m \rightarrow 0) \\ &= \text{Diag} \{ \langle u_s^c \rangle; \langle u_s^f \rangle; \langle u_2^c \rangle; \langle u_2^f \rangle; \langle u_1^c \rangle; \langle u_1^f \rangle \}_i \end{aligned}$$

where the brackets $\langle \rangle$ indicate that each u is taken as $k_m \rightarrow 0$. The limiting value of the absorber path is given by

$$u_i(k_m \rightarrow 0) = -\lim_{k_m \rightarrow 0} \bar{F}_{0,i}^{-1} \frac{\partial}{\partial k_m} \bar{F}_{m,i} = \text{Diag} \{ \langle u_s^c \rangle; \langle u_s^f \rangle; \langle u_2^c \rangle; \langle u_2^f \rangle; \langle u_1^c \rangle; \langle u_1^f \rangle \}_i$$

That this definition produces optical paths can be demonstrated by performing the indicated operations on a simple monochromatic Beer's law equation.

The fluxes approximated with the effective absorber amount require the definition of a transmittance matrix,

$$\Pi_{m,i}^{EAM} = \text{Diag} \left\{ \sum_{j=1}^{L_m} a_{m,j} \left[\exp(-k_{m,j} \langle u \rangle_s^c) ; \exp(-k_{m,j} \langle u \rangle_s^f) ; \exp(-k_{m,j} \langle u \rangle_2^c) ; \right. \right. \\ \left. \left. \exp(-k_{m,j} \langle u \rangle_2^f) ; \exp(-k_{m,j} \langle u \rangle_1^c) ; \exp(-k_{m,j} \langle u \rangle_1^f) \right] \right\}_i$$

After which the flux vector may be written as

$$\bar{F}_{m,i} \sim \bar{F}_{m,i}^{EAM} = \Pi_{m,i}^{EAM} \cdot \bar{F}_{0,i}$$

For the case where absorbers spectrally overlap a separate transmission matrix must be supplied for each absorber. That is in the case of two gases m and n which absorb in the same spectral interval; the flux vector may be computed from

$$\bar{F}_{m,n,i} = \Pi_{m,i} \cdot \Pi_{n,i} \cdot \bar{F}_{0,i}$$

The authors note that the above is always true for the case of a grey body absorber and a band absorber and approximately true for two band absorbers.

The authors choose to treat the infrared emission by dividing the spectrum into three parts (3.5-8.75 μm), (8.75-12.25 μm) and (12.25-100 μm). The window region is treated in a similar manner as the solar region as described above. The other two parts of the infrared spectrum are treated using a flux emissivity method which includes emission by water vapor, carbon dioxide and grey body absorbers. Regions of spectral overlap are accounted for by pre-tabulating the wave number integration of the overlap integrals so that the remaining integration can be carried out in an expedient manner. The authors list for the origin of their flux emissivity method the following sources: Elsasser and Culbertson (1960), Zdunkowski *et al* (1966) and Zdunkowski and Breslin (1979). The method is represented by the following formulas:

$$F_1(u, w, m) = [\pi B(T_G) - \pi B(T(U))] \tau_f(M-m) + \pi B(T(U)) \\ - \int_{T(u)}^{T(u)} \tau_f(\mu(T)-m) [R^*(\eta(T)-u, T) + \Delta R^*(\eta(T)-u, \xi(T)-w, T)] dT \\ - \int_{T(u)}^{T(u)} (1 - \tau_f(\mu(T)-m)) \pi \frac{dB}{dT} dT \\ - \tau_f(M-m) \int_{T(u)}^{T_0} [R^*(U-u, T) + \Delta R^*(U-u, W-w, T)] dT$$

where the symbols are defined in the following table.

Integrated absorbing mass measured from top of atmosphere	H ₂ O-Vapor	CO ₂	Grey Absorber
Dummy variable	η	ξ	μ
Reference level	u	w	m
Ground	U	W	M

Top of Atmosphere	Reference Level	T _{air} at ground	T _{surf}
T_t	$T(u)=T(w)=T(m)$	$T(U)=T(W)=T(M)$	T_g

The quantities R^* and ΔR^* represent the water and water vapor-carbon dioxide overlap emissivities weighted with the temperature derivative of the Planckian function instead of the Planck function itself. The equations above are applicable to an atmosphere containing water vapor, carbon dioxide and a grey body emitter. The authors note that the emissivity approach is a good approximation due to the strong absorption by water vapor but would not be a good approach in a cirrus cloud layer where scattering is likely to contribute in a relatively stronger fashion when compared to the weaker water vapor absorption at high altitudes.

The equation for the upward diffuse infrared irradiance is written as

$$\begin{aligned}
 F_2(u, w, m) = & \pi B(T_t) [1 - \tau_f(m)] + \int_{T_t}^{T(u)} \tau_f(m - \mu(T)) [R^*(u - \eta(T), T) \\
 & + \Delta R^*(u - \eta(T), w - \xi(T), T)] dT \\
 & + \int_{T_t}^{T(u)} [1 - \tau_f(m - \mu(T))] \pi \frac{dB}{dT} dT \\
 & + \tau_f(m) \int_0^{T_t} [R^*(u, T) + \Delta R^*(u, w, T)] dT
 \end{aligned}$$

The grey body transmission function is calculated from

$$\tau_f(m) = 2 Ei_3 \left(- \int_{-\infty}^{Z_{RL}} \beta_{ABS}(z') dz' \right),$$

where Ei_3 is the exponential integral of the third order, β_{ABS} is the grey body absorption coefficient and Z_{RL} is the height of the reference level.

The authors state that when used in a general circulation model partial cloudiness presents no particular difficulties. This statement is presumably made with the assumption that the effects of radiative transfer through finite clouds is treated only approximately by assuming a plane parallel approximation for clouds in designated grid cells of the model, since the method does not in fact include the effects of finite cloud geometry. In order to avoid making several calculations of grey body transmittance the authors choose to treat clouds as black body radiators and to limit the types of clouds to high, middle and low levels. In the one dimensional fog modeling application partial cloudiness has no meaning since a layer is either foggy or fog free.

The authors describe the treatment of droplet distributions for stratus and cumulus type cloudiness and describe the accuracy of the effective absorber amount method versus the exponential fit method in the solar spectrum. The following two tables summarize the scattering and non-scattering parts of the model.

Spectral interval in μm	Attenuating material	Treatment of Attenuation in presence of emission
8.75-12.25	O ₃ H ₂ O-Vapor H ₂ O-Dimer Aerosol Particles Droplets	EFM-4 Terms Continuum E-Type Absorption, Scattering Absorption, Scattering
3.50-8.75 12.25-100	H ₂ O-Vapor CO ₂ Aerosol Particles Droplets	Emissivity Method

Authors' summary of model configuration in the infrared. EFM-4 implies the Exponential Fit Method using 4 terms.

Spectral interval in μm	Attenuating material	Treatment of Attenuation in presence of emission
0.28-1.00	H ₂ O-Vapor O ₃ NO ₂ Dry Air Aerosol Particles Droplets	EFM - 5 Terms EAM - 5 Terms EFM - 5 Terms Scattering Absorption, Scattering Absorption, Scattering
1.00-1.53	H ₂ O-Vapor Dry Air Aerosol Particles Droplets	EFM - 7 Terms Scattering Absorption, Scattering Absorption, Scattering
1.53-2.20	H ₂ O-Vapor CO ₂ Dry Air Aerosol Particles Droplets	EFM - 6 Terms EAM - 6 Terms Scattering Absorption Scattering Absorption Scattering
2.20-6.00	H ₂ O-Vapor CO ₂ Aerosol Particles Droplets	EAM - 7 Terms EAM - 6 Terms Absorption Scattering Absorption Scattering

Authors' summary of configuration of the model in the solar portion of the spectrum. EFM represents the Exponential Fit Method and EAM the Effective Absorber Method.

A.3.4 The radiation fog model of Brown and Roach (1976)

The next model considered is a model of radiation fog, Brown and Roach (1976), which was formulated in consideration of experimental results gathered at Cardington; see Roach *et al* (1976). The model is formulated in one dimension in accordance with the interpretation of experimental findings. The model is formulated without advective effects. Equations governing the perturbation quantities are not presented although the authors note that the turbulent flux components are included in the numerical integration. For example, the radiative influence is included in the thermodynamic equation simply as

$$\frac{\partial T}{\partial t} = -\frac{1}{\rho c_p} \frac{\partial F_N}{\partial z} + \frac{\partial}{\partial z} (K_h \frac{\partial \theta}{\partial z}) + \frac{L}{c_p} C,$$

where T , ρ , θ and z represent dry bulb temperature, density, potential temperature and height, F_N is the net radiation, C the rate of condensation per mass of air, L is the latent heat of vaporization, K_h the exchange coefficient for heat, and c_p the specific heat of air at constant pressure. Also, the flux of sensible heat F_H is modeled in the traditional manner in terms of the exchange coefficient K_h as, $F_H = \rho c_p K_h \partial \theta / \partial z$. K_h is modeled in terms of the Monin-

Obukhov length scale as $K_h = K_0 / \Phi_H(z/L)$, where K_0 is the adiabatic value ($= k u_*$), where k is von Karman's constant and u_* is the friction velocity. The authors choose a formulation of $\Phi_H(z/L)$ from Pruitt, Morgan and Lourence (1973):

$$\begin{aligned} \Phi_H(z/L) &= 0.855 (1 + 34 Ri)^{0.4} & 0 \leq Ri < 0.3 \\ \Phi_H(z/L) &= 0.855 (1 - 22 Ri)^{-0.4} & -3.5 \leq Ri < 0 \end{aligned}$$

The microphysics of condensation are not explicitly included in the numerical scheme. Rather, at each time step and at each grid point the temperature and water vapor mixing ratio are examined. If these imply supersaturation then condensation takes place until the air is just saturated. Conversely, if liquid water is present at a relative humidity less than 100%, evaporation takes place until saturation is reached or until all liquid is evaporated. The flux of liquid water due to gravitational settling is parameterized in terms of the liquid water content as $v = 6.25w$.

The radiative heating is calculated in a plane parallel setting with consideration of infrared irradiances only. The radiative heating rate is calculated as

$$\begin{aligned} H(z) = & -\frac{1}{\rho c_p} \{ [B(0) - F_G] \frac{\partial \tau(z, 0)}{\partial z} + [F_I(z_c) - B(z_c)] \frac{\partial \tau(z, z_c)}{\partial z} + \\ & + \int_0^{z_c} \frac{\partial \tau(z, z')}{\partial z} \frac{\partial B(z')}{\partial z} dz' \} \end{aligned}$$

where $H(z)$ is the heating rate in $^{\circ}\text{C}/\text{sec}$ at height z , $\tau(z, z')$ is the layer transmissivity between levels z and z' , $B(z')$ the Planck function, F_g the radiative flux incident from levels below the limit of integration, z_c the height to which the radiative integration is carried, 250 m, and $F\downarrow(z_c)$ the radiative flux incident from levels above z_c . The authors note that they ignore the first term in the above equation with one exception (mentioned below in the approximate treatment to include the effects of surface vegetation), and that the equation is evaluated separately inside and outside the atmospheric window region. The transmissivity due to carbon dioxide and water vapor are evaluated in two broad spectral regions, 4-8 μm and 13-50 μm using the random band model of Goody (1952), and combined into a single transmissivity. Spectral data for water vapor was taken from Cowling (1950) and for carbon dioxide from Howard, Burch and Williams (1956). The atmospheric window is treated as being transparent in the presence of gases.

The transmittance due to water droplets is calculated according to

$$\tau_f(z, z') = \exp[-\phi(z, z')] \quad \text{where}$$

$$\phi(z, z') = \int_0^{z'} \int_0^\infty 1.66 N(r, z'') \pi r^2 Q_a(r) dr dz''.$$

Above, $Q_a(r)$ is the absorption efficiency for droplets of radius r , and the factor 1.66 is a diffusivity factor to approximate the conversion from collimated to hemispheric radiation. Scattering by water droplets and gases is ignored. The authors note that an approximation to

$Q_a(r)$ has been offered by Herman (1962), as $Q_a = Q_{\max} (1 - e^{-\alpha r})$, where Q_{\max} and α are empirical constants. The authors choose instead a form due to Herman (1962) which greatly simplifies the radiation computations, $Q_a = \beta r$, in which the value of β is 0.12 μm^{-1} in the atmospheric window and 0.18 μm^{-1} outside. This results in the familiar parameterization of droplet transmissivity in terms of liquid water content $w(z)$, the particular form here is

$$\partial(\ln \tau_f(z, z')) / \partial z = -\alpha w(z), \quad \text{where } \alpha \text{ is a constant. The following boundary conditions}$$

are applied at the surface-air interface: $F_H + F_N + F_L + F_S = 0$; $\partial T_s / \partial z = \partial T / \partial z$; $T_s = T$; $w = 0$ for $z = 0$ and $t \geq 0$, where F represents a flux quantity and the subscripts H, N, L, S stand for sensible heat, net radiation, latent heat and soil heat.

Also it is assumed that at the top of the model, held at 250 m the following conditions hold:

$$\begin{aligned} q &= \text{constant}, w = 0 \\ \left. \begin{aligned} F\downarrow &= 235 \text{ W m}^{-2} \text{ outside} \\ F\downarrow &= 30 \text{ W m}^{-2} \text{ inside} \end{aligned} \right\} \begin{aligned} &8-13 \mu\text{m} \\ &\text{window} \end{aligned} \left. \begin{aligned} & \\ & \end{aligned} \right\} \begin{aligned} &z = 250 \text{ m} \\ &t \geq 0 \end{aligned} \\ T_s &= 5^{\circ}\text{C for } z = -1 \text{ m}, t \geq 0 \end{aligned}$$

It is evident that the downwelling fluxes have been fixed at the top of the model. Outside the atmospheric window the value is based on calculations assuming a sky emission temperature of 4°C , which is 1°C cooler than the initial temperature at 250 m. Outside the window the value is based on calculations made using the data from a single sounding.

One note of interest is a rough attempt to use the model to estimate the role of vegetation on the radiative aspects of fog formation. This exercise was conducted in order to attempt an explanation for an observed decrease in surface temperature during a period immediately after skies had cleared which was of greater magnitude than could be predicted by the model. Basically, by introducing an additional layer above the ground and 3 cm thick with a smaller heat capacity than the bare soil, and assuming the layer to radiate as a black body at a temperature 2°C below the soil temperature, the models cooling rate at a height of 1m and subsequent fog formation were brought more in line with observations. Although the method of accounting for the radiative effects of surface vegetation are crude, the authors remark that the results indicate surface vegetation may play a significant role on the timing of formation of radiation fog onset.

A.3.5 A numerical study of radiation fog by Brown (1980)

This study enhances the Brown and Roach (1976) model discussed above in two ways. First the model includes a scheme which approximates the actual fog droplet spectrum as a function of the fog life cycle. The model also couples the rate of growth of the droplets to the infrared radiation field using Roach's (1976) version of the droplet growth equation. This equation features an additional term which treats radiation budget of the droplet as an important influence in determining its rate of growth. This approach represents an interesting enhancement of the treatment of the coupling of the radiative, thermodynamic and water budgets when compared to other models reviewed thus far.

The droplet growth equation is written as

$$\frac{\partial r_{ij}}{\partial t} = \left(\frac{\sigma}{r_{ij}} - \frac{a_1}{r_{ij}^2} + \frac{a_2 m_j}{r_{ij}^4} - a_3 Q_i R \right) (A1 + f_{\beta} A2)^{-1},$$

where

$$\begin{aligned} a_1 &= \frac{2SM}{\rho_1 R_G T}, & a_2 &= 6.05 \cdot 10^{-5} \text{ m}^3 \text{ kg}^{-1}, & a_3 &= \frac{1}{kT} \left(\frac{LM}{R_G T} - 1 \right) \\ R &= \frac{1}{2} (F\downarrow + F\uparrow) - \sigma T^4, & Q_i &= 1.18 (1 - \exp(-0.28 r)) \\ A1 &= \frac{L\rho_1}{kT} \left(\frac{LM}{R_G T} - 1 \right), & A2 &= \frac{\rho_1 R_G T}{DM e_s(T)} \\ f_{\beta} &= 1 + l_{\beta} / r_{ij}, & l_{\beta} &= \left(\frac{2\pi M}{R_G T} \right)^{\frac{1}{2}} \frac{D}{\beta} \end{aligned}$$

In the equation above, σ is the supersaturation, r_i is the radius at the center of the i^{th} size bin with condensation nucleus mass m_i , S is the surface tension for pure water, M the molecular weight of water vapor, ρ_l the density of liquid water, R_g is the universal gas constant, T is the air temperature, k is the thermal conductivity of air, L is the latent heat of vaporization, R is the net radiation per unit area of drop for unit Q , the droplet absorption efficiency factor averaged over wavelength, $F\uparrow$ and $F\downarrow$ are the upwelling and downwelling longwave fluxes at height z , s is the Stephan-Boltzmann constant, D the diffusivity of water vapor in air, M the molecular weight of water vapor, $e_s(T)$ the saturation vapor pressure at temperature T , β is the condensation coefficient, and D is the diffusivity of water vapor in air.

The droplet size distribution equation is written as

$$\begin{aligned} \frac{\partial N_{ij}}{\partial t} - \gamma r_{ij}^2 \frac{\partial N_{ij}}{\partial z} + \frac{\partial}{\partial z} \left(K \frac{\partial N_{ij}}{\partial z} \right) - \frac{N_{ij}}{\Delta r_i} \left| \frac{\partial r_{ij}}{\partial t} \right| + \\ + \frac{N_{i-1,j}}{\Delta r_{i-1}} \left| \frac{\partial r_{i-1,j}}{\partial t} \right| \quad \text{when} \quad \frac{\partial r_{i-1,j}}{\partial t} > 0 \\ + \frac{N_{i+1,j}}{\Delta r_{i+1}} \left| \frac{\partial r_{i+1,j}}{\partial t} \right| \quad \text{when} \quad \frac{\partial r_{i+1,j}}{\partial t} < 0, \end{aligned}$$

where $\gamma = v_T / r^2$ and v_T is the droplet's terminal velocity defined by Stokes law. This equation is introduced because it is not at all practical to try to integrate the droplet growth equation for each droplet history. So the latter equation is used to predict the concentration of droplets within a fixed radius interval. This type of treatment was introduced by Kovetz and

Olund (1969). The assumption is that during a time τ a fraction $\Delta N_{ij} = \frac{N_{ij}}{\Delta r_i} \left| \frac{\partial r_{ij}}{\partial t} \right| \tau$ of

the drops in bin i grow into bin $(i+1)$. The model uses 55 bins across the radius range from 0.3 to 20 μm . The author notes that use of this form of prognostic equation for the droplet distribution has some drawbacks. The major problem is the discrete nature of the formulation which forces some fraction of droplets into the bins for larger drops at each time step even though the continuous droplet growth equation may predict no drops in the larger bins after an equal amount of time. Steps have been taken to control the "spreading" in the drop size distribution which the method produces. Another problem is that the method does not conserve liquid water (again because of the spreading) but deviations are small enough that value of knowing the approximate droplet size distribution more than compensates.

The model does nothing to advance the treatment of turbulence beyond the previous offering except to include a term for turbulent diffusion of droplets in the vertical for which an eddy diffusion formulation is used.

As far as the formalism for the treatment of radiation, little was changed from the previous paper except that knowledge of the droplet spectrum now allows the flux version of the optical depth to be evaluated for a changing microphysical distribution, rather than invoking a form of the absorption efficiency which results in a parameterization in terms of liquid water. Thus, the transmission due to droplets between the levels z and z' is again modeled as

$$\tau_d(z, z') = \exp[-\Phi(z, z')] \quad , \text{ where}$$

$$\Phi(z, z') = 1.66 \int_z^{z'} \int_0^\infty N(r, z'') \pi r^2 Q_a(r) dr dz''.$$

Here, $N(r, z)$ is the concentration of droplets of radius r found at height z , $Q_a(r)$ is the absorption efficiency and the factor 1.66 is a diffusivity factor to approximate conversion from parallel to hemispheric radiation. The data of Herman (1962) are again used to compute the mean value of Q_a separately for regions inside and outside the atmospheric window as was done previously. However, whereas it was previously necessary to further approximate Q_a as proportional to r , in order to obtain Φ as a function of the liquid water content, since N is predicted, the integral may be evaluated. Scattering by droplets and gases is neglected. The author quotes Stephens (1978) as an indication that scattering makes only a 4% difference in the cooling rate at cloud top. Effects of solar radiation are neglected completely.

The model includes the effects of cloud condensation nuclei (CCN) by beginning with a specified CCN concentration. Droplets are assumed to be activated when the radius of the swelling nuclei reaches $0.3 \mu m$. At that point the particle is classified as a droplet and subsequently is subject to growth by condensation with release of latent heat, gravitational settling and turbulent diffusion. Before this critical radius the CCN do not participate in the physical processes.

One interesting benefit of approximating the droplet distribution is the ability to make a rough approximation of the visual range. Even though scattering has not been included as an important process in the radiative energy exchange of the fog layer, since the droplet distribution is

predicted the scattering coefficient σ_s may be evaluated as $\sigma_s = \pi \sum_i \sum_j N_{ij} r_{ij}^2 Q_{sij}$, where

Q_s is the scattering efficiency factor appropriate to the i th radius bin. Thus, it is possible to approximate the visual range as $V = 3.0 / \sigma_s$, utilizing values of the scattering efficiency at the wavelength of interest.

Several interesting effects of the radiative-microphysical coupling are given and this report will not attempt to summarize these findings because they must be explained in some detail to be appreciated. Suffice it to say that prognosis of the droplet distribution seems to be a significant advancement to the modeling of the fog life cycle even in the approximate form offered in this model.

A.3.6 Formation and evolution of radiation fog and stratus fogs in the atmospheric boundary layer, by Buykov and Khvorost'yanov (1977).

This model is in many respects similar to the previous offering by Brown (1980), in the sense that it includes a prognostic equation for the droplet distribution and a droplet growth equation. The formulations of the equations differ primarily in that the current offering couples the dynamics of the boundary layer to the mean wind field and to the time rate of change of the turbulent kinetic energy, whereas the previous model is decoupled in the sense that it relies solely on a one-dimensional characterization of vertical transports by turbulence for fog formation and evolution. The current model is in this sense more complete but some of its detail requires a more thorough search of the Soviet literature since it relies on previous relations (perhaps parameterizations) and conclusions to which the reader is referred. For example, after introducing equations for the time rate of change of u , v and b , which represent the horizontal components of the wind and the turbulent kinetic energy, the authors quote a finding in the literature which allows the time derivatives to be neglected with respect to other terms in the respective equations.

Continuing with the comparison it is noted that the droplet growth equation used here is

Maxwell's relation, $\frac{dr}{dt} = D \rho_a \Delta / \Gamma \rho r$, where D and Δ are the diffusion coefficient and

supersaturation of the water vapor, ρ and ρ_a the density of water and air and Γ the correction for the difference between the air and drop temperature. This contrasts to the droplet growth equation in Brown (1980) which includes terms for radiative cooling, droplet surface tension and condensation. Also, the current model neglects gravitational settling but includes a continuous rather than discrete form of the droplet distribution function.

The formulation of radiation is similar in many respects to the two stream methods used elsewhere. The divergence of the upward and downward streams is given as

$$\begin{aligned}\frac{dF_{\uparrow}}{dz} &= \beta (\alpha_{\lambda L} + \alpha_{\lambda V}) (B_{\lambda} - F_{\uparrow \lambda}) \\ \frac{dF_{\downarrow}}{dz} &= \beta (\alpha_{\lambda L} + \alpha_{\lambda V}) (F_{\downarrow \lambda} - B_{\lambda})\end{aligned}$$

where F_{\uparrow} and F_{\downarrow} are the upwelling and downwelling fluxes at height z , and wavelength λ , $\alpha_{\lambda L}$ and $\alpha_{\lambda V}$ are the volume absorption coefficients for liquid and vapor and β is a diffusivity factor of 1.66. The droplet absorption coefficient is linked in the usual way to the droplet distribution $f(r, z, t)$,

$$\alpha_{\lambda L}(r, z, t) = \rho_a \int_0^{\infty} dr \sigma_{\lambda}(r) f(r, z, t),$$

where σ_λ is the absorption cross section. Model results were generated with σ_λ calculated from Mie theory and also from an approximation due to Shifrin (1955),

$$\sigma_\lambda(r) = \pi r^2 (1 - R_\lambda^{(1)}) (1 - \exp(-8\pi\kappa_\lambda r/\lambda)),$$

where $R_\lambda^{(1)}$ is the single particle scattering albedo and κ_λ the imaginary part of the index of refraction. With this formulation the radiative heating rate is calculated as

$$\left(\frac{\partial T}{\partial t}\right)_{rad} = \frac{\beta}{c_p \rho_a} \int_{\lambda_1}^{\lambda_2} d\lambda (\sigma_{\lambda L} + \sigma_{\lambda V}) (F_{\lambda \uparrow} + F_{\lambda \downarrow} - 2B_\lambda)$$

and the radiative heating couples with the thermodynamic balance through

$$\partial T / \partial t - (\partial / \partial z) k (\partial T / \partial z + \gamma_a) = L e_c / c_p (\partial T / \partial t)_{rad},$$

where γ_a is the dry adiabatic lapse rate, L is the latent heat of condensation, and k the turbulent exchange coefficient. e_c is related to the droplet distribution function as follows,

$$e_c = 4\pi\rho \int_0^\infty dr \frac{dr}{dt} r^2 f(r, z, t).$$

The radiative heating is evaluated at 32 wavelengths between 5 and 35 μm which the authors admit only accounts for the trend in the spectral variation of water vapor absorption and is not sufficient to account for the fine structure in the absorption coefficient.

Regarding the degree of spectral resolution as it affects the accuracy of the vapor absorption and emission, the authors note that it would be preferable to use transmission functions which account for the "mass" of vapor. This is apparently a reference to using a model in which the absorption coefficient is adjusted for the effects of non-homogeneous path, since they quote a constant value for α_v of $0.1 \text{ cm}^2 \text{ gm}^{-1}$. However, they note that in the region of the atmospheric window, which is chiefly responsible for the longwave energetic exchange, the absorption coefficient depends only weakly on the mass of the vapor. Outside the window region the authors note that the dependence of the absorption coefficient can be significant only in the subcloud layer and since the dependence is not particularly strong, it has little effect on the energetics. The authors present a comparison using their spectral approach and previously published transmission functions which shows "fair" agreement and indicates that their spectral approximation is sufficient without detailed accounting of the line structure.

A.3.7 A numerical study of the formation and the dissipation of radiation fogs by Ohta and Tanaka (1986)

This model differs somewhat from others looked at so far mainly in its treatment of radiation exchange. Although the model is different it is questionable if much is gained by the particular

algorithm chosen. The radiation method is described below. As for the dynamic and thermodynamic treatment, although very clearly presented, the model is similar in most respects to others in this review. The model considers the mean flow above a certain level to be geostrophic and casts the equations for the variation of the u and v components below this level what is basically an horizontally homogeneous Ekman boundary layer. The model includes turbulent flux budget equations for momentum, heat, water vapor and liquid water. Droplet settling is included using a constant preset velocity for the falling droplets. The eddy diffusivity coefficients are adjusted for stability using the Monin Obukhov length scale with nondimensional shear functions for momentum and sensible heat. The flux of heat into the ground is included as a contributing process down to a level of 80 cm where the local time rate of temperature change is considered constant.

The simulation of daytime conditions is included in this model. In the clear atmosphere, either before fog formation or after fog dissipation, the flux of solar radiation is affected by absorption by water vapor and ozone and scattering by air molecules as well as surface reflection. The value of the surface albedo used in the calculations is not presented. The spectral resolution is basically at the level required for band models. Ozone absorption is calculated using a single coefficient in the visible which was taken from The Handbook of Geophysics by Campen *et al.* In the near infrared at 0.72 and 0.81 μm , the transmission functions due to Fowle (1915) were used and the transmission data from Howard, Burch and Williams (1955) were used for water vapor at 0.94, 1.10, 1.38, 1.87, 2.70, and 3.40 μm . A matrix adding method Tanaka (1971) was used to calculate scattering in the visible due to air molecules. The effects of scattering are not included in the near infrared region covered by the band models. The authors indicate that the absorption by CO_2 is small and is not included in the calculation in the solar region. For clear sky in the infrared region the spectral resolution is limited to division into three regions: from 4.2-8.0 μm in which the 6.3 μm water vapor absorption is included, from 8.0 to 12.0 μm for which a continuum calculation is made, and from 12.0-62.5 μm in which the pure rotation band of water vapor and the 15.0 μm CO_2 band are included.

When fog is present the flux of radiation is calculated using a P_3 method described in Ohta and Tanaka (1984), to solve the radiative transfer equation. This method is somewhat more detailed than the two stream models used to treat the transfer of radiation in most other models reviewed. The method assumes the specific radiation intensity $I_\nu(\tau, \mu)$ at a frequency ν and optical depth τ in the direction that makes an angle with the vertical whose cosine is μ , and phase function $p(\tau; \mu, \mu')$ which may be expressed as a sum of Legendre polynomials $P_l(\mu)$ such that

$$I_\nu(\tau_\nu, \mu) = \sum_l I_l(\mu) P_l(\mu),$$

$$p_\nu(\tau_\nu; \mu, \mu') = \sum_l G_{l,\nu} P_l(\mu) P_l(\mu').$$

When the above is substituted into the equation of radiative transfer the results for near infrared or solar radiation,

$$\begin{aligned} \frac{l+1}{2l+3} \frac{dI_{l+1,v}}{d\tau_v} - \left[1 - \frac{G_{l,v}}{2l+1} \right] I_{l,v} \\ + \frac{l}{2l-1} \frac{dI_{l-1,v}}{d\tau_v} = -\frac{1}{4} F_v G_{l,v} P_l(-\mu_0) e^{-\tau_v/\mu_0}, \end{aligned}$$

where πF_v is the flux of solar radiation at the top of the atmosphere, and μ_0 is the cosine of the solar zenith angle. For the infrared portion of the spectrum the relation becomes

$$\begin{aligned} \frac{l+1}{2l+3} \frac{dI_{l+1,v}}{d\tau_v} - \left[1 - \frac{G_{l,v}}{2l+1} \right] I_{l,v} \\ + \frac{l}{2l-1} \frac{dI_{l-1,v}}{d\tau_v} = -\delta_{l,0} [1 - G_{0,v}] B_v(T), \end{aligned}$$

where, $B_v(T)$ is the Planck function at temperature T , and $\delta_{l,0} = 1$ for $l=0$ and $\delta_{l,0} = 0$ for $l \neq 0$. When these equations are solved for $l = 0, 1, 2$ and 3 and $dI_{4,v}/d\tau_v = 0$, the result has been termed the P_3 approximation. In order to obtain a solution in closed form the coefficients G and the Planck function B must be a function only of τ . In order to accomplish this the Planck function is expanded as a third order polynomial in τ . The absorption properties of the gases are treated in the same manner as in the clear atmosphere. A gamma distribution is used to describe the droplet distribution, but the distribution does not change with the fog life cycle. Scattering by droplets is included in the radiative calculation. The scattering characteristics are calculated from Mie theory.

Although the treatment of radiation by the P_3 method is more rigorous in that it is a higher moment calculation as compared to the more standard two stream methods, its value in this application is questionable. The two stream methods have been shown to be quite accurate in most situations for the determination of fluxes. If radiances or specific intensities are required for some application the P_3 method may be worthy of consideration. It would seem that if additional computational effort is to be invested it is better expended in either more detailed spectral information or in more realistic microphysical evolutions.

In addition, it would seem that only a small amount of additional effort would be required to make the droplet fall speeds a function of their radii, but this is not done. Rather a constant fall speed is adopted.

The strongest part of this model is its clearly defined treatment of the boundary layer, including a detailed account of boundary and initial conditions and an explicit presentation of the spatial and temporal grid used in the numerical calculations.

A.3.8 Prediction of quasi-periodic oscillations in radiation fogs. Part I: Comparison of simple similarity approaches by Welch, Ravichandran and Cox (1986)

This paper offers nothing additional in terms of modeling of radiative processes over the previous entry by Welch *et al.* Rather, it is both a comparison of some of the similarity approaches offered by various authors and a detailed accounting of the life cycle of the radiation fog scenario complete with comparison to observations. Following a thorough description of the modeling equations, with optional forms of the turbulent exchange schemes, the paper discusses the quasi-periodic oscillations in the height of the boundary/fog layer, including variations in liquid water content, which have been noted in some field observations. Also, the model clearly indicates that fog formation occurs during periods of active turbulent activity and not at a time of a lull in the turbulent exchange as was indicated in the observations of Roach *et al.* (1976). The authors identify five distinct periods of importance in the fog life cycle, which they classify as the sundown stage, the conditioning stage, the mature stage, the sunrise stage, and the fog dissipation stage.

A.3.9 Assessing the role of latent heat in the development of nighttime cooling fogs, by L.P. Bykova (1986).

This effort presents a relatively brief accounting of the heat budget in a radiation fog. There is little detail presented in the method of solving for the radiational heating/cooling, except to refer to published transmission functions in the Soviet literature for longwave and shortwave transfer. The model includes prognostic equations for the average energy of turbulent fluctuations, the rate of dissipation of turbulent energy, a surface heat transport equation and air-ground interface equation as well as including mean geostrophic wind components. Lacking in the model is any dynamic accounting of the droplet size distribution, droplet growth or of dew deposition. These equations are not required for radiative considerations in this model presentation since the transmission functions are presented for clear and cloudy atmospheres and are thus preset with regards to drop size distribution.

There is minimal descriptive information on the models formulation. It is similar to that used by Buykov *et al.* (1977), with the exception of radiative and droplet growth equation included in the latter. Almost no detail of the radiative formulation is given other than the mention of the transmission functions. What makes this model noteworthy is the author's conclusion, based on the model results, that radiative cooling plays a minor role in fog formation and in the maintenance of the inversion at the top of the layer. Rather, the author presents model results which indicate that the primary mechanism for the maintenance of the temperature inversion and the growth of the fog is the turbulent evaporation of the droplets. The analysis separates the time rate of evaporation into a local rate of change and a turbulent rate of change. Results indicate that the rate of temperature change attributable to the divergence of radiation is only a small fraction (usually less than 10%) of the cooling rate due to turbulent evaporation. This finding is at odds with other interpretations; however, this study is the first to specifically separate out the evaporation due to turbulent exchange. It may be that the treatment of radiative energy was

inappropriate or not resolved on a vertical grid structure of sufficiently to indicate the actual magnitude of the radiative contribution in various layers.

A.3.10 A comparison of a numerical model of radiation fog with detailed observations by Turton and Brown (1987)

This paper adds virtually nothing regarding the modeling aspects of radiation fog to the previous entry by Brown (1980). Rather it offers a detailed comparison of various model predictions to the observed counterparts. Of significance in these comparisons is the reaffirmation that fog forms during a lull in the turbulent process which is again in conflict with the findings of at least one other line of thought. For example, Welch *et al* (1986) indicate that fog forms during periods of active turbulence. The authors attribute some of the disagreement between modeled results and observations to the lack of topography in the model. They contend the turbulence parameterizations are tuned to observations taken of flat surfaces and the presence of rolling hills, shrubs and even distant buildings may violate assumptions about the turbulence.

A.3.11 The effects of radiative exchange on the growth by condensation of a population of droplets by Guzzi (1980)

This paper summarizes a model of the growth of a population of droplets as in the case of a radiation fog. It is not a fog model in the complete sense though since it simulates only the growth of the drops due to condensation in a moist environment and has no mechanism for turbulent exchanges or vertical transport of heat, momentum or water. The main emphasis is to examine the effects of radiative exchange on droplet growth. The treatment of radiation is limited to the infrared with scattering ignored. The upward and downward fluxes are given as

$$F_{\uparrow}^{\Delta\lambda}(z) = [F_{\uparrow}^{\Delta\lambda} - \pi \overline{B^{\Delta\lambda}}(z_0)] 2 E_3^{\Delta\lambda}(z_0, z) - \int_0^z \pi \frac{dB^{\Delta\lambda}}{dz} 2 E_3^{\Delta\lambda}(z, z') dz + \pi \overline{B^{\Delta\lambda}}(z)'$$

and

$$F_{\downarrow}^{\Delta\lambda}(z) = [F_{\downarrow}^{\Delta\lambda} - \pi \overline{B^{\Delta\lambda}}(z_{\max})] 2 E_3^{\Delta\lambda}(z, z_{\max}) + \int_z^{z_{\max}} \pi \frac{dB^{\Delta\lambda}}{dz} 2 E_3^{\Delta\lambda}(z, z') dz' + \pi \overline{B^{\Delta\lambda}}(z)'$$

where $F_{\uparrow}^{\Delta\lambda}$ and $F_{\downarrow}^{\Delta\lambda}$ are the boundary conditions for the fluxes; $2E_3(z, z')$ is twice the GOLD function of the third order and represents the diffuse transmission function between two different levels z and z' ; $dB/dz = (dB/dT)(dT/dz)$ is the derivative of the Planck function with respect to height in terms of its derivative with respect to temperature and the lapse rate. The superscript $\Delta\lambda$ represents a three-point weighted average in the spectral interval $\Delta\lambda$. The treatment of the

water vapor and carbon dioxide emission is reportedly similar to that of Rogers and Walshaw (1966). The water vapor continuum in the window is divided into five spectral intervals and an approximation to the absorption coefficient due to Bignell (1979) is used in which

$$K(\lambda) = K_1(\lambda) \frac{p}{p_s} + K_2(\lambda) \frac{e}{p_s},$$

where K_1 and K_2 are the foreign and self-broadening coefficients respectively, and p , p_s , and e are respectively the total, standard and partial pressure of water vapor. A contribution from ozone is estimated using Lowtran 3B as described in Selby *et al.* (1976). A surface emissivity of 0.98 is assumed in the calculations. The contribution due to the droplet population is calculated as

$$E_3^{\Delta\lambda}(z, z') = \int_0^{\pi/2} \exp \left[- \int_z^{z'} \left(\sum_i K_{gi}^{\Delta\lambda} \rho_{gi} + \sigma_a^{\Delta\lambda} \right) dz \sec \theta \right] \sin \theta \cos \theta d\theta,$$

where K_{gi} is the absorption coefficient in the range $\Delta\lambda$, and ρ_{gi} is the density of the gases. The volume absorption coefficient is calculated in the standard manner by

$$\sigma_a^{\Delta\lambda} = \int n(r) \pi r^2 \overline{Q^{\Delta\lambda}}(r, \lambda, m) dr,$$

where $n(r)$ is the droplet distribution, m is the complex index of refraction, λ the wavelength and Q the absorption efficiency factor from Mie theory.

The most interesting result from this work is the role of infrared radiation in preferentially enhancing the growth of larger droplets through the droplet growth equation

$$r \frac{dr}{dt} = \frac{\frac{De}{R_v T \rho_s} \left\{ \frac{e}{e_s} - \left[1 - \frac{LrR}{R_v K T^2} \right] b \exp(a/r) \right\}}{1 + \frac{L^2 D \rho_s}{K R_v T^3} b \exp(a/r)},$$

where D is the water vapor diffusivity in air, e and e_s the partial and saturation pressure of water vapor, R , the specific gas constant of water vapor, L the latent heat of vaporization, ρ , the solution density, r the droplet radius, K the coefficient of heat conduction in air, and T the ambient temperature. In the above R is the radiative heat exchange per unit surface as defined by Roach (1976), and is defined as

$$R = Q_A(r) \left[\frac{1}{2} (F\downarrow + 1.015 F\uparrow) - \sigma T^4 \right],$$

where Q_λ is a mean longwave absorption efficiency factor defined as

$$Q_\lambda = \frac{\sum_i (F_{\uparrow}^{\Delta\lambda_i} + F_{\downarrow}^{\Delta\lambda_i}) \int_{\Delta\lambda_i} Q(r, \lambda, m) d\lambda}{\sum_i (F_{\uparrow}^{\Delta\lambda_i} + F_{\downarrow}^{\Delta\lambda_i}) \Delta\lambda_i}.$$

The remaining factors in the growth equation are given by

$$\begin{aligned} a &= \frac{2\sigma}{\rho_s R_v T} \\ b &= \frac{m}{m + i e M_w \rho_d r_0^3} \\ m &= M_s \{ \rho_s [r^3 - r_0^3 (1 - e)] - e \rho_d r_0^3 \}, \end{aligned}$$

where σ is the surface tension of pure water, e is the solubility or fraction of soluble matter, M_w is the molecular weight of water, M_s is the molecular weight of the solute, ρ_d is the density of dry nuclei, r_0 is the radius of the aerosol and i is the VAN'T HOFF factor.

One of the aspects of the presentation of the treatment of radiative effects which has not been totally explained is the amount of spectral resolution used in the calculation of the absorption coefficients for gases. While it is stated that the symbol $\Delta\lambda$ represents a three-point average over the spectral interval, it is not clear exactly what spectral interval was chosen and thus to what extent the entire spectrum is represented. Of course any suitable average over the emissive spectrum could be substituted in applying the model.

The results of this study, although incomplete from the standpoint of offering results in a real radiation fog scenario, point to the role of radiative cooling of the droplets in preferentially enhancing the growth of larger droplets. In the model experiments presented total water is conserved. If the model is started with sufficient water vapor the growth of medium and larger droplets is accelerated because of the radiative term in the droplet growth equation. If the initial humidity is decreased somewhat only the largest drops are affected. This is an interesting result although not necessarily obtained in nature since additional water may be exchanged in the volume by turbulent mixing or evaporation from the surface. Nevertheless, this is the type of droplet growth equation that could be introduced into a radiation fog model to track the growth of the population, thereby allowing more detailed computations of visibility or acquisition ranges.

A.3.12 Numerical simulation of a fog event with a one-dimensional boundary layer model by Luc Musson-Genon (1987)

This model of fog is a 1-D turbulent calculation of the boundary layer evolution which takes into account radiative effects, transport of heat and water by turbulence and gravitational settling of droplets. The model is meant to be used in conjunction with a larger scale boundary layer model that predicts temperature, wind and moisture on a larger scale and is intended as an operational

forecasting tool. As such the parameterizations used for the different processes are not necessarily the most sophisticated according to the author; however, they seem to be on a level comparable to the other models examined in this study. There are some limitations that are related to the treatment of radiative exchange. For example, the flux of liquid water due to droplet settling is parameterized in terms of the mean droplet fall speed which is in turn expressed as a function of the liquid water content. This treatment of the fall speed was adopted by other modelers, for example in the evolution of the Welch, Zdunkowski and Cox effort. The other approach is to use the Stokes terminal velocity as was done in Brown (1980) and others, apparently as a function of droplet radius. Thus, the current treatment does not seem inadequate at least in a relative sense. One aspect unique to the model is a statistical treatment of saturation which is termed a sub-grid scale treatment. It allows a layer to be saturated in some grid areas and unsaturated in others according to a preset distribution function.

The treatment of longwave radiative exchange is similar to that described in Sasamori (1968), where the heating rate in the infrared denoted by $\overline{R_d IR}$ is given as

$$\overline{R_d IR} = -\frac{\theta}{T} \frac{1}{\rho C_p} \frac{\partial \overline{F}}{\partial z}$$

where the vertical flux divergence is given by

$$\begin{aligned} \frac{\partial \overline{F}}{\partial z} = & (1 - \epsilon_g) \left[B(0) - \int_0^{\infty} B(z') \frac{\partial A(0, z')}{\partial z'} dz' \right] \frac{\partial A(0, z)}{\partial z} \\ & + \int_0^z \frac{\partial A(z, z')}{\partial z'} \frac{\partial B}{\partial z'} dz' + \int_z^{zt} \frac{\partial A(z, z')}{\partial z'} dz' \\ & - \frac{\partial A(z, \infty)}{\partial z} B(zt) \end{aligned}$$

where ϵ_g is the ground emissivity, $B(z)$ is the Planck black body function at a temperature $T(z)$ at altitude z , zt the altitude above which the atmosphere is assumed to be isothermal, $A(z, z')$ is the total absorptivity between levels z and z' and is given by

$$A(z, z') = 1 - (1 - A_{gas}(z, z')) T_{H_2O}.$$

The symbol A_{gas} represents absorptivity of water vapor, carbon dioxide or the water dimer in the window region, while the factor T_{H_2O} represents the transmission by liquid water. The absorption due to gases is computed from band models. Two different models are used for the water vapor rotation and vibration transitions. These are given in Sasamori (1968) and Shaffer and Long (1975). The carbon dioxide model is taken from Sasamori (1968) and the dimer absorption from Veyre (1980). The transmissivity due to liquid water takes the simple form

$$T_{H_2O} = \exp(-K_{ext} U_{H_2O}),$$

where the extinction coefficient is given a constant value of $120 \text{ m}^2 \text{ gm}^{-1}$. The author takes the position invoked in some of the other simpler schemes for the treatment of the infrared radiation, namely that the transmission due to liquid water does not depend strongly on the microphysical droplet distribution. Also neglected in this treatment is the effect of scattering by the droplets. Using the same level of approximation the downward infrared flux is given by

$$F_{\downarrow}(0) = \int_0^{z\tau} B(z') \frac{\partial A(0, z')}{\partial z'} dz' = B(z\tau) [A(0, z\tau) - A(0, \infty)].$$

The contribution to the radiative exchange in the solar portion of the spectrum is derived from a model by Fouquart and Bonnel (1980). There is only a short (one paragraph) description of how the model is applied to the radiation fog scenario but it is indicated that the effects of Rayleigh scattering, ozone absorption in the near ultraviolet and in the visible, absorptions by carbon dioxide, water vapor and cloud droplets are accounted for. A mean value of $5 \mu\text{m}$ is used for the droplet radius indicating the absence of a detailed microphysical model. Although the notion of cloud fraction is included in the boundary layer model it is discarded in the radiative computations because, according to the author, "fog or low clouds will be stratiform."

The solar model of Fouquart and Bonnel (1980) was reviewed separately. The model is one intended to be used in a general circulation model. The model utilizes the modified exponential kernel approximation to solve a conservative scattering process and then applies a predetermined photon path distribution to implement absorptions by ozone, carbon dioxide and water vapor. The exponential kernel method divides the problem into spectral intervals such that mean transmission functions may be written for each in the form

$$\Psi_{\Delta\nu}(u) = \frac{1}{\Delta\nu} \int_{\Delta\nu} \exp(-k_\nu u) d\nu = \sum_{i=1}^N a_i \exp(-k_i u).$$

The scattering problem is solved for each extinction coefficient k_i and the individual results are recombined as

$$F_{\Delta\nu} = \sum_{i=1}^N a_i F_i(k_i),$$

in which F is the flux density. The method of solution to the scattering problem utilizes a "delta phase function" to avoid complications attributable to the strong forward peak. In this aspect the solution is similar to the delta-Eddington approximation and is likely to be of the same order of accuracy as the PIFM discussed in Zdunkowski *et al.* (1980) mentioned above. The details of the exponential kernel may be found in Wang (1972) or Brogniez (1975) and are only outlined in the discussion of the parameterization of solar heating. The algorithm takes an interesting approach to the problem of specifying absorber amounts, based on an approximation that the monochromatic intensity I_ν may be represented in terms of the conservative intensity I_c according to

$$I_\nu(\tau_\nu; \mu, \phi; \mu_0, \phi_0) = I_c(\tau; \mu, \phi; \mu_0, \phi_0) \int_0^\infty p(\lambda, \tau; \mu, \phi; \mu_0, \phi_0) e^{-k_\nu \lambda / \sigma} d\lambda,$$

where $p(\lambda, \tau; \mu, \phi; \mu_0, \phi_0)$ is the probability distribution that a photon contributing to the conservative intensity and traveling in a direction specified by the cosine of the zenith μ , and azimuth angle ϕ , has traversed an optical path between λ and $d\lambda$, for a scattering medium of optical thickness τ , and cosine of the solar zenith μ_0 and azimuth angle ϕ_0 . The distribution of photon paths is derived *a priori* from Monte Carlo calculations or from numerical methods using the inverse Laplace transform, Fouquart (1974). In the parameterization this approach is simplified and the absorber amount is obtained from $u = -\ln(F/F_0)/k$. In this way the optical path u may be obtained from conservative scattering calculations of F and then the scattering medium may be immersed in an atmosphere of variable gaseous composition.

The parameterization when used in a general circulation model uses precalculated layer reflectivities and transmissivities for high, middle or low level clouds. It is presumed that constants for these quantities are set in a single layer for the fog model application; however, the microphysics apparently have not been adjusted until a later paper; see the entry for Vehil and Bonnel (1987). The parameterization also makes a first order approximation for the effects of broken cloudiness. This is accomplished by assuming the radiation field beneath a cloud is isotropic, thus only the clear fraction areas beneath cloud base are illuminated with radiation at the solar zenith angle. In the application to the fog model this aspect of the parameterization is not invoked.

In its development as a parameterization for heating due to solar radiation in a general circulation model this approach has been carefully implemented and has been favorably compared to other parameterizations (Lacis and Hansen (1974) and even to more exact solutions of the radiative transfer equation such as the solution by spherical harmonics, for example. What is not evident however, is the applicability to the radiation fog scenario. The possible shortcomings of such an application have been identified, and due to the lack of detail in the explanation of its implementation, the virtues of the solar heating algorithm in this application can not be further identified. There appears to be no capability to account for the effects of a changing droplet distribution even through parameterization in terms of liquid water content. This is probably due to the fact that the general circulation model for which this parameterization was designed does

not currently predict liquid water content. Also, the parameterization is evaluated more on the basis of its performance throughout the entire atmospheric column and not specifically within a cloud or fog layer. The degree of spectral resolution is also somewhat obscure. In the general circulation model it appears that the clouds have a layer reflectivity and transmissivity evaluated at a single conservative wavelength after which the absorptivities due to the gases are calculated with an approximation divided into two terms, one for strong absorption and one for weak absorption.

A.3.13 A one-dimensional numerical study to simulate the influence of soil moisture, pollution and vertical exchange on the evolution of a radiation fog by Forkel, Panhans, Welch and Zdunkowski (1984)

This article details the treatment of the soil moisture and energy budget model that is used in the Welch-Zdunkowski model; see related sections 3.1, 3.2 and 3.3. The article details the formalism of the Welch-Zdunkowski model and outlines the radiative treatment which has already been described above. The main emphasis of the article is the treatment of the soil layer and results of model simulation for dry and moist soil conditions and high and low pollution conditions. There is nothing additional to note regarding the treatment of radiation.

A.3.14 Fog Modeling with a new treatment of the chemical equilibrium condition by Forkel *et al.* (1987)

This paper describes a two-dimensional model of radiation fog for application in the mesoscale- γ range (2.5-25 km). The paper introduces a new way to calculate the liquid water content diagnostically from the chemical equilibrium requirement between vapor and droplets. The method is attributed to Sievers (1984) and is equivalent to the saturation adjustment proposed by McDonald (1963) but is stated to be more appropriate at the boundaries of the fog regions. The radiative energy exchange is computed according to the model of Zdunkowski *et al.* (1982), described above. There is nothing additional in the description of the method which impacts the accounting for the radiational exchange.

A.3.15 The diurnal cycle of the marine stratocumulus layer. A higher-order model study by Bougeault (1981).

This paper presents a detailed accounting of the modeling of the turbulent fluxes in the marine boundary layer using a higher order closure. Many of the fluxes are third order correlations; however, the radiative cooling is introduced as a constant in the model. Thus, in a sense there is no radiative model at all.

A.3.16 A radiative fog model with a detailed treatment of the interaction between radiative transfer and fog microphysics, by Bott, Sievers and Zdunkowski (1990).

This paper presents the results of numerical experiments using a one-dimensional fog model with a detailed treatment of the interaction between radiative transfer and fog microphysics. In many ways the model is a more up to date version of the model by Brown (1980), described above in that it includes a prognostic equation for the growth of droplets and also includes a radiative term in the droplet growth equation. The model improves on the earlier offerings by the Zdunkowski group by including the more detailed interaction. Thus, the model includes the more fully developed surface heat and moisture sub-model; see Forkel *et al* (1984), mentioned above and uses the radiation scheme of Zdunkowski *et al* (1982) described at length above. There are refinements to the model that affect the radiation scheme and these will be described.

First, a prognostic equation for the joint distribution of aerosol nuclei and water droplets is introduced as

$$\frac{\partial f(a, r)}{\partial t} - \frac{\partial}{\partial z} \left(k_h \frac{\partial f(a, r)}{\partial z} \right) - \frac{\partial}{\partial z} (w_t f(a, r)) - \frac{\partial}{\partial r} \left(r f(a, r) \right),$$

where k_m and k_h are the exchange coefficients for momentum and heat, a and r are the radius of the aerosol component and the total radius of the droplet, and w_t is the terminal velocity of the droplet due to gravitational settling. The solution of this equation replaces the *a priori* specification of droplet size as a function of fog life cycle as used in earlier versions of the model.

Second, the calculation of the scattering and absorption coefficients include the effects of the aerosol's contribution to the index of refraction. The index of refraction of a nucleus containing water sphere is given by $n(r_a, r_w, \lambda) = i\kappa(r_a, r_w, \lambda)$, where

$$\begin{aligned} n(r_a, r_w, \lambda) &= n_w(\lambda) + [n_a(\lambda) - n_w(\lambda)] \alpha(r_a, r_w) \\ \kappa(r_a, r_w, \lambda) &= (n(r_a, r_w, \lambda)^2 + 2) \left[\frac{\kappa_w(\lambda)}{n_w(\lambda)^2 + 2} \right. \\ &\quad \left. + \left(\frac{\kappa_a(\lambda)}{n_a(\lambda)^2 + 2} - \frac{\kappa_w(\lambda)}{n_w(\lambda)^2 + 2} \right) \alpha(r_a, r_w) \right] \end{aligned}$$

The quantity $\alpha(r_a, r_w) = [r_a / (r_a + r_w)]^3$ is the volume mixing ratio of the aerosol particle of radius r_a in the droplet of radius r_w , for which the index a denotes dry aerosol and w pure water. The authors relate that Mie calculations were performed for 11 values of α ranging from zero (pure water) and with decreasing increments towards one (pure aerosol). This

yielded a concentration of the available data at the higher relative humidities. The mean values of the radiation quantities were obtained for two infrared regions (one of them pertaining to the atmospheric window) and four solar spectral regions. The extinction and absorption efficiency factors $Q_{ext}(r_a, r_w)$ and $Q_{abs}(r_a, r_w)$ and asymmetry parameter $g_i(r_a, r_w)$ were tabulated for 440 combinations of (r_a, r_w) . In total, an extensive series of 1,200,000 Mie calculations were performed. The time dependent absorption coefficient may be obtained from

$$B_{abs} = \int_0^\infty \int_0^\infty f(a, r, t) Q_{abs}(a, r) \pi r^2 da dr.$$

The value of the efficiency factor for absorption $Q_{abs}(a, r)$ is obtained from linear interpolation of the tabulated values. A similar process is carried out for the extinction coefficient and the asymmetry parameter.

Third, the droplet growth equation includes the effects of the radiation budget, as prescribed by Davies (1985). This equation has the added benefit that the time constant of the temperature excess has been calculated to be much smaller than the time step of the numerical model so that the steady state solution may be used. The droplet growth is entered as

$$r \frac{dr}{dt} = \frac{1}{C_1} \left[C_2 \left(\frac{S_a}{S_r} - 1 \right) - \frac{F_d(a, r) - m_w(a, r) C_w dT/dt}{4 \pi r} \right],$$

where

$$C_1 = \rho_w L + \frac{\rho_w C_2}{D'_v S_r \rho_s}$$

$$C_2 = k' T \left[\frac{L}{R_v T} - 1 \right]^{-1}.$$

Here, $F_d(a, r)$ is the net radiation flux at the droplet's surface. The quantity k' denotes the thermal conductivity of moist air and D' , the diffusivity of water vapor where both terms have been modified for gas kinetic effects following Pruppacher and Klett (1980). S_a is the ratio of the actual water vapor pressure e_a of the ambient air and its saturation value $e_{a,s}$, and S_r is given by Kohler's equation:

$$S_a = \frac{e_a}{e_{a,s}}$$

$$S_r = \exp \left[\frac{A}{r} - \frac{B}{r^3 - a^3} \right].$$

The values of A and B describe the curvature and solution effects, respectively were taken from Pruppacher and Klett (1980). The net radiative flux at the droplet's surface is given by

$$F_d(a, r) = \pi r^2 \int_0^\infty Q_{abs}(\lambda, a, r) \left[\int_0^{2\pi} \int_0^\pi L(\lambda, \theta, \phi) \sin\theta d\theta d\phi + S(\lambda, \theta_0, \phi_0) - 4B(\lambda) \right] d\lambda.$$

The term $L(\lambda, \theta, \phi)$ is the spectral diffuse radiance incident at the droplet's surface, $S(\lambda, \theta_0, \phi_0)$ is the radiant flux density of the sun, and $B(\lambda)$ is the thermal emission of the droplet. Subdivision of the spectrum into the four solar and two infrared bands as in the description of the radiation code of Zdunkowski *et al.* (1982) above in section 3.3 and integration over azimuth yields

$$F_d(a, r) = \sum_{i=1}^6 F_{d,i}(a, r)$$

with

$$F_{d,i}(a, r) = \pi r^2 \int_{\Delta\lambda_i} Q_{abs}(\lambda, a, r) \left[2\pi \int_0^\pi L(\lambda, \theta) \sin\theta d\theta + S(\lambda, \theta_0) \right] d\lambda \quad i = 1, \dots, 4$$

and

$$F_{d,i}(a, r) = \pi r^2 \int_{\Delta\lambda_i} Q_{abs}(\lambda, a, r) \left[2\pi \int_0^\pi L(\lambda, \theta) \times \sin\theta d\theta - 4B(\lambda) \right] d\lambda \quad i = 5, 6$$

If the integrations of the absorption efficiencies are replaced by the mean values for the spectral interval one obtains

$$F_{d,i}(a, r) = \pi r^2 Q_{abs,i} \left[2\pi \int_0^\pi L_i(\theta) \sin\theta d\theta + S_i(\theta_0) \right] \quad i = 1, \dots, 4$$

and

$$F_{d,i}(a,r) = \pi r^2 Q_{abs,i}(a,r) \left[2\pi \int_0^\pi L_i(\theta) \sin\theta d\theta - 4B_i \right] \quad i = 5,6 ,$$

in which the following have been defined:

$$\begin{aligned} L_i(\theta) &= \int_{\Delta\lambda_i} L(\lambda, \theta) d\lambda \quad i = 1, \dots, 6 \\ S_i(\theta_0) &= \int_{\Delta\lambda_i} S(\lambda, \theta_0) d\lambda \quad i = 1, \dots, 4 \\ B_i &= \int_{\Delta\lambda_i} B(\lambda) d\lambda \quad i = 5, 6 \end{aligned}$$

Several of the equations above involve the integral over zenith angle of the diffuse spectral radiance $L(\lambda, \theta)$; however, since the radiation model is a two stream solution the functional dependence of the radiance on zenith is not known. Instead, the upward and downward directed flux densities are formulated according to the following:

$$\begin{aligned} E_i^+ &= 2\pi \int_0^{\pi/2} L_i(\theta) \cos\theta \sin\theta d\theta \\ E_i^- &= 2\pi \int_{\pi/2}^\pi L_i(\theta) \cos\theta \sin\theta d\theta \end{aligned}$$

Then, since in the original Eddington approximation (Shettle and Weinman 1970)

$$L_i(\theta) = L_{i,0} + \cos\theta L_{i,1} ,$$

a substitution into the formulation for the flux densities yields

$$\begin{aligned} L_{i,0} &= \frac{E_i^+ + E_i^-}{2\pi} \\ L_{i,1} &= \frac{3(E_i^+ - E_i^-)}{4\pi} \end{aligned}$$

Use of these relations allows the radiation incident on the droplet to be written as

$$F_{d,i}(a,r) = \pi r^2 Q_{abs,i}(a,r) [2(E_i^+ + E_i^-) + S_i]$$

for $i = 1, \dots, 4$ and

$$F_{d,i} = \pi r^2 Q_{abs,i}(a,r) [2(E_i^+ + E_i^-) - 4B_i]$$

for $i = 5, 6$.

The authors note that substitution of the above into the droplet growth equations shows analytically that the radiation term is a linear function of the absorption cross section of the droplets. Thus, with increasing radius the effect of the radiation term becomes more and more important. The paper continues with examples demonstrating the importance of the interaction between the radiative effect on the growth of the droplets and the gravitational settling of the droplets. The net effect is to cause oscillations in the liquid water content of the fog as the fog alternately grows large droplets and then loses them to gravitational settling. An interesting consequence is after each oscillation the supersaturation required to grow large droplets increases since after each oscillation more of the large aerosols have been scavenged out of the fog and the remaining smaller aerosols require a higher supersaturation for activation. The model is also able to study the evolution of the microphysical droplet distribution and the variations in the liquid water content as they are influenced by the radiational effects on droplet growth.

A.3.17 Properties of aerosols on the life cycle of radiation fogs, by Bott (1991)

This paper presents a detailed study of the effects of three different aerosols on the life cycle of a radiation fog. The effort is actually a continuation of the Bott *et al.* (1990) study discussed in section 3.16 in that it uses the same radiation model and droplet growth submodel. The major differences are the use of a different scheme for the transfer of heat and moisture in the surface so that the effects of different soils and vegetation may be eventually investigated. The author has chosen the soil model described in McCumber and Pielke (1981) and Pielke (1984). The paper concentrates on the effects of the different aerosols (urban, rural and oceanic) on the development of the fog properties and explains differences in fog life cycle evolution in terms of the different radiative properties resulting from the various aerosol nuclei. The model uses 40 aerosol size bins for each of 30 water size bins resulting in 1200 possible combinations of radii. Thus, 40 droplet growth equations must be solved for each model iteration. When combined with the possible variation of volume fraction ($\alpha = a^3 / r^3$), where a is the aerosol radius and r is the total droplet radius, and the variation over wavelength, the 1,200,000 total of Mie calculations is arrived at. The model uses the same droplet growth equation as used in Bott *et al.* (1990), but uses the level 2.5 turbulent model of Mellor and Yamada (1974, 1982), in order to calculate the eddy coefficients for heat and momentum transfer k_h and k_m . The paper proceeds with an excellent depiction of the behavior of the absorption and scattering efficiencies of the different aerosols and examines the behavior of a radiation fog evolving in the presence of the three aerosols. Notable among the examples is the rapid onset of fog with the urban

aerosol and the inability of the incoming solar radiation to "burn off" the fog. The article also does a good job of depicting differences in the droplet concentration spectrum, the liquid water spectrum and the aerosol mass spectrum as a function of fog evolution and aerosol type. There is nothing additional presented regarding the treatment or effects of radiation beyond the previous entry by Bott et al.(1990).

A.3.18 Radiation fog: A comparison of model simulations with detailed observations by Duynkerke (1991)

This paper describes the comparison of a radiation fog model with observations of the same in August of 1988 in the Netherlands. The model is one-dimensional with the familiar parameterization of the turbulent fluxes in terms of the turbulent diffusion coefficients which are calculated using the local gradient Richardson number and scaling in terms of the local Monin-Obukhov length. The model considers gravitational settling of the droplets for which the flux is written as

$$\overline{w_t q_l} = -10^6 q_l^{5/3} N_0^{-2/3},$$

where N_0 is the number of droplets per unit volume, q_l is the liquid water content and in which it is assumed that the terminal velocity of a drop of radius r , w_r , can be written as $w_r = w_0 r^2$, where w_0 has the value $1.27 \times 10^{-4} \text{ m}^2 \text{ s}^{-1}$. The model also includes a soil-vegetation model which specifies the vegetation temperature and soil temperature based on the emissivity of the vegetation and the net radiation at the surface.

The radiation model is described in Duynkerke and Driedonks (1988). Basically, a grey-body flux emissivity model is used in the infrared in which the downward and upward flux densities are given by

$$F^\downarrow = \int_z^\infty B(T(z')) \frac{\partial \epsilon(z, z')}{\partial z'} dz',$$

and

$$F^\uparrow = \int_z^0 B(T(z')) \frac{\partial \epsilon(z, z')}{\partial z'} dz' + B(T_s) [1 - \epsilon(z, 0)],$$

in which B is the Planck function, $\epsilon(z, z')$ is the emissivity for the corrected mass of absorber $u(z, z')$ corresponding to the vertical path from z to z' , and T_s is the surface temperature. In order to handle the spectral overlap of emitters the transmissivity is written as

$$(1 - \epsilon) = (1 - \epsilon_v) (1 - \epsilon_{\text{CO}_2}) (1 - \epsilon_c),$$

where v represents water vapor and c stands for droplets. The authors use a revised scheme for water vapor absorber attributable to Welch and Zdunkowski (1976), for which

$$\epsilon_v = \epsilon_{v1} + \epsilon_{v2} \left(\frac{u e}{p_*} \right),$$

where

$$u = \left| \int_z^{z'} 100 \cdot C \left(\frac{p}{p_*} \right) \left(\frac{p}{p_*} \right)^{0.9} dz \right|,$$

in which $C = 330 \times 10^6$ ppm at all levels and u is in atm-cm. For droplets or clouds, the authors state they use a method due to Stephens (1978), but then do not completely state the formulation which is basically a parameterization in terms of liquid water path.

The shortwave radiative fluxes are calculated using the SUNRAY model described by Fouquart and Bonnel (1980), discussed in section 3.12 above; however the authors indicate that they utilize a delta-Eddington approximation instead of the exponential kernel method for the solution of the monochromatic problem. As described above the model includes the effects of Rayleigh scattering, of absorption by water vapor ozone and carbon dioxide, and the scattering and absorption by water droplets. The optical thickness is parameterized using the relation $\tau = 3W/2r_e$, where r_e is the equivalent radius of the droplet distribution which is set to $10 \mu\text{m}$ in the model and W is the liquid water path. The single particle scattering albedo is given by

$$\omega_0 = 0.9989 - 4 \times 10^{-3} \exp(-0.15 \tau_c),$$

where τ_c is the optical thickness of the whole cloud layer.

The use of the SUNRAY model for a fog layer is questioned again as it was in its use in the fog model by Luc-Musson described in section 3.12 above, because it was derived for use in a general circulation model and has ostensibly been tuned to produce the best results for an entire tropospheric column and not necessarily a particular cloud layer. This shortfall is apparently addressed in a paper by Vehil *et al.* (1988), which discusses a new parameterization for the asymmetry factor and single particle scattering albedo and is meant to allow the monospectral model of Fouquart and Bonnel (1980) to be used in a fog layer.

A.3.19 Computing solar heating in a fog layer: a new parameterization, by Vehil and Bonnel (1988)

This paper presents a revision of the Fouquart and Bonnel (1980) model specifically for application to fog layers. As mentioned in the discussion of the Musson-Genon model in section 3.12, in which the Fouquart and Bonnel model was used for the solar radiative transfer, the model was tailored for use in a general circulation model and not necessarily applicable to a fog layer. This paper presents a comparison of the original Fouquart and Bonnel model with a more accurate exponential kernel method and reveals large errors in both the transmitted and absorbed solar energy. The errors are attributed to the tuning of the original model atmospheric columns containing clouds, and points especially to the values of the asymmetry parameter and the single particle scattering albedo as the cause of the discrepancies. New values of these parameters are derived using the optical depth and effective radius as parameters in the fit. The new values are shown to provide much better estimates of the absorbed and transmitted flux densities.

A.3.20 Study of the radiative effects (long-wave and short-wave) within a fog layer, Vehil *et al.* (1989)

This paper presents results of modeled and measured radiation quantities from a fog event. It is not a description of a radiation fog model, rather it presents a comparison of the measured and modeled infrared fluxes at the surface and infrared and visible optical thicknesses inferred from surface flux measurements. The study utilizes an infrared integration divided into 232 spectral intervals to evaluate the expressions for the upward and downward fluxes

$$F\uparrow(z) = \pi \int_0^\infty \left\{ I\uparrow_\lambda(0) t_\lambda(0, z, r) + \int_0^z B_\lambda(z') dt_\lambda(z, z', r) \right\} d\lambda$$

$$F\downarrow(z) = \pi \int_0^\infty \int_0^z B_\lambda(z') dt_\lambda(z, z', r) d\lambda$$

where $I\uparrow_\lambda(0)$ is the upward monochromatic radiative intensity at ground level, $B_\lambda(z')$ is the monochromatic Planck function for a temperature at altitude z' , $r = 1.66$ is the diffusivity factor and $t_\lambda(z, z', r)$ is the spectral transmissivity across the layer. The model uses gaseous transmittance values from Goody (1952), Golubitski and Moskalenko (1968) and Moskalenko (1969). The transmittance of water droplets is evaluated using a constant absorption coefficient and only in the atmospheric window (7-13 μm). The model uses the liquid water content to estimate an optical thickness $\delta(z, z') = k \cdot \text{LWC} \cdot \Delta z$, where k is taken as a constant at 149.5 $\text{kg}^{-1} \text{m}^2$, according to Herman (1962). Then the simple exponential transmission calculation is made as $t(z, z', r) = \exp[-\delta(z'/z)]$. This model does not take scattering into account in the infrared.

The shortwave fluxes are calculated using the modified model of Fouquart and Bonnel as

described in section 3.19 to calculate the fluxes arriving at the surface and the absorption of shortwave radiation within the layer. There is no additional modeling reported in this paper. There is no discussion of the dynamics of the fog development. The paper continues on to discuss a comparison of flux values measured during a fog event and compares measured and modeled flux values using no knowledge of the fog microphysics in the process. The radiation results are afterward used to infer the optical thickness of the layer without any experimental verification.

A.3.21 A numerical study of radiation fog over the Changjiang River by Qian and Lei (1990)

This paper presents a case study of radiation fog over the Changjiang River. The model is one dimensional with parameterized turbulence and considers only the effects of longwave radiation in a form attributed to Zdunkowski and Nielson (1969). The paper presents a single equation for the calculation of longwave fluxes but gives no information about spectral resolution, accounting for cloud microphysics etc.

A.3.22 Numerical simulations with a three-dimensional cloud model: Lateral boundary condition experiments and multicellular severe storm simulations, by Clark (1979)

This paper describes a cloud dynamics model used to simulate the evolution of cloud cells as in building storm cloud systems. No radiation model is described.

A.3.23 Mathematical modeling of acid deposition due to radiation fog, by Pandis and Seinfeld (1989)

This model is primarily a chemical model incorporating chemical rate equations into a radiation fog model. The fog model uses the radiation submodel of Zdunkowski *et al.* (1982), with no apparent modification for the modified solution properties introduced by the presence of the acid. In order to properly account for this effect the Mie calculations for the droplets would require recalculation using an index of refraction modified according to the acid solution. There is no indication that this has been done in the model.